Prepared for:

Rijkswaterstaat

RIZA-Arnhem

Morphodynamic Development of Secondary Channel Systems Along Rhine Branches in The Netherlands

November 1994

Q 1963

delft hydraulics

Morphodynamic Development of Secondary Channel Systems Along Rhine Branches in The Netherlands

Z.B. Wang
Th. van der Kaaij

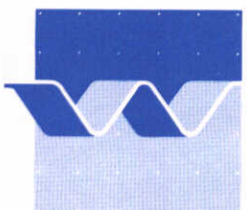

delft hydraulics

Contents

Samenvatting

In dit rapport wordt een studie naar de morfologische gevolgen van de aanleg van nevengeulen naast de Rijntakken beschreven. De nadruk ligt op de gevoeligheid van de voorspelde morfologische ontwikkeling voor de aangenomen waarden van de morfologische parameters. Met name de invloed van de zogenoemde splitsingspuntrelatie, waarmee de sedimentverdeling over hoofd- en nevengeul wordt beschreven, is uitvoerig geanalyseerd.

De studie is opgebouwd uit 2 delen: een theoretische analyse gevolgd door numerieke berekeningen met het 1-dimensionale model SOBEK.

Bij aanvang van de studie is als eerste de data verzameld door Akkerman (1993) die betrekking heeft op de sedimentverdeling over splitsingspunten geanalyseerd. Op basis van deze analyse en op basis van model-technische overwegingen wordt aanbevolen een machtsrelatie tussen debietverhouding en transportverhouding als splitsingspuntrelatie te hanteren.

De theoretische analyse beschouwt de mogelijke evenwichtstoestanden na aanleg van de nevengeul, de stabiliteit van deze evenwichtstoestanden en de tijdschaal van de morfologische ontwikkelingen wanneer het systeem niet in evenwicht is. Deze analyse is vergelijkbaar met die van Wang e.a. (1993) echter hier toegepast op de Meyer-Peter-Muller (MPM) transport formule. Toegevoegd is een analyse van de morfologische tijdschaal van het systeem.

De drempelwaarde voor stroomsnelheid in de MPM formule blijkt een grote invloed op het gedrag van het systeem te hebben. Zonder drempelwaarde bestaan 3 mogelijke evenwichtstoestanden: 2 waarbij slechts één van beide geulen stroomvoerend is en 1 waarbij beide geulen stroomvoerend zijn. De stabiliteit van de mogelijke evenwichtstoestanden wordt bepaald door de splitsingspuntrelatie. Met drempelwaarde voor stroomsnelheid blijken 3 of 5 mogelijke evenwichtstoestanden te bestaan. De 2 evenwichtstoestanden waarbij slechts één geul stroomvoerend is zijn stabiel onafhankelijk van de splitsingspuntrelatie. Alleen wanneer 3 evenwichtstoestanden bestaan waarbij beide geulen stroomvoerend zijn is één daarvan ook stabiel.

De end evenwichtsituatie die het systeem zal bereiken is dus niet alleen afhankelijk van de splitsingspuntrelatie, maar ook van de begintoestand van het systeem. Voor de nevengeul waarop zowel de analyse als de numerieke berekeningen betrekking heeft, de nevengeul gepland bij Stiftse Waard naast de Waal, betekent dit dat de nevengeul op lange-termijn afgesloten wordt. De situatie waarbij beide geulen stroomvoerend blijven kan alleen gerealiseerd worden indien de nevengeul voldoende diepte heeft en indien de splitsingspuntrelatie aan bepaalde voorwaarden voldoet, wat echter onzeker is.

In principe bestaan er twee morfologische tijdschalen van totaal verschillende orde van grootte. Als gevolg hiervan kan een korte en een lange termijn ontwikkeling van het systeem worden onderscheiden. Het afsluiten van de nevengeul is een lange-termijn ontwikkeling. Dit betekent dat in de eerste periode de kleine veranderingen in de nevengeul verwaarloost mag worden bij het beschouwen van de veranderingen in de hoofdgeul. Daarom wordt snelle aanzanding in de hoofdgeul verwacht in de eerste periode. Samenhangend met de langzame afsluiting van de nevengeul begint daarna de hoofdgeul te eroderen om op langere-termijn naar de oorspronkelijke situatie terug te keren.

De numerieke berekeningen zijn uitgevoerd met SOBEK, een 1-dimensionaal netwerk model recent ontwikkeld door het Waterloopkundig Laboratorium en Rijkswaterstaat. De geschematiseerde nevengeul zoals gepland bij Stiftse Waard is als referentie gehanteerd. Om de gevoeligheden te onderzoeken zijn gevarieerd:

- Het bovenstrooms debiet, een tijdsafhankelijk debiet i.p.v. een constant debiet;
- De splitsingspuntrelatie;
- De geometrie van de nevengeul;
- De grootte van het sedimenttransport;
- De korreldiameter in de nevengeul;
- De ruwheid in de nevengeul.

In de meeste berekeningen vertoont het systeem hetzelfde gedrag als in de referentiesituatie. Alleen een tijdsafhankelijk debiet en een kleinere korreldiameter in de nevengeul resulteren in een ander gedrag. Als gevolg hiervan dient bij verdere morfologische evaluatie uitgegaan te worden van een tijdsafhankelijk debiet en moet speciale aandacht besteed worden aan de korrelgrootte in de nevengeul.

De berekeningsresultaten stemmen goed overeen met de resultaten van de theoretische analyse naar de stabiliteit van de evenwichtstoestanden en de morfologische tijdschalen.

Voor het ontwerp van een nevengeul zijn de volgende punten belangrijk:

- Er moet rekening gehouden worden met benodigd onderhoud-baggerwerk.
- Bij de evaluatie op morfologische aspecten van een ontwerp moet men uitgaan van tijdsafhankelijk bovenafvoer.
- Speciale aandacht moet geschonken worden aan de korrelgrootte van het bodemmateriaal van de nevengeul. Als het materiaal duidelijk fijner dan dat in het hoofdgeul zal zijn, moet er nadere studie gedaan worden op de morfologische consequenties.
- Het simpele analytische model ontwikkeld in deze studie kan een nuttig middel zijn bij de evaluatie van morfologische aspecten bij het ontwerp van een nevengeul.

Summary

The present study describes the results of a short study on the morphological development induced by the construction of a secondary channel along the Rhine branches in the Netherlands. Emphasis is put on the sensitivity of a number of parameters on the morphological development. Especially the influence of the uncertain nodal point relation representing the sediment distribution to the two branches at the bifurcation has been analyzed.

The study consists of two parts: a theoretical analysis part and a numerical simulation part.

First the data collected by Akkerman (1993) on the sediment transport at bifurcations have been analyzed. Based on the results of the analysis and based on model-technical considerations it is recommended to use the power relation between the discharge ratio and sediment transport ratio as nodal point relation.

In the theoretical analysis the possible equilibrium states after the construction of the secondary channel, the stability of these equilibrium states and the time scale of the morphological development when the system is not in equilibrium are investigated. The analysis is similar to that of Wang et al (1993) but it is extended with the use of the Meyer-Peter-Muller (MPM) sediment transport formula. Another extension is the analysis on the morphological time scale of the system.

The threshold value for the flow velocity in the MPM transport formula appears to have important influence on the behaviour of the system. Without this threshold value there are three possible equilibrium states: two with only one branch open and the other with both branches open. The stabilities of them are determined by the nodal point relation. Either the two with only one branch open are stable or the one with both branches open is stable. With the threshold value, there are either three or five possible equilibrium states depending on the applied nodal point relation. In all the cases the two equilibrium states with only one branch open are stable, independent of the nodal point relation. Only when there are three equilibrium states with both branches open one of them is stable.

The final equilibrium state that the system will reach is thus not only dependent on the nodal point relation but it is also dependent on the initial condition. For the secondary channel system under consideration, i.e. the one designed at Stiftse Waard along the Waal river, this means that in all the situations the system tends to go to the situation that the secondary channel is closed. The situation with both branches open can only be reached if the secondary channel is deep enough at the beginning (which can be realised) and that the nodal point relation satisfies a certain condition (which is very uncertain).

There are basically two morphological time scales with different order of magnitude. As a consequence the system will first react with the smaller time scale and then develop with the larger time scale. The closure of the secondary channel is related to the larger time scale. This means that for the first period the minor change of the secondary channel may be neglected. Therefore rapid siltation in the main channel is expected in this period. Corresponding to the slow closure of the secondary channel the main channel starts to erode after the first period, tending to restore the original bed level.

The numerical simulations have been carried out with SOBEK, a one-dimensional network package recently developed by Rijkswaterstaat and DELFT HYDRAULICS. The schematised secondary channel system designed at Stiftse Waard is used as reference. In addition to the reference case various simulations have been carried out in order to investigate the sensitivity of time-varying discharge, the nodal point relation, the geometry of the secondary channel, the upstream sediment transport supply, the grain size of the sediment in the secondary channel and the roughness of the secondary channel.

Most of the simulations show a similar behaviour of the system as in the reference case. Only the case with time-varying discharge and the case with finer sediment in the secondary channel show significant difference in the behaviour of the system. This means that the final morphological evaluation on the design of the secondary channel should be based on the time-varying discharge and that special attention should be paid to the grain size in the secondary channel in further study.

The results of the numerical simulations agree very well with the conclusions from the theoretical analysis on the stability of the equilibrium states and the time scales.

For the design of a secondary channel the following points are important:

- The needed maintenance dredging work must be taken into account.
- For the evaluation on morphological aspects of a design the time-varying discharge has to be used.
- Special attention should be paid to the grain size of the bed material in the secondary channel. If it is much smaller than that of the bed material in the main channel, further study on the morphological consequences should be carried out.
- The simple analytical model developed in this study can be a useful tool for the evaluation of the morphological aspects of a secondary channel design.

List of Figures

List of Symbols

B	width	[m]
C	Chezy coefficient	[$m^{0.5}/s$]
D_m	mean grain size of sediment	[m]
D_{90}	grain size for which 90% of sediment is finer	[m]
g	gravity accelaration	[m/s^2]
h	water depth	[m]
i	water surface slope	[-]
j	constant	[-]
k	constant power in the nodal point relation	[-]
L	length	[m]
m	constant	[$m^{3-n}s^{n-1}$]
n	constant	[-]
Q	discharge	[m^3/s]
S	sediment transport	[m^3/s]
u	flow velocity	[m/s]
α	constant	[-]
β	constant	[-]
Δ	relative density of sediment	[-]
Δx	spatial step	[m]

Index

e	equilibrium
i	inflow
m	main channel
o	outflow
s	secondary channel

1 Introduction

1.1 General

To improve the ecological conditions along the Rhine branches in the Netherlands secondary channels are planned at various locations. These secondary channels can be considered as human interferences on the existing river system which will lead to various impacts on the river. One of the impacts, morphological changes caused by a secondary channel, is still far from fully understood up to now.

By the letter CXBC/8325 dated 22 September, RIZA, Rijkswaterstaat commissioned DELFT HYDRAULICS to investigate the sensitivity of a number of parameters influencing the morphological development of a secondary channel system. The study has been carried out by Ir. G.J. Akkerman (project leader), Ir. Th. van der Kaaij and Dr.ir. Z.B. Wang under the supervision of Ir. M.H.I. Schropp from Rijkswaterstaat.

The major objective of the present study is to obtain more insight into the morphological development caused by the construction of a secondary channel, in the river as well as in the secondary channel itself. The sensitivities of various parameters are analyzed in order to cope with the uncertainties of these parameters.

1.2 State of the art

The morphological processes of the planned secondary channel systems along the Rhine branches have already been investigated in a number of studies.

Schropp (1991) carried out a case study on the morphological development of the secondary channel system planned at Bemmelerwaard. Theoretical analysis as well as numerical computations using an one-dimensional model have been carried out in this study. With the theoretical approach the morphological equilibrium situation of a main and secondary channel system have been determined. It is also pointed out that the equilibrium is an unstable one; the secondary channel will only remain open if the sediment supply to it is stopped.

It appeared that the sediment distribution to the main and the secondary channel at the bifurcation is very important for the system. However, knowledge on this subject is very limited. A literature survey on the sediment distribution at bifurcation points in natural rivers and artificial channels have been carried out by Akkerman (1993). It is found that the curvature effect at the bifurcation and immediately upstream of the bifurcation is very important for the sediment distribution. This indicates that the sediment distribution relation, or the nodal point relation is different from bifurcation to bifurcation. The scarce available data have been well documented by Akkerman (1993).

In an one-dimensional network model the behaviour of the morphological development according to the model simulation is strongly influenced by the nodal point relation at bifurcations. For a simple case: one river bifurcates into two branches both flowing into a lake, it is shown by Wang et al (1993) that the behaviour of the long-term morphological development is totally determined by the used nodal point relation. For certain relations the bifurcation is stable (both branches tend to remain open) and otherwise it is unstable (one

of the branches tends to be closed). Based on model-technical considerations they recommend the following type of nodal point relation:

$$\frac{S_1}{S_2} = \left(\frac{B_1}{B_2}\right)^j \left(\frac{Q_1}{Q_2}\right)^k \quad (1)$$

Herein $S_{1,2}$ = sediment transport to the branches,
$Q_{1,2}$ = discharge through the branches,
$B_{1,2}$ = width of the branches.

Other alternatives presented in the literature are

$$\frac{S_1}{S_2} = \alpha \frac{Q_1}{Q_2} + \beta \quad (2)$$

and

$$\frac{S_1}{S_2} = \frac{B_1}{B_2} \quad (3)$$

Relation (1) is preferable to relations (2) and (3) because

(i) it is symmetric, i.e. it does not depend on the choice of the indices (note that this is not the case for relation (2));
(ii) it can represent both the stable case and the unstable case, whereas relations (2) and (3) always lead to the unstable situation.

Especially the case that $j = 1-k$, which implies that the ratio of the specific sediment transport rate (transport rate per unit of width) is related to the power of the specific discharge ratio, is recommended.

In the analysis the following simple sediment transport formula is used:

$$S = B\, m\, u^n \quad (4)$$

where u = flow velocity,
m, n = constants.

If equation (1) is used as nodal point relation, the bifurcation is stable if $k > n/3$, and otherwise it is unstable. These conclusions from the analysis have been verified by numerical simulations (Fokkink and Wang, 1993, Den Dekker and Voorthuizen, 1994) using WENDY, a one-dimensional network package developed at DELFT HYDRAULICS. It is also shown that the conclusions apply for the two channel system between a bifurcation and a confluence.

Another related study is carried out by Busnelli (1994), who investigated a two-channel system formed by a longitudinal dike in Rhine branch. This study concerns mainly the equilibrium state without considering the stability of the system.

All the analysis mentioned above uses the relatively simple sediment transport formula (4).

1.3 Set up of the study

The present study consists of two parts, a numerical simulation part and a theoretical analysis part.

The numerical simulations are carried out with SOBEK, a one-dimensional network package recently developed by Rijkswaterstaat and DELFT HYDRAULICS. The major objectives of the simulations is to investigate the sensitivity of a number of parameters. Here the secondary channel planned at Stiftse Waard (Schropp, 1994) is used as reference for the investigation.

In the theoretical part the analysis on bifurcations carried out by Wang et al (1993) is extended with the sediment transport formula of Meyer-Peter-Muller, which appears to have the best performance for the Rhine branches in the Netherlands (Kamphuis, 1990). The equilibrium situation, the stability of the system as well as the morphological time scale of the system have been considered in the analysis. The data collected by Akkerman (1993) for the sediment distribution at bifurcations have been analyzed in order to support the choice of a nodal point relation.

The two parts of the study are complementary. The conclusions drawn from the theoretical analysis have been verified by the results of the numerical simulations. On the other hand, the theoretical analysis makes it possible to extend the conclusions drawn from the numerical study, which refers only to one single secondary channel system, to other cases.

2 Numerical Simulations with SOBEK

2.1 General

In order to investigate the influence of various morphological parameters a sensitivity analysis based on SOBEK simulations is carried out. As reference case for the analysis the design of the secondary channel at Stiftse Waard is schematised into a one-dimensional network model. Based on this reference case a series of simulations are carried out, each time with one of the relevant parameters modified with respect to the reference case.

The schematised network system as described in this chapter is also used as reference for the theoretical analysis in Chapter 3.

The simulation periods will depend on the morphological time scale of the individual cases. However, the simulation time will not be longer than 25 year even when the time scale is much larger. This is based on the consideration that beyond a period of 25 years the morphological evolution will be significantly influenced by human interferences.

The results of the simulations are presented as much as possible in dimensionless form so that the conclusions drawn can be extended to other secondary channels along the Rhine branches.

2.2 Reference Case

The reference case for the study is based on the schematisation of the designed secondary channel at Stiftse Waard (Figure 2.1). The design of this secondary channel is described by Schropp (1994).

The schematised network model is shown in Figure 2.2. The length of the river section parallel to which the secondary channel is located is 2400 m and secondary channel is 2940 m of length. The secondary channel will also influence the upstream river and downstream river. Therefore a river section of 50 km (order of magnitude of water depth divided by slope of the Waal river, which is approximately the length scale of back water curves) at both ends is included in the network model.

The river Waal (the main channel) as well as the secondary channel are assumed to be prismatic, i.e. the cross-section is the same over the entire length and rectangular of shape. For the main channel this assumption agrees quite well with the reality but the cross-section of the secondary channel does vary in the length direction and it is triangular rather than rectangular of shape. However, the main purpose of the present study is to investigate influences of various morphological parameters rather than to make predictions for a particular case. A more detailed representation of the geometry will induce morphological evolutions which only make the analysis of the computational results more complicated.

The width of the main channel is 260 m and the width of the secondary channel is taken such that the discharge through the secondary channel will be about 5% of the total discharge at the initial state. The bottom of the secondary channel is about 3 m higher than that of the main channel. Based on the assumption that the secondary channel does not cause significant

influence on the water level in the main channel because it only transports a small part of the discharge the width of the secondary channel can be estimated as follows:

$$\frac{B_s}{B_m} = \frac{Q_s}{Q_m}\frac{C_m}{C_s}\left(\frac{h_m}{h_s}\right)^{\frac{3}{2}}\left(\frac{i_m}{i_s}\right)^{\frac{1}{2}} \quad (5)$$

For Q_s/Q_m = 5/95, C_s/C_m = 40/45, h_m/h_s = 5.61/(5.61-3) en i_m/i_s = 2940/2400 it follows that B_s/B_m = 0.19, Or B_s = 50 m.

Here the subscripts m and s indicate main and secondary channel respectively and

B = channel width;
Q = discharge;
C = Chezy coefficient;
h = water depth;
i = water surface slope.

However, the first SOBEK run shows that B_s should be 55 m instead of 50 m in order to have 5% discharge through the secondary channel. The difference is enplaned by the fact that the hydraulic radius is not equal to the water depth.

The bed-forming discharge, Q = 1600 m^3/s (Schropp, 1991, 1994), is prescribed at the upstream boundary. At the downstream boundary of the model the equilibrium water depth h_e of the undisturbed Waal river is prescribed as boundary condition. With C = 45 $m^{0.5}/s$ and i_m=0.00011 it follows from the following equation that h_e = 5.61 m.

$$Q = BCh\sqrt{\frac{Bh}{B+2h}i} \quad (6)$$

The grid size Δx in the area of interest is set to 100 m, whereas in the other areas it gradually increases to 6000 m. The time step for the simulations are determined based on the consideration of stability and accuracy of the numerical computations.

The sand in the main channel and in the secondary channel is the same having a mean grain size of D_m = 0.00145 m. The sand transport in the undisturbed situation is assumed to be in equilibrium and it is assumed that the transport formula of Meyer-Peter-Muller applies for the Waal. Thus the sediment transport at the upstream boundary is: 400160 m^3/year. This is rather large compared to measurements (see Kamphuis, 1990). However, the sensitivity of the sediment transport rate will be investigated (section 4.6).

In summary the input parameters for the reference case are as follows:

- length of the main channel L_m = 2400 m,
- length of the secondary channel L_s = 2940 m,
- width of the main channel B_m = 260 m,
- width of the secondary channel B_s = 55 m,
- Chezy coefficient of the main channel C_m = 45 $m^{0.5}/s$,
- Chezy coefficient of the secondary channel C_s = 40 $m^{0.5}/s$,

- Bottom slope of the main channel $i_m = 1.1*10^{-4}$,
- Bottom of the secondary channel at the node points is 3 m above that of the main channel.
- Upstream discharge Q = 1600 m^3/s,
- Water depth at down stream boundary h = 5.61 m,
- grain size of sand D_m = 0.00145 m,
- sediment transport at upstream boundary S = 400160 m^3/year
- grid size Δx = 100 m to 6000 m.

2.3 Set up of the sensitivity analysis

The sensitivity analysis is carried out such that each time only one of the relevant physical parameters is modified with respect to the reference case as described in the previous section. It is possible that the numerical parameters need to be adjusted due to the modification of the physical parameters.

The following relevant physical parameters are considered in the analysis:

- upstream river discharge;
- nodal point relation for sediment transport at the bifurcation point;
- upstream sediment transport;
- grain size of the sediment in the secondary channel;
- roughness (Chezy coefficient) of the secondary channel;
- initial discharge distribution via the width of the secondary channel.

In the following the variations of these parameters are analyzed.

Upstream river discharge

In the reference case the river discharge at the upstream boundary is kept constant. However, in reality the river discharge is varying all the time. In order to investigate the influence of the time variation of the river discharge a simulation is carried out with the discharge as shown in Figure 2.3 instead of a constant value. The hydrograph of the Waal river as shown in Figure 2.3 is based on a characteristic hydrologic year of the Rhine (Schropp, 1994).

Nodal point relation

An important drawback induced by the schematisation of a river channel system into a 1D network model is that the sediment distribution at a bifurcation point has to be prescribed. Physically the sediment distribution into the downstream branches at a bifurcation point is determined by the local three-dimensional flow conditions. This three-dimensional phenomenon cannot be represented in a 1D model and it has to be parameterised via a nodal point relation. Based on the results of the analysis on the data collected by Akkerman (1993) (see Chapter 3) it is decided to use equation (1) as nodal point relation and in the reference case k=2.5 is chosen. For this value of k the bifurcation will be unstable during the simulation as shown in the analysis in chapter 3. One more simulation is carried out with k=5 for which the bifurcation can be stable.

Width of the secondary channel

In the reference case the width of the secondary channel is determined such that the discharge through the secondary channel is about 5% of the total river discharge. One more simulation is carried out with two times the width of the secondary channel, i.e. the discharge through the secondary channel is about 10% of the total discharge.

Total sediment transport

The sediment transport rate in the river is an important uncertain parameter because it is difficult to measure. The value of this parameter in the reference case is assumed to have the equilibrium value according to the transport formula of Meyer-Peter-Muller. In order to cope with the uncertainties with respect to this parameter two more computations are carried out, one with a smaller value (300000 m^3/year) and one with a larger value (450000 m^3/year). The variation range of this parameter is determined based on the range of difference in the value of this parameter from different source of data.

Grain size of sediment in secondary channel

The grain size of sediment in the secondary channel in the reference case is assumed to be the same as that in the main channel. However, the sediment in the secondary channel may differ from that in the main channel due to two reasons. First, immediately after the construction of the secondary channel the sediment on its bed will be dependent on the local geological conditions. Second, at the intake selection of sediment may occur depending on the local flow conditions. In order to cope with this uncertainty it is decided to carry out two more computations, one with a coarser bed (grain size doubled) for the secondary channel and one with finer (grain size halved) secondary channel bed.

Roughness of the secondary channel

The chezy coefficient in the reference case is set to 40 $m^{0.5}$/s. According to Schropp (1994) this will be about the case immediately after the construction of the secondary channel. Later due to the grow of vegetation the roughness in the secondary channel will tend to increase resulting in a Chezy value of about 25 $m^{0.5}$/s. Therefore one more computation is carried out with this value.

In total there are thus 8 computations in addition to the reference case. The definition of these computations are summarised in Table 2.1.

Table 2.1 Definition of the runs

Run nr.	Description
000	Reference case
001	Time-varying upstream discharge and sediment transport
002	k=5 instead of k=2.5
003	B_s = 110 m instead of 55 m
004	Decreased upstream sediment transport
005	Increased upstream sediment transport
006	Grain size secondary channel halved
007	Grain size secondary channel doubled
008	C_s=25 $m^{0.5}/s$ instead of 40 $m^{0.5}/s$

3 Theoretical analysis

3.1 General

The analysis of Wang et al (1993) shows that the behaviour of a morphodynamic model for a one-dimensional network system is strongly influenced by the nodal point relation used in the model. However, this analysis is not only for a very simplified system but it is also based on a relatively simple sediment transport formula (4).

The sediment in the Waal river, along which the secondary channel Stiftse Waard will be located, is relatively coarse. According to Kamphuis (1990) the Meyer-Peter-Muller transport formula performs the best here among the existing formulas. A characteristic of this formula is that there is a threshold value for the flow velocity under which the sediment transport rate vanishes. This makes the things much more complicated. It will not only make the analysis more cumbersome but it also seems to cause a paradox. According to the earlier analysis the bifurcation will be stable if the constant k in equation (1) will be large enough. It is expected that this remains true if the Meyer-Peter-Muller formula is applied instead of equation (4). However, a simple physical reasoning leads to the conclusion that when one of the channels is small enough it will tend to be closed independent of the value of k. A very shallow channel will only discharge a very small part of the water, thus the flow velocity will be small. When the flow velocity is lower than the threshold value the sediment transport capacity of the branch will be zero but the branch will still receive sediment at the bifurcation according to the nodal point relation, provided that there is sediment transport towards the bifurcation. Therefore the branch will tend to be closed. This will thus lead to a situation that all three equilibrium situations are stable which is in contradiction with the general mathematical theory: three sinks on the phase diagram without source nor saddle is impossible. Therefore the analysis is extended here for the case that the Meyer-Peter-Muller formula is applied.

Before the analysis on the morphological system is described the data collected by Akkerman (1993) is analyzed in order to find an indication for physically valid nodal point relations.

3.2 Nodal Point Relation

Up to now the nodal point relation (1) has been recommended only because it is able to represent both the stable situation and the unstable situation in the model. Here the three data sets collected by Akkerman (1993) are fitted to this relation and to the linear relation (2) in order to investigate the validity of the relation and in order to find an indication of the value of the power k in the relation.

The fitting is done by a regression analysis using the least-square method. A separate analysis is carried out for each data set because it is expected that the nodal point relation is different from case to case due to the different local flow condition. The results are as follows (see Figure 3.1):

For the Pannerdens Channel:

$$\frac{S_1}{S_2} = 2.346 \left(\frac{Q_1}{Q_2}\right)^{2.326} \quad (7)$$

As Figure 3.1 shows, the agreement between the data and this relation is good and it is certainly better than that between the data and the linear relation (2). Note that both the power relation and the linear relation contain two free parameters. The width ratio of the two branches is not exactly known. For j=1-k, this relation leads to $B_1/B_2=0.52$, which agrees well with the map.

It is noted that the data is from scale model measurements which means that the quality of the data is high. Furthermore, the data cover a relatively large range of Q_1/Q_2.

For the Bifurcation at Westervoort the data does not fit the relation at all. The data suggests the tendency that the larger the ratio Q_1/Q_2 the smaller the ratio S_1/S_2 which is of course strange. It is noted by Akkerman (1993) that the sediment distribution at this bifurcation is disturbed by various human measures.

For the Jonglei Channel:

$$\frac{S_1}{S_2} = 2.977 \left(\frac{Q_1}{Q_2}\right)^{2.938} \quad (8)$$

The agreement between the relation and the data seems to be good but it is noted that in this case the data only cover three values of Q_1/Q_2. The relation leads to $B_1/B_2=0.57$ if j=1-k is chosen, which also agrees well with the map. Also for this case the power relation is clearly better than the linear relation.

Furthermore, a prototype data set from the Pannerdens Channel has been analyzed by Fokkink (1994), who found the following relation (see Figure 3.2):

$$\frac{S_1}{S_2} = 50 \left(\frac{Q_1}{Q_2}\right)^{5.99} \quad (9)$$

The coefficients are clearly different from those from the scale model data sets. However, it must be mentioned that measurements in nature is much more difficult than in a scale model, which means that the quality of the prototype data is usually much lower. It is also noted that the range of Q_1/Q_2 covered by the data set is very small. For j=1-k, this relation leads to $B_1/B_2=0.47$, which is still not far from what the map indicates.

In summary the following conclusions can be drawn:

- The sediment distribution ratio S_1/S_2 clearly depends on the discharge ratio. the suggested power relation works well for most situations but the coefficients vary from case to case.

- The suggested correction with the width ratio (j=1-k) agrees well with reality in most cases, independent of the value of the power in the relation. This indicates that the assumption that the transport per unit width is related to the discharge per unit width is correct.

- The suggested nodal point relation (1) is not only model-technically, but also physically preferable to equations (2) and (3).

3.3 Equilibrium State and Stability

Generally the change of the volume of the bed of a river branch is determined by the difference of sediment transport rate at the two ends of the branch. For the main channel and the secondary channel between the bifurcation and the confluence (Figure 2.2) this gives:

$$B_m L_m \frac{dh_m}{dt} = S_{mo} - S_{mi} \tag{10}$$

and

$$B_s L_s \frac{dh_s}{dt} = S_{so} - S_{si} \tag{11}$$

The out-going sediment transport rate at the downstream end is equal to the transport capacity whereas the in-going sediment transport rate at the upstream end is determined by the nodal point relation.

Under the assumption that the bathymetry of each branch can be represented by the averaged depth both terms can be related to this depth if the discharge through the two branches are known. In this way equations (10) and (11) become a system of first order ordinary differential equations for the water depths in the two branches.

The discharges through the two branches can be determined as follows.

$$Q_m = B_m C_m h_m \sqrt{\frac{B_m h_m}{B_m + 2h_m} i_m} \tag{12}$$

$$Q_s = B_s C_s h_s \sqrt{\frac{B_s h_s}{B_s + 2h_s} i_s} \tag{13}$$

$$Q_m + Q_s = Q_0 \tag{14}$$

$$\frac{i_m}{i_s} = \frac{L_s}{L_m} \tag{15}$$

Here Q_0 is the discharge from the upstream branch. From these four equations the four variables Q_m, Q_s, i_m and i_s can be expressed in h_m and h_s. The expressions for the discharges into the two branches are

$$Q_s = Q_0 \frac{B_s^{\frac{3}{2}} C_s h_s^{\frac{3}{2}} L_s^{-\frac{1}{2}} (B_s+2h_s)^{-\frac{1}{2}}}{B_s^{\frac{3}{2}} C_s h_s^{\frac{3}{2}} L_s^{-\frac{1}{2}} (B_s+2h_s)^{-\frac{1}{2}} + B_m^{\frac{3}{2}} C_m h_m^{\frac{3}{2}} L_m^{-\frac{1}{2}} (B_m+2h_m)^{-\frac{1}{2}}} \quad (16)$$

$$Q_m = Q_0 \frac{B_m^{\frac{3}{2}} C_m h_m^{\frac{3}{2}} L_m^{-\frac{1}{2}} (B_m+2h_m)^{-\frac{1}{2}}}{B_s^{\frac{3}{2}} C_s h_s^{\frac{3}{2}} L_s^{-\frac{1}{2}} (B_s+2h_s)^{-\frac{1}{2}} + B_m^{\frac{3}{2}} C_m h_m^{\frac{3}{2}} L_m^{-\frac{1}{2}} (B_m+2h_m)^{-\frac{1}{2}}} \quad (17)$$

The flow velocities are

$$u_s = Q_0 \frac{B_s^{\frac{1}{2}} C_s h_s^{\frac{1}{2}} L_s^{-\frac{1}{2}} (B_s+2h_s)^{-\frac{1}{2}}}{B_s^{\frac{3}{2}} C_s h_s^{\frac{3}{2}} L_s^{-\frac{1}{2}} (B_s+2h_s)^{-\frac{1}{2}} + B_m^{\frac{3}{2}} C_m h_m^{\frac{3}{2}} L_m^{-\frac{1}{2}} (B_m+2h_m)^{-\frac{1}{2}}} \quad (18)$$

$$u_m = Q_0 \frac{B_m^{\frac{1}{2}} C_m h_m^{\frac{1}{2}} L_m^{-\frac{1}{2}} (B_m+2h_m)^{-\frac{1}{2}}}{B_s^{\frac{3}{2}} C_s h_s^{\frac{3}{2}} L_s^{-\frac{1}{2}} (B_s+2h_s)^{-\frac{1}{2}} + B_m^{\frac{3}{2}} C_m h_m^{\frac{3}{2}} L_m^{-\frac{1}{2}} (B_m+2h_m)^{-\frac{1}{2}}} \quad (19)$$

The sediment transport capacities S_{mo} and S_{so} can then also be expressed in h_m and h_s by applying the sediment transport formula:

$$S = 13.3\, B \frac{\sqrt{g}}{\Delta} \left(\frac{u^2}{\sqrt{C_{D90}^3 C}} - 0.047 \Delta D_m \right)^{\frac{3}{2}} \quad (20)$$

Herein C_{D90} is the Chezy coefficient related D_{90}.

At the bifurcation point the mass-balance for sediment reads:

$$S_{mi} + S_{si} = S_0 \quad (21)$$

where S_0 is the sediment transport rate from the upstream branch. Together with equation (1) S_{mi} and S_{si} can be expressed in Q_m and Q_s and thus in h_m and h_s.

$$S_{si} = S_0 \frac{B_s^{1+\frac{k}{2}} C_s^k h_s^{\frac{3k}{2}} L_s^{-\frac{k}{2}} (B_s+2h_s)^{-\frac{k}{2}}}{B_s^{1+\frac{k}{2}} C_s^k h_s^{\frac{3k}{2}} L_s^{-\frac{k}{2}} (B_s+2h_s)^{-\frac{k}{2}} + B_m^{1+\frac{k}{2}} C_m^k h_m^{\frac{3k}{2}} L_m^{-\frac{k}{2}} (B_m+2h_m)^{-\frac{k}{2}}} \quad (22)$$

$$S_{mi} = S_0 \frac{B_m^{1+\frac{k}{2}} C_m^k h_m^{\frac{3k}{2}} L_m^{-\frac{k}{2}} (B_m+2h_m)^{-\frac{k}{2}}}{B_s^{1+\frac{k}{2}} C_s^k h_s^{\frac{3k}{2}} L_s^{-\frac{k}{2}} (B_s+2h_s)^{-\frac{k}{2}} + B_m^{1+\frac{k}{2}} C_m^k h_m^{\frac{3k}{2}} L_m^{-\frac{k}{2}} (B_m+2h_m)^{-\frac{k}{2}}} \quad (23)$$

Substituting the expressions for S_{mo}, S_{so}, S_{mi} and S_{si} into equations (10) and (11) yields a system of two ordinary differential equations for h_m and h_s.

$$\frac{dh_m}{dt} = f_m(h_m, h_s) \quad (24)$$

$$\frac{dh_s}{dt} = f_s(h_m, h_s) \quad (25)$$

The behaviour of the solution of this system of equations is mainly determined by the singular points (or physically the equilibrium states) at which both time derivatives in (10) and (11) are zero ($f_m=f_s=0$) and the stability of these singular points. The stability is analyzed as follows.

In the vicinity of singular point (h_{me}, h_{se}) the system of differential equations (24) and (25) can be linearized as

$$\begin{bmatrix} \frac{dh'_m}{dt} \\ \frac{dh'_s}{dt} \end{bmatrix} = \begin{bmatrix} \frac{\partial f_m}{\partial h_m} & \frac{\partial f_m}{\partial h_s} \\ \frac{\partial f_s}{\partial h_m} & \frac{\partial f_s}{\partial h_s} \end{bmatrix} \begin{bmatrix} h'_m \\ h'_s \end{bmatrix} \quad (26)$$

where

$$h'_m = h_m - h_{me} \quad (27)$$

(27)

$$h'_s = h_s - h_{se} \quad (28)$$

The matrix on the right hand side of equation (26) is called the Jacobian denoted by J. Try to find a solution of equation (26) in the form of

$$\begin{bmatrix} h'_m \\ h'_s \end{bmatrix} = \begin{bmatrix} H_m \\ H_s \end{bmatrix} \exp(\lambda t) \quad (29)$$

Substituting equation (29) into equation (26) yields

$$J \begin{bmatrix} H_m \\ H_s \end{bmatrix} = \lambda \begin{bmatrix} H_m \\ H_s \end{bmatrix} \quad (30)$$

Thus λ is the eigenvalue of the Jacobian with the corresponding eigenvector (H_m, H_s). The eigenvalue is solved from

$$\det \begin{bmatrix} \frac{\partial f_m}{\partial h_m} - \lambda & \frac{\partial f_m}{\partial h_s} \\ \frac{\partial f_s}{\partial h_m} & \frac{\partial f_s}{\partial h_s} - \lambda \end{bmatrix} = 0 \qquad (31)$$

At each singular point there are thus two eigenvalues (λ_1 and λ_2) and the corresponding eigenvector is found by substituting λ into equation (30).

The solution of equation (26) can thus be written as

$$\begin{bmatrix} H_m \\ H_s \end{bmatrix} = \alpha_1 \begin{bmatrix} H_{m1} \\ H_{s1} \end{bmatrix} \exp(\lambda_1 t) + \alpha_2 \begin{bmatrix} H_{m2} \\ H_{s2} \end{bmatrix} \exp(\lambda_2 t) \qquad (32)$$

where α_1 and α_2 are constant coefficients.

It is clear that the sign of the eigenvalues determine the stability of the equilibrium state represented by the singular point. If both eigenvalues are negative the equilibrium is stable and otherwise it is unstable.

For the case that the power law (4) is applied for the transport capacity the position of the singular points as well as the eigenvalues of the Jacobian can be calculated analytically. If the sediment transport formula of Meyer-Peter-Muller is used instead of the power law this is no more possible. Even the equilibrium states (singular points) can no more be expressed in an analytical form. Therefore the system is analyzed numerically:

- an area on the h_m-h_s plane, which covers all possible singular points, is divided in a grid;
- at each grid point the time derivatives according to equations (10) and (11) are calculated numerically;
- isolines $dh_m/dt=0$ and $dh_s/dt=0$ are drawn on the plane, the cross-points of these two lines determine the singular points;
- on the same plane the normalised vectors (dh_m/dt, dh_s/dt) at a selected number of points (a coarser grid) are depicted; this vector field shows the behaviour of all the singular points. Note that the normalisation of the vectors as well as coarsening of the grid are necessary to keep the vector field visible.

For each set of parameters such a figure gives the same information as the phase diagram as presented by Wang et al (1993). A number of examples are shown in Figures 3.3 through 3.9.

Figure 3.3, 3.4 and 3.5 present the symmetric case. Here all the parameters for the upstream branch are as that of the Waal river considered in this study (see Chapter 2). The two branches downstream of the bifurcation are identical, each with the half of the width of the upstream branch. For this case the point (h_e, h_e) is thus always a singular point independent

of k, where h_e is the equilibrium depth of the upstream branch. The following observations are made:

- For small values of k (smaller than about 1.3 in this case), there are three singular points (indicated by A, B and C, see Figure 3.3), of which one represents the case that both branches are open (A) and the other two represent the cases that one of the branches is closed (B and C). The equilibrium state with both branches open is a saddle point, thus unstable. The other two equilibrium states with only one of the branches open are stable. This is the same as the conclusion drawn from the analysis of Wang et al (1993).

  However, the critical value of k is no more a constant. It depends on the sediment transport parameter: the larger the difference between the flow velocity and its critical value the smaller the critical value of k. For the limit situation that the flow velocity is infinitely large the critical value for k is 1.

- For a large values of k (larger than about 1.3 in this case), there are in total five singular points (A, B, C, D and E, see Figure 3.4 and 3.5), three with both branches open (A, D and E). The three singular points, which are the same as in the case that k is small (A, B and C), are all stable now. The two additional singular points (D and E), of which the positions depend on the value of k, are saddles, thus unstable. These results solve the paradox mentioned in section 3.1. For this case the end results of a simulation will thus depend on the initial condition.

For the Figures 3.6 through 3.9 the parameters are chosen as in the reference case defined in Chapter 2, i.e. the schematised secondary channel system at Stiftse Waard. The basic behaviour of the system is the same as in the symmetric case. Only the positions of the three singular points are strongly asymmetric. This has the following consequences as the vector fields shows:

- Independent of the value of k, the situation that the main river is silted up and only the secondary channel remains open (indicated by B in Figures 3.6 through 3.9) will practically never be reached, which is physically logical. Only if the initial depth of the main channel is very small this situation can be reached.

- For large values of k (larger than about 5 in this case), there are practically two possible end situations: only the main river is open (C) or both branches are open (D) depending on the initial condition. See Figures 3.8 and 3.9.

- The designed secondary channel as schematised in Chapter 2 will always tend to be closed, independent of the value of k. See Figure 3.6 through 3.9 in which the initial state is indicated by a dot. To have the situation that both branches remain open not only a large value of k (larger than about 5) has to be chosen, but the initial depth of the secondary channel also has to be larger. The last condition can be easily realised but the first condition is uncertain.

3.4 Morphological time scale

Despite of the uncertainty in the value of k in the nodal point relation (1) the behaviour of the system appears to be predictable: the secondary channel tends to be closed and only the main river tends to remain open. Then it is very important to know on which time scale the development will happen. For this purpose the eigenvalues of the Jacobian at the singular points are considered again. Their signs determine the stability of the equilibrium state as mentioned in the previous section. Their values in absolute sense determine the time scale on which a disturbance from this equilibrium will decay or grow. In fact the eigenvalues are the reciprocal of the time scales.

3.4.1 The symmetric case

Before the secondary channel system under consideration is analyzed the symmetric case is investigated. Only the three possible stable equilibrium points, of which the positions are not influenced by k, are considered (A, B and C in Figures 3.3, 3.4 and 3.5). Because of symmetry only two points need to be analyzed. The two extra saddle points (D and E) for large values of k are not considered because they will never be reached in practise due to instability. The dimensionless time scales for the two equilibrium states as function of k are calculated numerically and shown in Figure 3.10. The time scale is the time needed for a disturbance along the corresponding eigenvector to decay (or to grow in case of instability, i.e. time scale $>$ 0) with a factor e (see Equation (32)). They have been normalised with

$$\frac{B_1 L_1 H_1}{S_0} \tag{33}$$

which is the time needed to fill one of the branch if all the sediment from the upstream branch is trapped in the branch.

For the case that only one branch is open (B or C), one of the time scale is constant (i.e. independent of k) with the corresponding eigenvector (1,0), i.e. disturbance only in the open channel (see Figure 3.10). The other time scale is not shown in the figure because it is infinitely large with the corresponding eigenvector (0, 1). This means that a very shallow branch tends to be closed but the closure will take a very long time. This behaviour can also be observed in Figures 3.3, 3.4 and 3.5 as the vectors near B and C are almost parallel to the axes.

For the case that both branches are open (A) both time scales are shown in Figure 3.10. One of the time scales does not depend on k, which is for the disturbances along the line $h_1 = h_2$ (eigenvector (1,1)). The other one changes of sign at a certain value of k, which is the critical k value for the stability. Below this value the equilibrium is unstable. Above the critical value the magnitude of the time scale decreases with k and it becomes constant for large values of k with the same order of magnitude as the other time scale (see also Figures 3.4 and 3.5, and compare the directions of the vectors near point A).

3.4.2 Secondary channel case

As mentioned earlier there is only one relevant stable equilibrium state, i.e. only the main channel is open. Other stable equilibrium states can only be reached for large values of h_s. Like the symmetric case, there are two time scales independent of the value of k, one with a infinitely large magnitude and the other with a magnitude of about one third of the time needed to close the branch if the total sediment transport is trapped.

According to this analysis it will take a very long time before the secondary channel is closed. It is then important to know about the development immediately after the construction of the secondary channel. Therefore, the initial depth change rates in the secondary channel (dh_s/dt) as well as in the main channel (dh_m/dt) have been calculated and shown in Figure 3.11 as function of k. They have been made dimensionless with the depth change rate which will happen if all the sediment from the upstream branch is trapped in the channel:

$$\frac{S_0}{BL} \tag{34}$$

where B and L are the width and length of the corresponding channel.

It is noted that at the initial state the flow velocity in the secondary channel is under the threshold value which means that the secondary channel is an ideal sand trap (e.g. for k=1 the relative bed level change rate is 5% of magnitude which is exactly the discharge distribution rate).

In the main channel the depth change rate at the initial state increases in magnitude with the value of k and it becomes constant for large values of k. It is clear that the initial bed level change in the main channel will be relatively fast. On the other hand, at long-term the system tends to go to the situation that only the main channel is open, which means that the original bed level will be restored. Based on this observations it can be expected that the bed level in the main channel will increase fast directly after the construction of the secondary channel. It first tends to go to the equilibrium situation if the secondary channel does not change, i.e. with a discharge withdraw of 5% and the corresponding sediment withdraw according to the nodal point relation. When this situation is almost reached, the bed level in the main channel will decrease slowly with the corresponding siltation in the secondary channel. This feature can also be observed from the Figures 3.6 through 3.9 as the vectors near the point indicating the initial state is almost parallel to the h_m-axis.

3.5 Sensitivity of other parameters

Up to now, especially the sensitivity of the parameter k is analyzed, which is of course the most uncertain parameter. From the analysis it appears that the "numerical phase diagram" as shown in Figures 3.3 through 3.9 gives the most insight. It shows the positions of the equilibrium states, their stability, and also the behaviour of the system with different initial conditions. Therefore such a figure is made for each case described in Chapter 2 for the sensitivity analysis, except the case that k=5 instead of 2.5 which is already presented in

Figure 3.8 and the case of time-varying discharge which cannot be represented in the simple model. See Figures 3.12 through 3.18. Note that the initial condition at present is h_m=5.618 m and h_s=2.618 m.

Based on these Figures it is expected that all the computations will show a similar behaviour of the system except the one with finer sediment in the secondary channel (see Figure 3.15).

Note that the parameters may also influence the equilibrium bed slope in the main channel. However, this has no influence on the behaviour of the system. Therefore this effect is not discussed here.

4 Results from SOBEK Simulations

4.1 SOBEK Input

The model is set to correspond with the designed secondary channel at Stiftse Waard along the river Waal. The relevant physical parameters have already been described in Chapter 2. Here the numerical parameters and the SOBEK input are described.

Computational Grid

The model consist of 2 nodes, a bifurcation node and a confluence node, 2 boundaries and 4 branches:

- An upstream branch, length 50,000 (m), located between the upstream boundary and the bifurcation node,
- A main channel, length 2,400 (m), and a secondary channel, length (2,940 (m), both located between the bifurcation and the confluence node,
- A downstream branch, length 50,000 (m) located between the adjoining node and the downstream boundary.

To ensure enough spatial resolution in the area of main interest, i.e. the main channel and the secondary channel, these channels are modelled with small grid cells of 100 (m) and 98 (m) respectively. Grid distances in the upstream and downstream branch vary between 100 (m) near the nodes connecting these branches with the main and secondary channel to 6,000 (m) near the model boundaries. This schematization results in 27 grid points in the upstream and downstream branch, 25 grid points in the main channel and 31 grid points in the secondary channel.

Initial bathymetry:

Since the aim of the study is to investigate the impact of parameter variations, i.e. a sensitivity analysis, the bathymetry schematisation is rather coarse. Rectangular cross-sections with a width of 260 (m) for the upstream branch, the downstream branch and the main channel are assumed. The secondary channel is modelled with a width of 55 (m).

A uniform bed slope of 0.00011 is assumed. This results in a difference of 11.264 m over the model (0,00011 * 102,400. m).

The bed level of the secondary channel is 3 m above the bed level of the main channel. The larger length of the secondary channel results in a bed level slope of the secondary channel equal to 2,400/2,940*0.00011.

Bed friction:

A uniform Chezy coefficient of 45 $m^{1/2}/s$ is used for the upstream branch, the main channel and the downstream branch. For the secondary channel a slightly smaller value of 40 $m^{1/2}/s$, indicating an larger roughness, is used.

Boundary conditions flow computation:

At the upstream boundary of the model a uniform discharge of 1600 m^3/s, bed forming discharge, is prescribed. The downstream, water level, boundary of the model uses the corresponding equilibrium water depth, i.e. 5.6184 (m), as boundary condition.

Numerical parameters flow computation:

The flow computation is a steady state computation. SOBEK utilizes a Preismann box scheme with 2 weight factors:

- ξ weight factor in space
- θ weight factor in time ($\theta=1$ represents a fully implicit scheme whereas $\theta=0$ represents a fully explicit scheme)

For the present computations the recommended values for these parameters are used, i.e. $\xi = 0.5$ and $\theta = 0.55$.

The maximum number of iterations to reach steady state was set to 7500.

The convergence criteria are set to 0.01 m for water levels (epsH) and 1.0 m^3/s for discharge (epsQ).

Sediment Transport:

SOBEK offers a number of transport formulae to be used for transport computations. Because the Meyer-Peter and Muller formula appeared to predict the transports in the river Waal, better than other formulae, this formula is used for the present computations.

The sediment properties are summarized below:

- relative density 1.65
- porosity of deposited sediment 0.4
- Main diameter of sediment 1.45 (mm)
- Grain size exceeded by 10% of the bed material (D_{90}) 3.75 (mm)

For the morphological computations the sediment transport rate at the upstream model boundary must be prescribed. A transport rate S equal to 400,160 m^3/year, corresponding with a discharge of 1600 m^3/s, a width of 260 (m) and a water depth of 5.61 (m) according to the Meyer-Peter and Muller formula is used as boundary condition.

Time frame:

The simulation period for the morphological computations is 25 years. A time step of 1 day is used for the morphological computations. This means that based upon the boundary conditions and the actual bathymetry a steady state flow computation is performed. Computed flow velocities and local water depths are used to compute the transports according to the Meyer-Peter and Muller formula. Computed transports are integrated over the morphological time step.

A new bathymetry schematization is computed using the continuity equation for sediment based upon differences in integrated transports. This new bathymetry is used in the next steady state flow computation.

Nodal point relation:

Equation (1) is used as nodal point relation at the bifurcation node, with k=2.5, j=-1.5. The relation between the discharge ratio and the sediment transport ratio is specified via a table in the input file.

Numerical parameters for morphology:

Sobek utilizes an explicit Lax-Wendroff type numerical scheme for the computation of bed level variations. The recommended value of 1.01 for the stability factor is used.

4.2 Results from Reference Case

The computed bed level changes along the main channel as well as along the secondary channel after 5, 10, 15, 20 and 25 year is shown in Figure 4.1. Note that the scales in the longitudinal direction are different for the different sections in order to make the figure more readable. The bed level change in the main channel is almost uniform in the longitudinal direction, which agrees with the assumption in the theoretical analysis in Chapter 3 that the bathymetry of a branch can be represented by a single depth value. In the secondary channel, on the other hand, the bed level change is clearly concentrated at the first part, which does not agree with this assumption. Nevertheless the results of the simulation do agree with the conclusions from the theoretical analysis (see Figure 3.7 and 3.11). It is clear that the secondary channel tends to close but the closure is slow and it becomes slower in the time. In the first short period rapid siltation occurs in the main channel. The bed level increase is almost 0.3 m after 5 years. After this period slow erosion occurs corresponding to the slow closure of the secondary channel.

In Figure 4.2 the relative discharge distribution is shown, which illustrates the same behaviour. Figures 4.3 and 4.4 show the bed level changes as function of time.

4.3 Influence of Time-Varying Boundary Condition

To investigate the influence of the variation in river discharge in time, a computation with time-varying boundary conditions is performed. The variation in boundary conditions is based upon a characteristic hydrologic year of the Rhine. In the table below, the used discharges at the upstream boundary and corresponding water levels at the downstream boundary and transport rates at the upstream boundary are given.

Tabel 4.1 Time-varying boundary condition

Month	Discharge (m^3/s)	Corresponding equilibrium water depth (m)	Corresponding transport rate (m^3/year)
January	1,950	6.4231	529,529
February	2,200	6.9703	618,308
March	1,875	6.2548	502,822
April	1,725	5.9117	449,343
May	1,600	5.6185	404,723
June	1,650	5.7366	422,571
July	1,600	5.6185	404,723
August	1,375	5.0717	324,431
September	1,075	4.2959	218,435
October	1,050	4.2283	209,714
November	1,575	5.5590	395,768
December	2,025	6.5895	556,204

The results of the run with time-varying discharge and sediment transport at the upstream boundary are shown in Figures 4.5 through 4.8.

Figure 4.5 shows the bed level change after 5, 10, 15 20 and 25 year. It seems strange that there is a wave in the bed of the main channel which remains at the same place all the time. However, this is only because the output is made at the same date in the corresponding year (1st of January). Figure 4.6 and 4.7 show that the bed level variation in the main channel is dominated by a wave with the period of one year. Besides this periodic variation there is a rapid siltation in the first period and slow erosion thereafter, the same behaviour as in the reference case. The bed level change in the secondary channel also shows a wave character. However, it is not clear here if it is a physical wave or numerical wave.

The averaged bed level changes in the main channel and in the secondary channel are about the same as in the reference case. However, because of the dominating wave character of the changes it is important to take the time variation of the discharge into account in a morphological prediction. The critical bed level change e.g. for the navigation may be seriously underestimated if this is not taken into account.

The importance of the time-varying discharge may be explained by the fact that there are two time scales for the morphological development of the system and one of them has the order of magnitude of a year.

4.4 Influence of Nodal Point Relation

The power in the nodal point relation largely determines the model behaviour. To examine the influence of the coefficient k, Two computations respectively with a value of 5 and 10 instead of 2.5 (reference case) for k are carried out.

The computed bed level change with k=5 is shown if Figure 4.9. It is observed that the secondary channel still tends to be closed but the closure is much slower than in the reference case. The siltation of the main channel in the first period is more rapid than in the reference case. All these observations agree well with the conclusions of the theoretical analysis (See Figures 3.8 and 3.11).

Figure 4.10, 4.11 and 4.12 show the discharge ratio, the bed level change in the two branches as function of time.

According to Figure 3.8 the situation that both channels remain open becomes stable for k=5. However, the secondary channel is not deep enough at the start of the simulation in order to reach this equilibrium. In order to verify the conclusion of the theoretical analysis an extra computation is carried out with the same input but then with a bed level of the secondary channel equal to that of the main channel at both nodes. The results are shown in Figure 4.13. It is clear that the system tends to develop to the situation that both channels remain open.

For k=10 the effect becomes even stronger (Figure 4.14). Now there is no siltation any more in the secondary channel. This is only because that the sediment input to the secondary channel according to the nodal point relation (1) now is smaller than the smallest number that the computer can still handle. In fact the secondary channel will still be silted up but the siltation is then very slow.

4.5 Influence of the Size of Secondary Channel

The width of the secondary channel, 55 (m) in the reference situation, induces a discharge through this channel equal to 5% of the total discharges. To examine the influence of the width of this channel, a computation with a doubled width, 110 (m), is performed.

The computed bed level change is shown in Figure 4.15. The basic behaviour of the system is the same as in the reference case. Only the impact of the secondary channel on the main channel is now stronger. The siltation in the first period is now about two times of that in the reference case. The bed level change in the secondary channel remains about the same but the total siltation volume is about doubled of course. See also Figures 4.16, 4.17 and 4.18.

4.6 Influence of Sediment Transport Rate

To examine the influence of transport rate, two computations are performed with respectively a decrease (300,000 m3/year) and an increase (450,000 m^3/year) of the sediment transport.

The computed transport in the all branches is multiplied by a factor (e.g. for the decrease case 300,000/400,000 = 0.75).

The results of the two computations are shown in Figures 4.19 through 4.26. Both computations show similar results as the reference case. The decreased sediment transport leads to slower siltation in the secondary channel (Figure 4.19), in the sense that the height of the bar is smaller (whereas the length of the bar is almost the same).

The increased sediment transport causes stronger siltation in the secondary channel (Figure 4.23).

4.7 Influence of Grain Size in Secondary Channel

To examine the influence of the grain size in the secondary channel, assumed to be equal to that in the main channel for the reference case, two computations are performed, one with a halved grain size in the secondary channel:

- mean diameter 0.000725 m,
- D_{90} = 0.001815 m;

and the other with a doubled grain size in the secondary channel:

- mean diameter 0.00290 m,
- D_{90} = 0.00726 m.

The results from the computations are shown in Figure 4.27 through 4.34.

For the increased grain size the behaviour of the system remains the same as the reference case, but the siltation in the secondary channel is now more concentrated in the first part of the channel (Figure 4.31).

For the decreased grain size the behaviour of the system is totally different: the secondary channel tends to remain open now (Figure 4.27). This behaviour is already expected on the basis of Figure 3.15. The simulation time was not long enough to show that the stable equilibrium with both channels open as shown in Figure 3.15 is indeed reached.

4.8 Influence of the Roughness of Secondary Channel

The Chézy coefficient in the reference case is 40 $m^{1/2}$/s. Due to grow of vegetation in the secondary channel the roughness will tend to increase in time. To examine the influence of enlarged friction a computation with increased roughness (C=25 $m^{1/2}$/s) has been performed. The results of the computation are shown in Figures 4.35 through Figure 4.38.

The difference with the reference case is mainly caused by the fact that now less water is distributed to the secondary channel (Figure 4.36). This means that the influence of the secondary channel on the main channel is now smaller. The flow velocity in the secondary channel is now much smaller which explains that the siltation in the secondary channel is more concentrated in the first part.

5 Conclusions

Theoretical analysis and numerical simulations have been carried out on the morphological development induced by secondary channels along the Rhine branches in The Netherlands. The secondary channel designed at Stiftse Waard is used as reference in the study. The main findings, especially the aspects which are important for the design of the secondary channel, are summarised in the following.

- The nodal-point relation (1) is model-technically as well as physically preferable to other relations proposed in the literature. The coefficient in the relation vary from case to case. Therefore the nodal-point relation remains the most uncertain factor in the study on the secondary channel system. Sensitivity analysis on this parameter is necessary when a secondary channel is designed.

- Despite of the uncertainty with respect to the sediment distribution into the secondary channel it is quite certain that the secondary channel tends to be closed. Only in the case that the bottom of the secondary channel is considerably finer than the main channel it is possible that the secondary channel remains open. Therefore maintenance dredging will probably be needed after the construction of the secondary channel. This must be kept in mind during the design phase.

- The morphological development induced by the construction of the secondary channel is characterized by two time scales: a short one having a magnitude of the order a year, and a long one which is orders larger. The development corresponding to the short time scale is the rapid siltation of the main channel. The development corresponding to the long time scale is the siltation of the secondary channel and the restoration of the original bed level in the main channel after the rapid siltation. However, if maintenance dredging is carried out the development corresponding to the long time scale will be compensated. This means that the bed level increase in the main channel will remain there, which may cause problems for navigation.

- Due to the fact that one of the time scales of the system is in the order of magnitude of a year the time-varying discharge (seasonal variation) is very important. Morphological evaluation of a design of a secondary channel has to be carried out with time-varying discharge. Otherwise the siltation problem in the main channel will be seriously under estimated.

- Another sensitive parameter is the grain size in the secondary channel. If the bed material of the secondary channel is much finer than that in the Waal river the behaviour can be totally different. The secondary channel then tends to be eroded and serious siltation problem in the main channel can occur. Therefore special attention should be paid to the bed material of the secondary channel during the design phase. If it is considerably finer than the material in the Waal extended research should be carried out on the morphological development.

- The analytical model set-up in the present study appears to be very effective for investigating the behaviour of the system. Up to now all the conclusions from the analytical model agree with the results from the numerical simulations with SOBEK. It is noted that an application of the analytical model can be done within a minute on a PC whereas a

run with the SOBEK model takes hours on a workstation. Therefor the analytical model is recommended as a tool for designing secondary channels.

References

Akkerman G.J. (1993) Zandverdeling bij splitsingspunten, Literatuurinventarisatie voor inlaten van nevengeulen, DELFT HYDRAULICS, Report Q 1573.

Busnelli M.M. (1994), Further normalisation Middenwaal and opportunities for nature restoration, M.Sc. Thesis H.H. 212, IHE.

Dekker P. den and J.M. van Voorthuizen (1994), Research on the morphological behaviour of bifurcations in rivers, M-Sc Thesis, Delft University of Technology, the Netherlands, 1994.

Fokkink R.J. and Z.B. Wang (1993), Study on fundamental aspects of 1D-network morphodynamic models, Delft Hydraulics, report Z654, 1993.

Fokkink R.J. (1994), Theoretical study of nodal point relations for suspended sediment transport, DELFT HYDRAULICS, Report Z 855.

Kamphuis H. (1990), Sediment-transportmetingen Rijntakken, Nota nr. 90.075, Rijkswaterstaat, RIZA.

Schropp M.H.I. (1991), Morfologische aspecten bij het ontwerpen van nevengeulen, Rijkswaterstaat, RIZA, Nota nr. 91.002.

Schropp M.H.I. (1994), Een ontwerp voor een nevengeul in de Stiftse Waard, Nota in voorbereiding, Rijkswaterstaat, RIZA.

Wang Z.B., Fokkink, R.J. and B. Karssen (1993), Theoretical analysis on nodal point relations in 1D network morphodynamic model, DELFT HYDRAULICS, Report Z473.

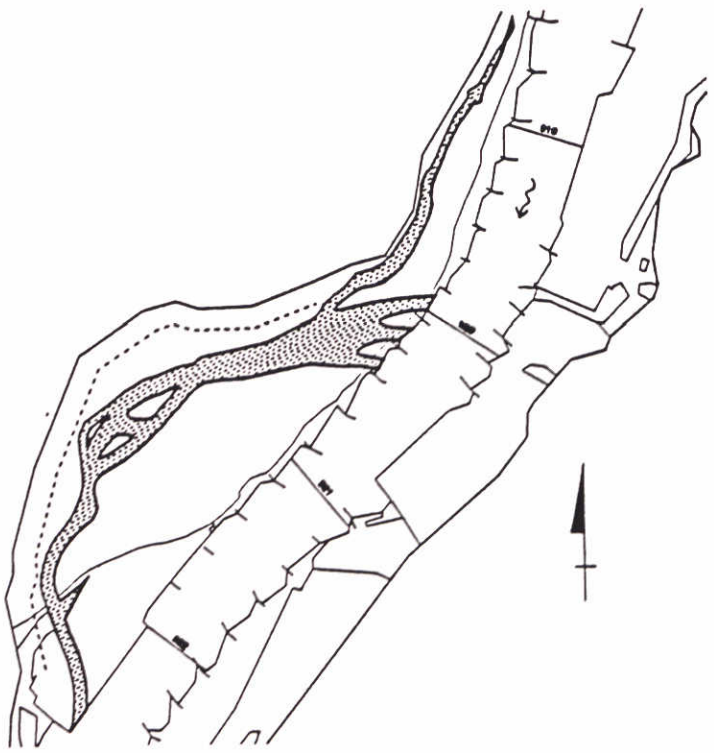

Design of the secondary channel at Stiftse Waard
After Schropp (1994)

1994-11-01

DELFT HYDRAULICS

Fig.2.1

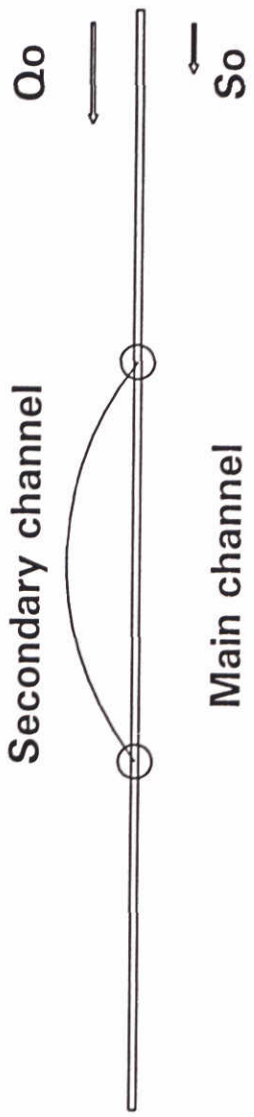

Schematised main and secondary channel system		1994-11-01
DELFT HYDRAULICS		Fig.2.2

Schematised hydrograph of the Waal river

DELFT HYDRAULICS

Fig.2.3

DELFT HYDRAULICS

Determination of the nodal point relation
Using data collected by Akkerman [1993]
Regression using power-relation

Fig.3.1

1994-11-01

Noal Point Relation
Pannerdens Channel

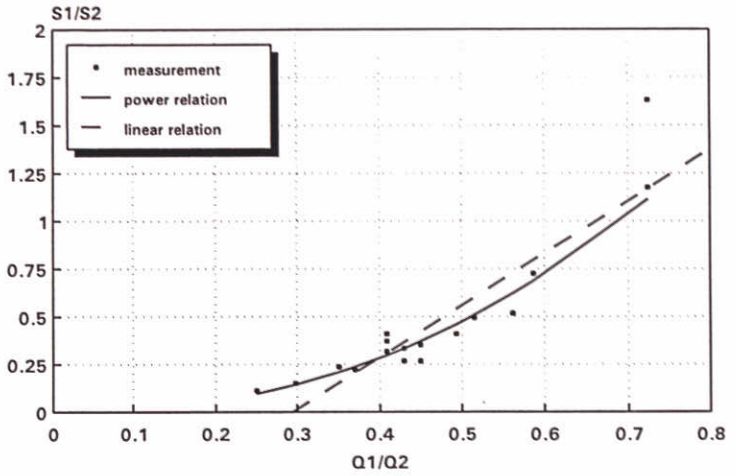

Nodal Point Relation
Bifurcation Westervoort

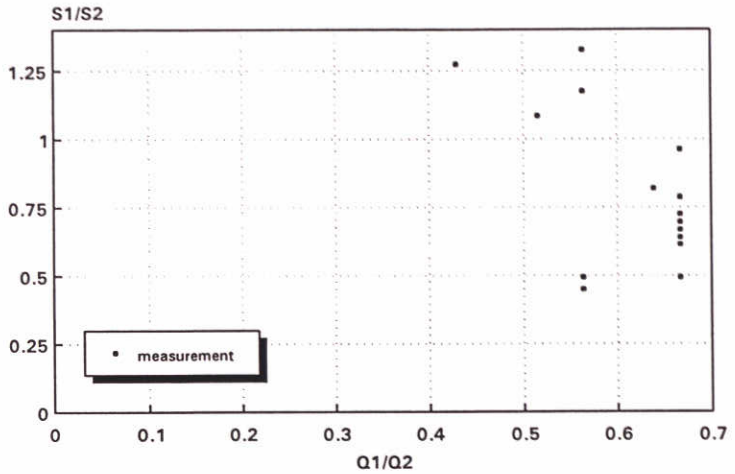

Nodal Point Relation
Jonglei Channel

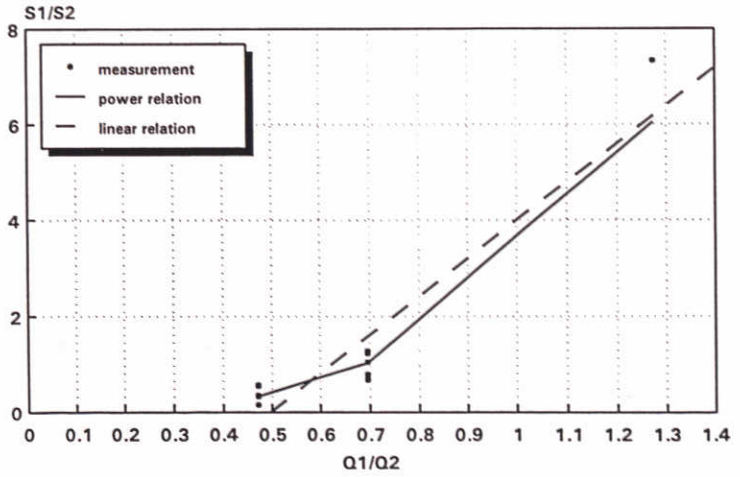

Pannerden
measured sediment distribution

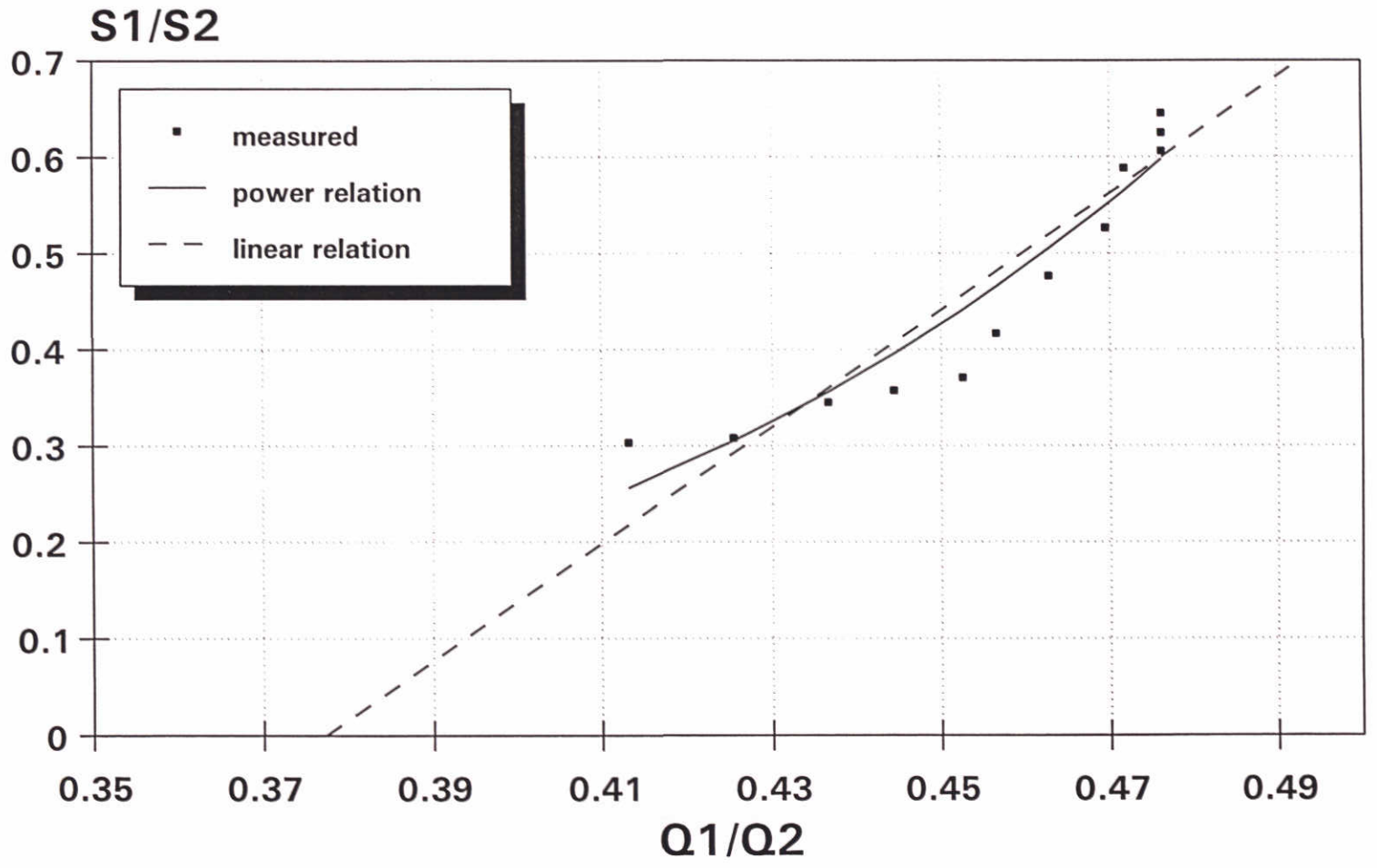

DELFT HYDRAULICS

Determination of the nodal point relation
Using proto-type data Pannerdens Channel
Regression using power-relation

Fig.3.2

1994-11-01

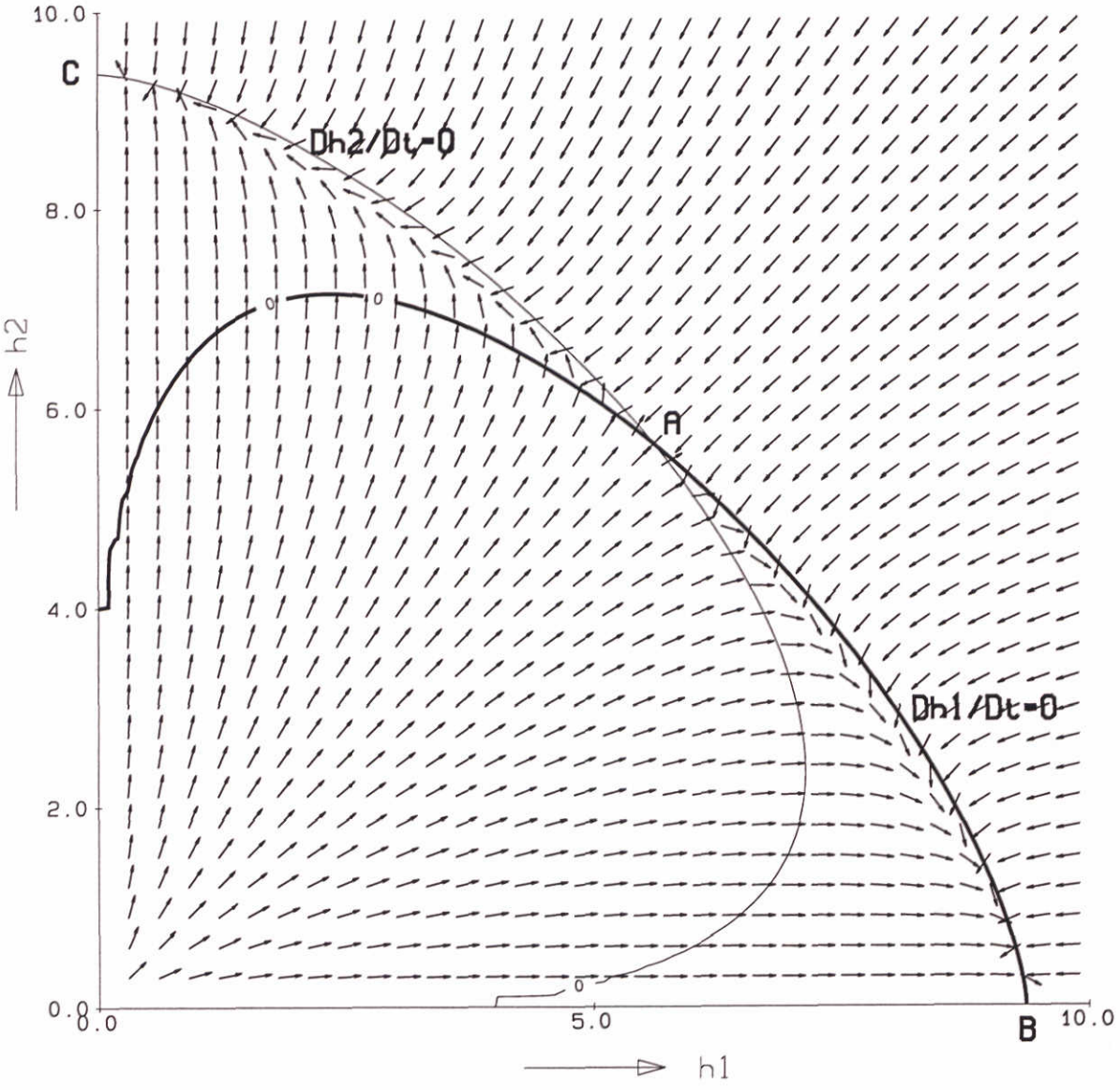

Equilibrium states and their stability Symmetric case k = 1		1994-11-01
DELFT HYDRAULICS		Fig.3.3

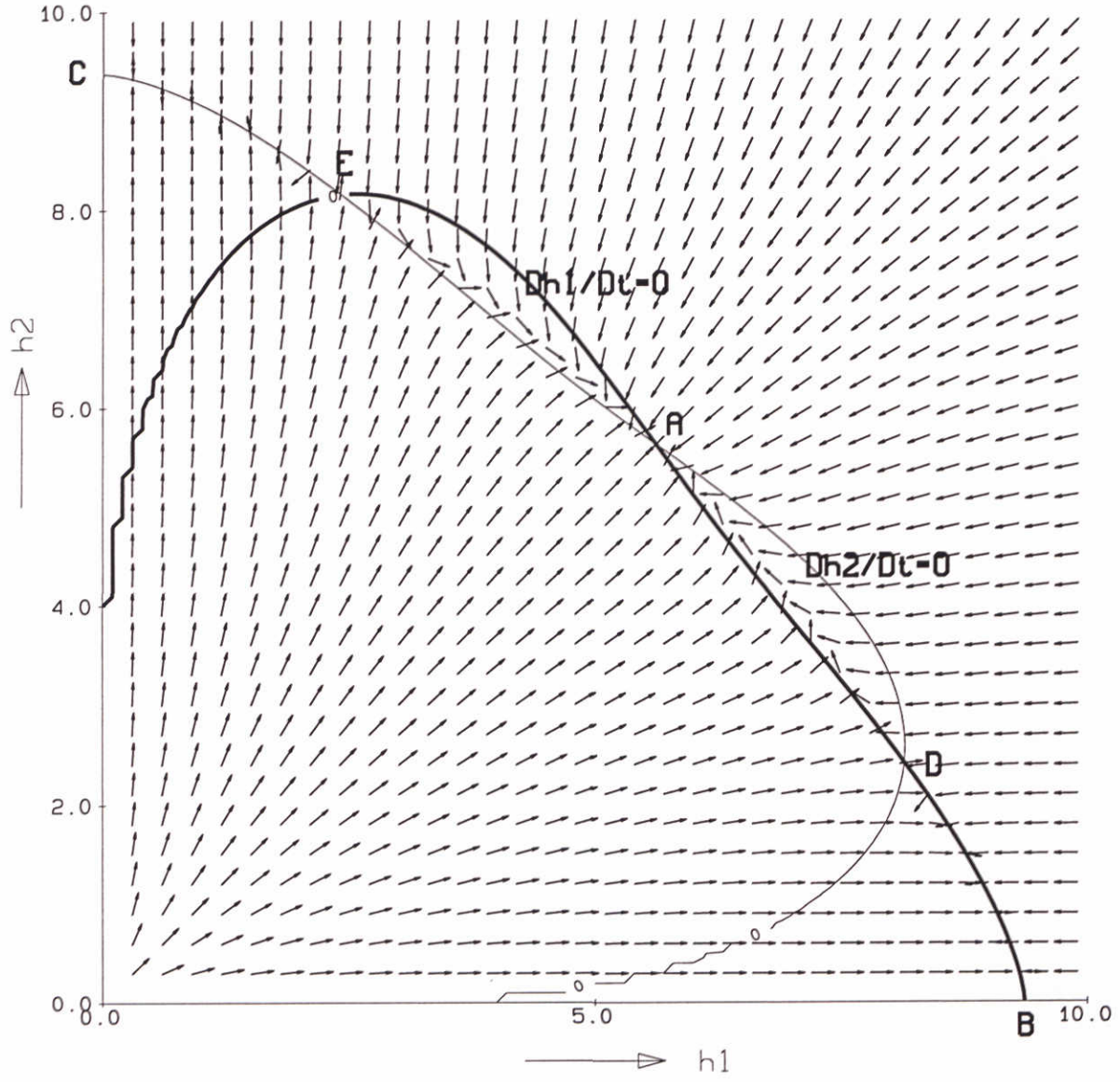

Equilibrium states and their stability Symmetric case k = 2		1994-11-01
DELFT HYDRAULICS		Fig.3.4

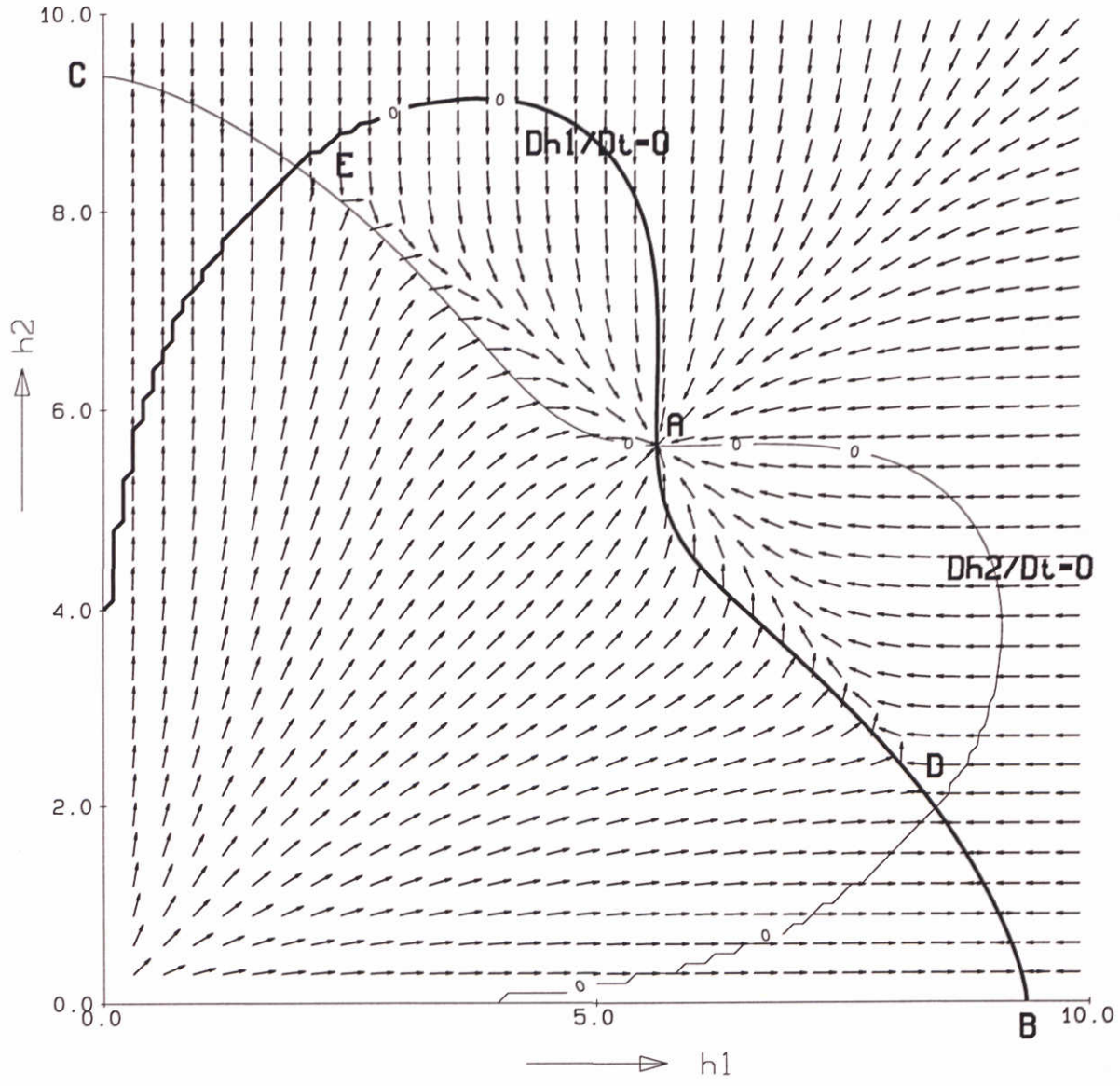

Equilibrium states and their stability
Symmetric case
k = 5

1994-11-01

DELFT HYDRAULICS

Fig.3.5

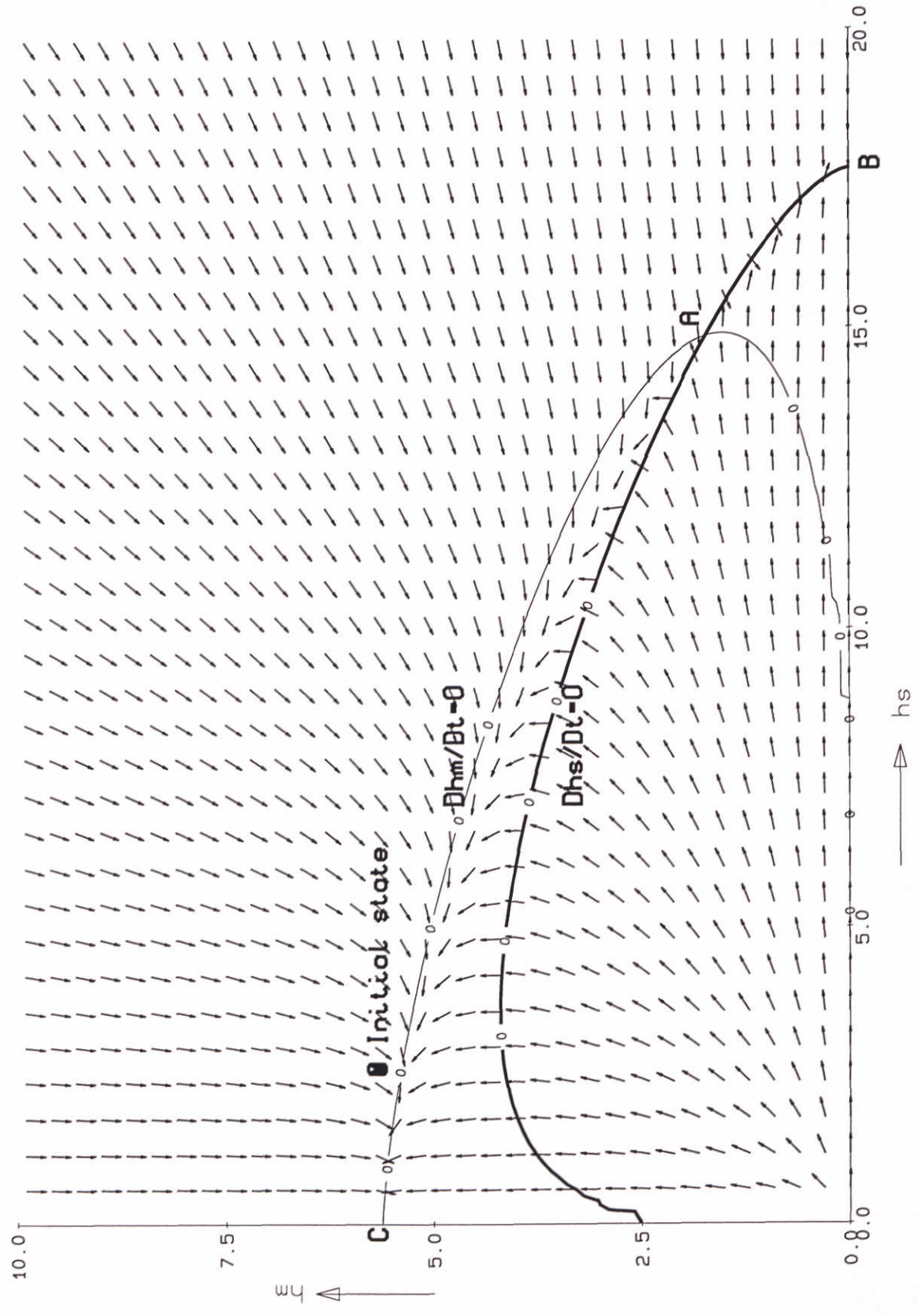

Equilibrium states and their stability
Secondary channel case
k = 1

1994-11-01

DELFT HYDRAULICS

Fig.3.6

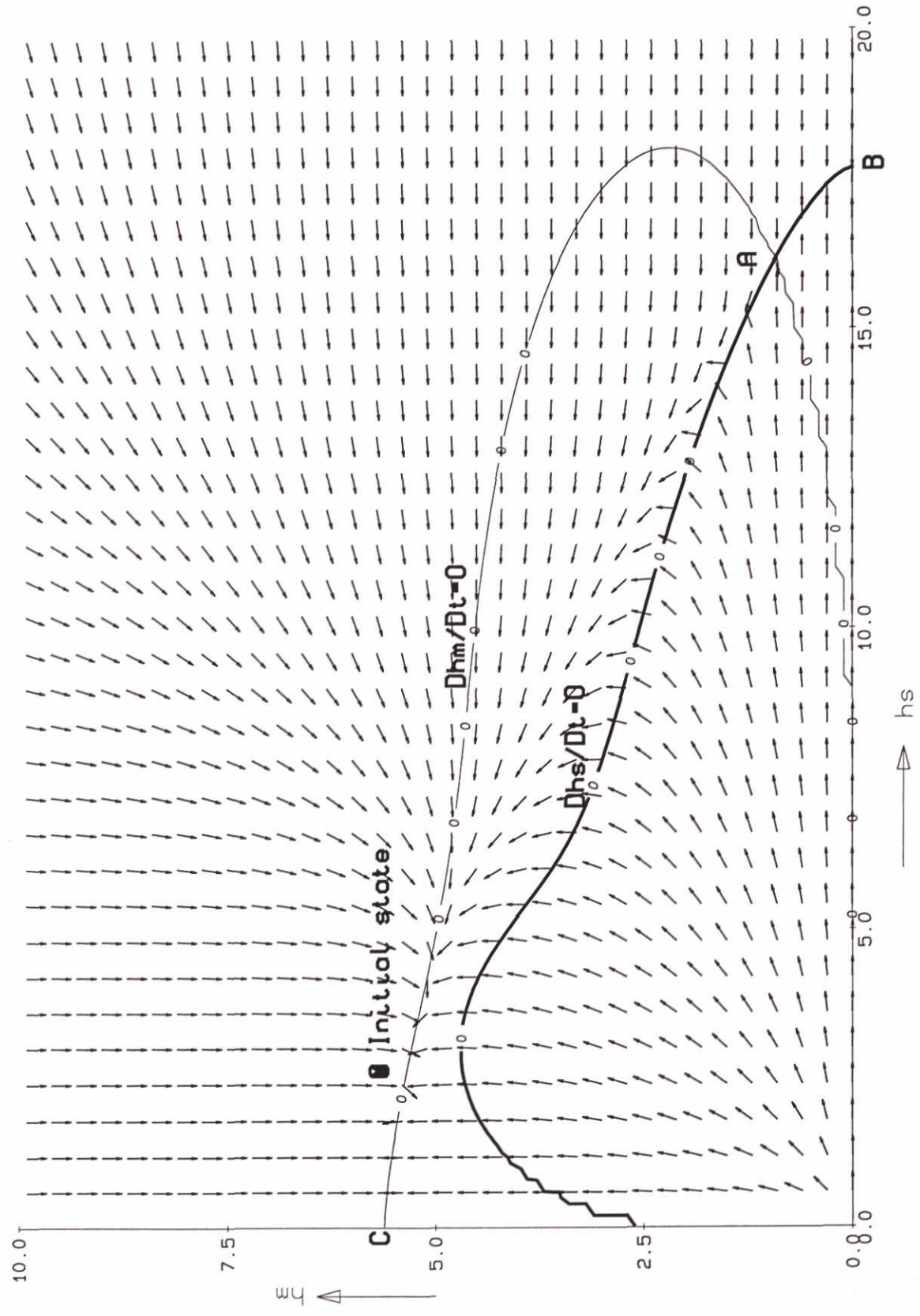

Equilibrium states and their stability
Secondary channel case
k = 2.5

1994-11-01

DELFT HYDRAULICS

Fig.3.7

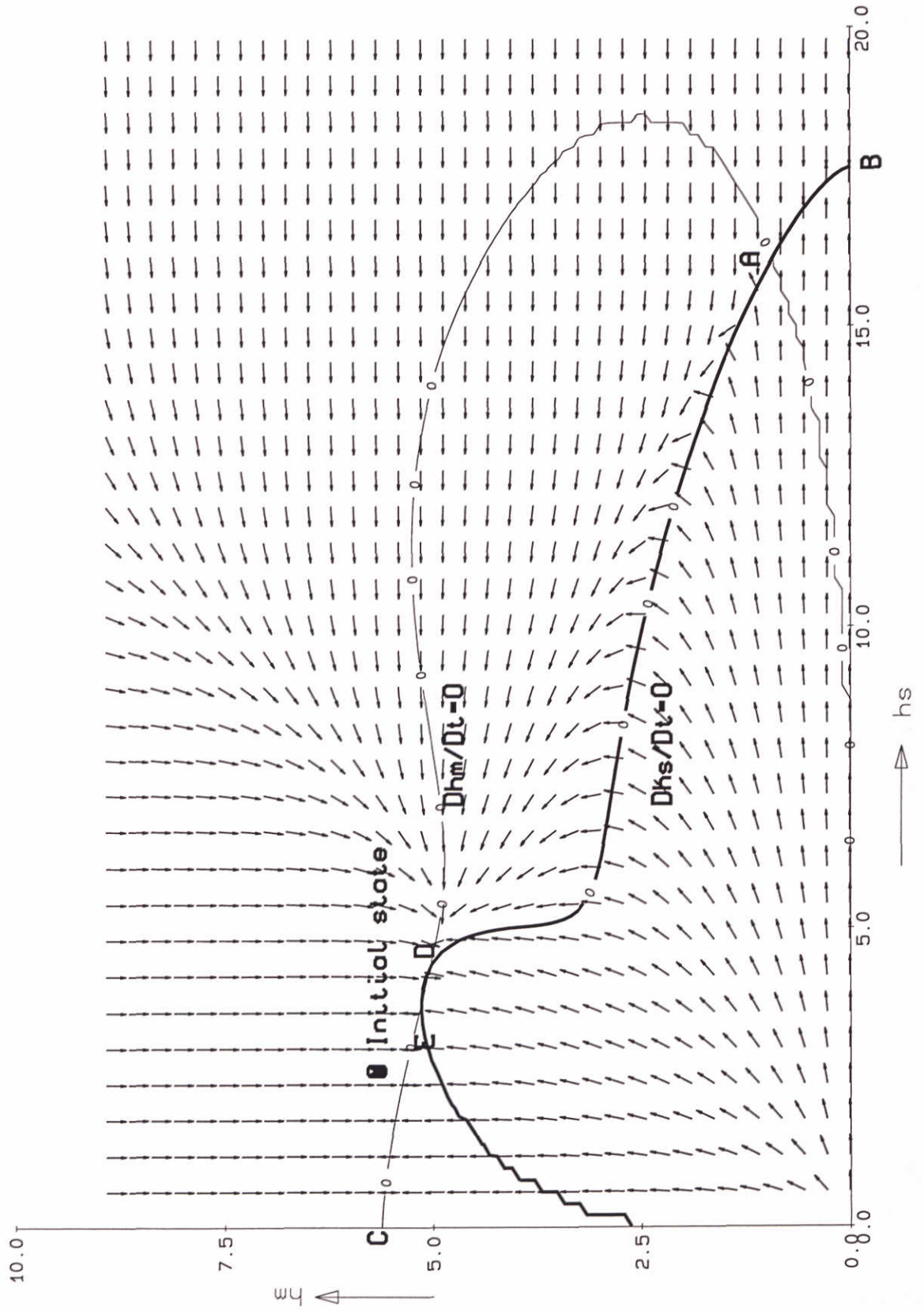

Equilibrium states and their stability
Secondary channel case
k = 5.0

1994-11-01

DELFT HYDRAULICS

Fig.3.8

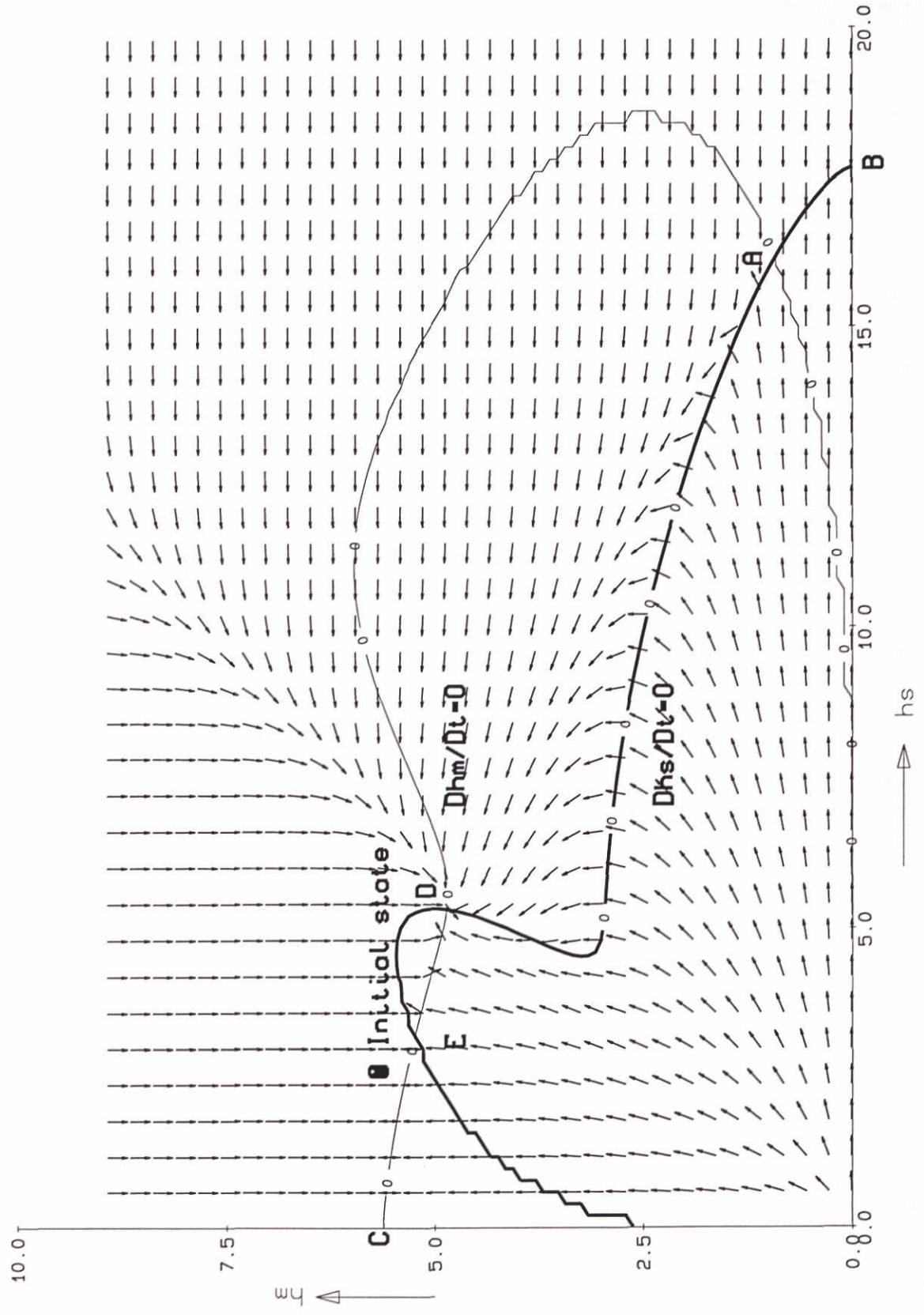

Equilibrium states and their stability
Secondary channel case
k = 10.0

1994-11-01

DELFT HYDRAULICS

Fig.3.9

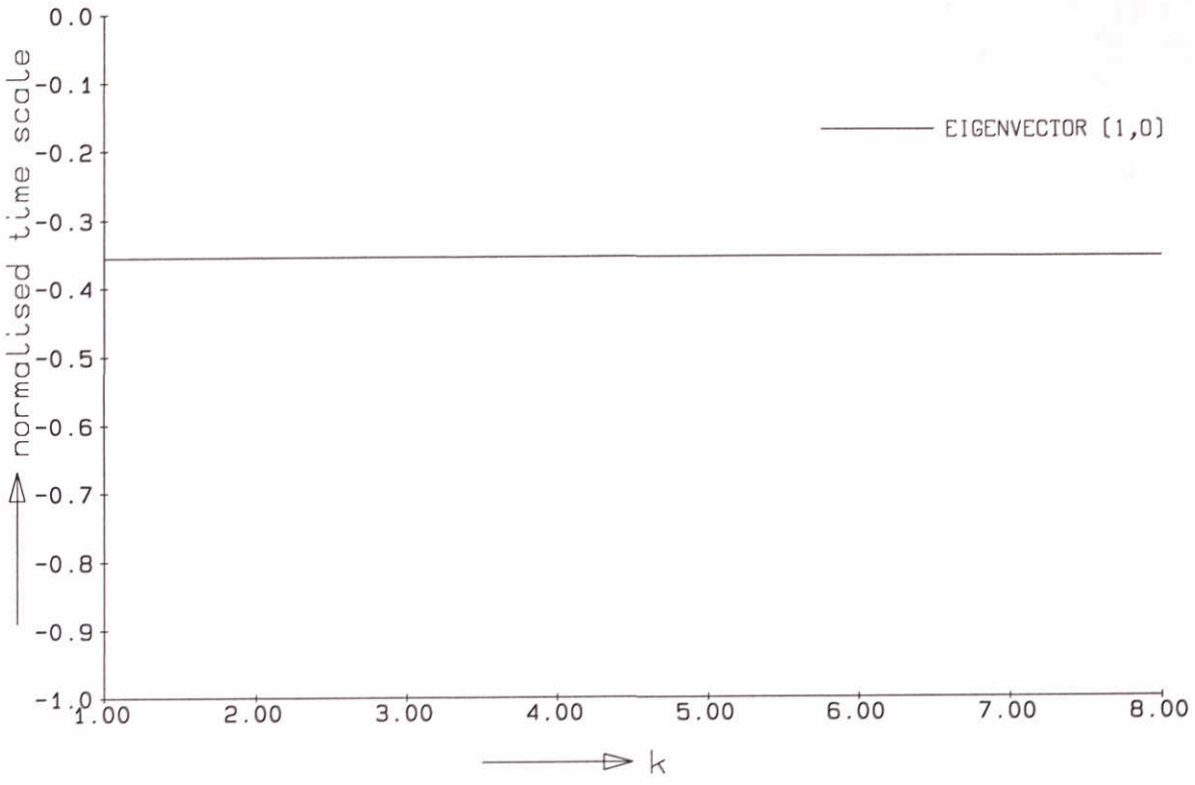

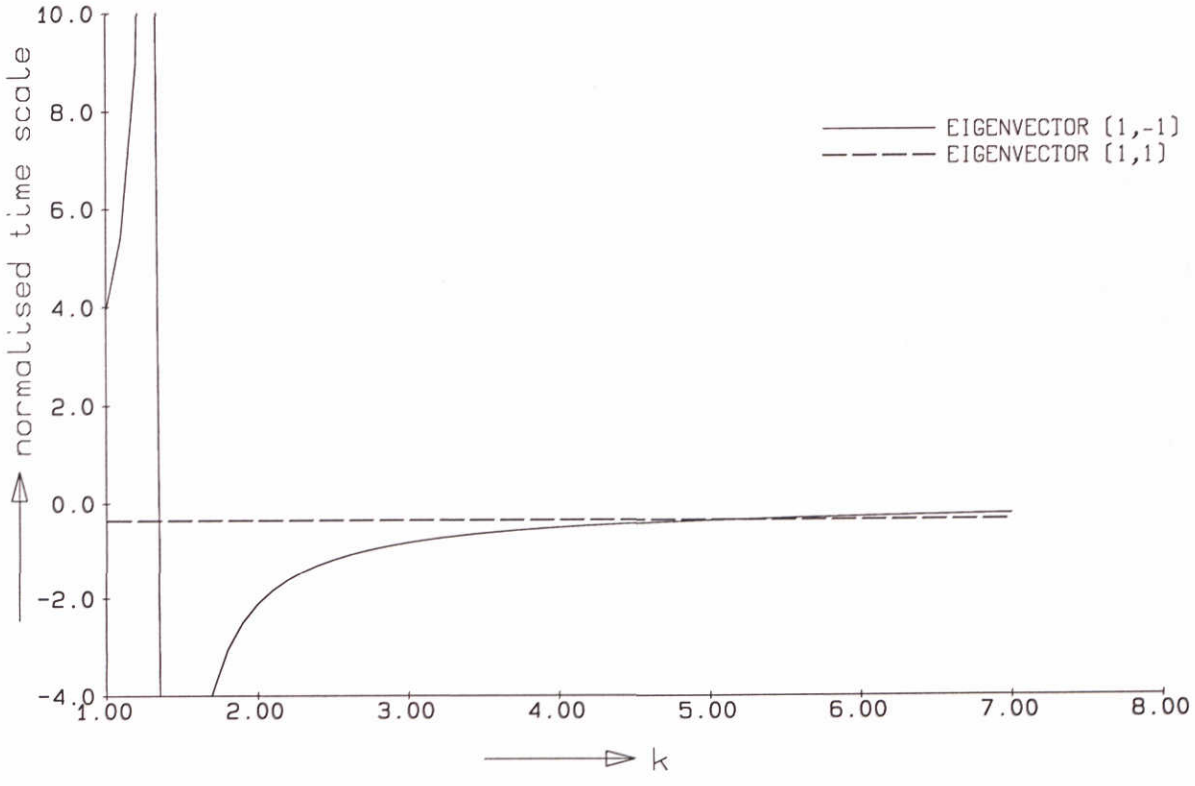

Time scale for the symmetric case as function of k
normalised with B1.L1.H1/S0
Top: with one branch open, Bottom: two branches open

1994-11-01

DELFT HYDRAULICS

Fig.3.10

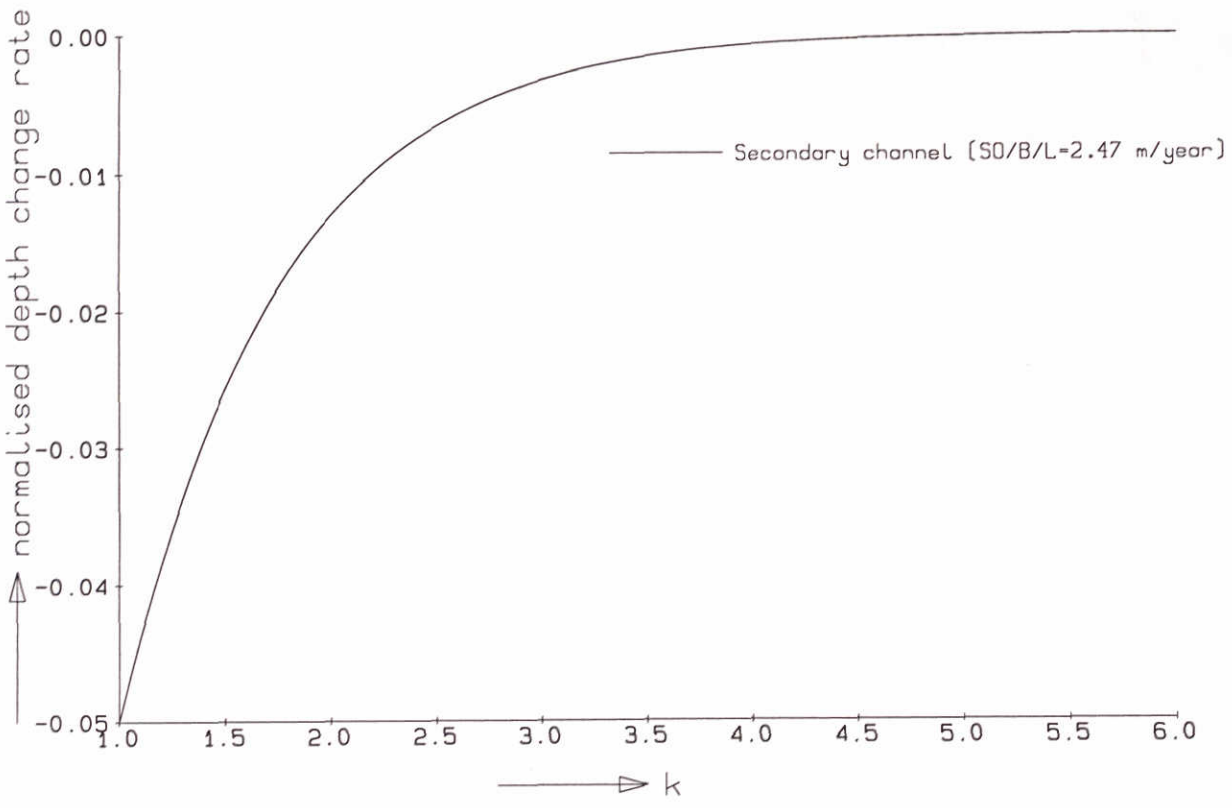

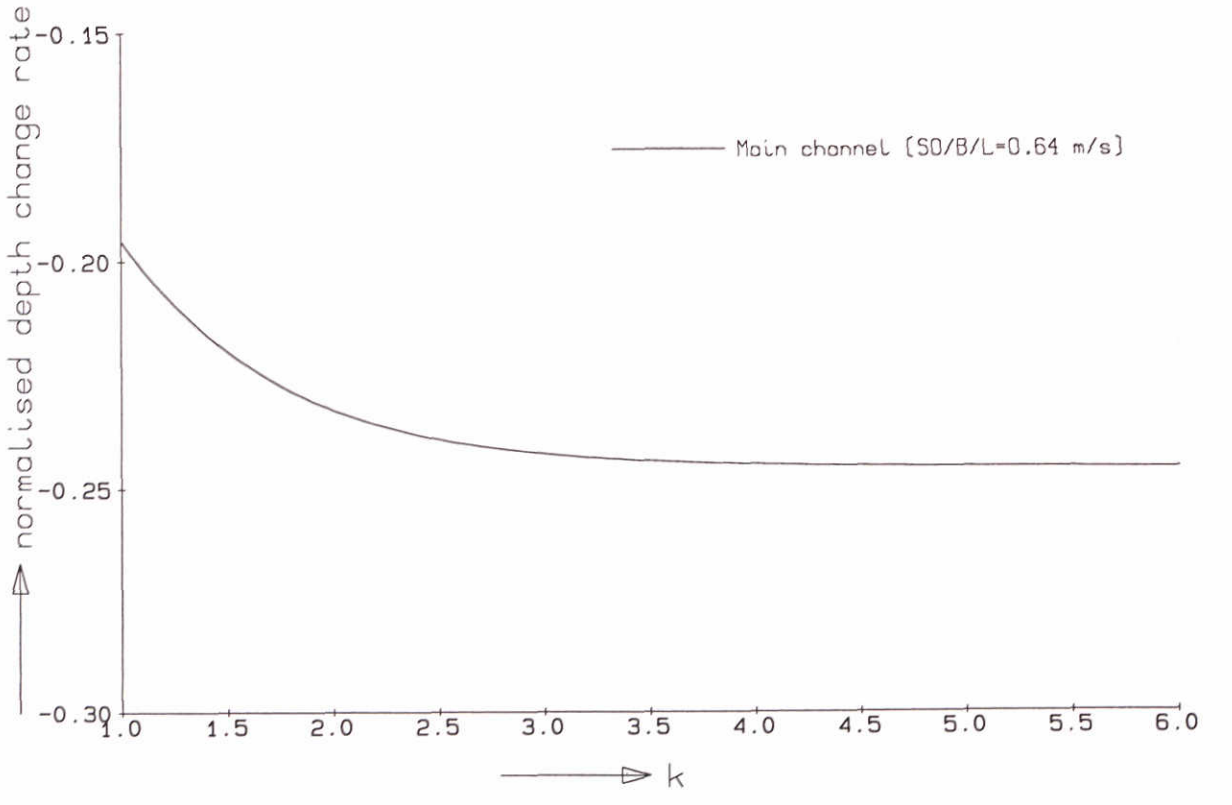

Initial depth change rate as function of k
normalised with S0/B/L
Secondary channel Stiftse Waard

DELFT HYDRAULICS

Fig.3.11

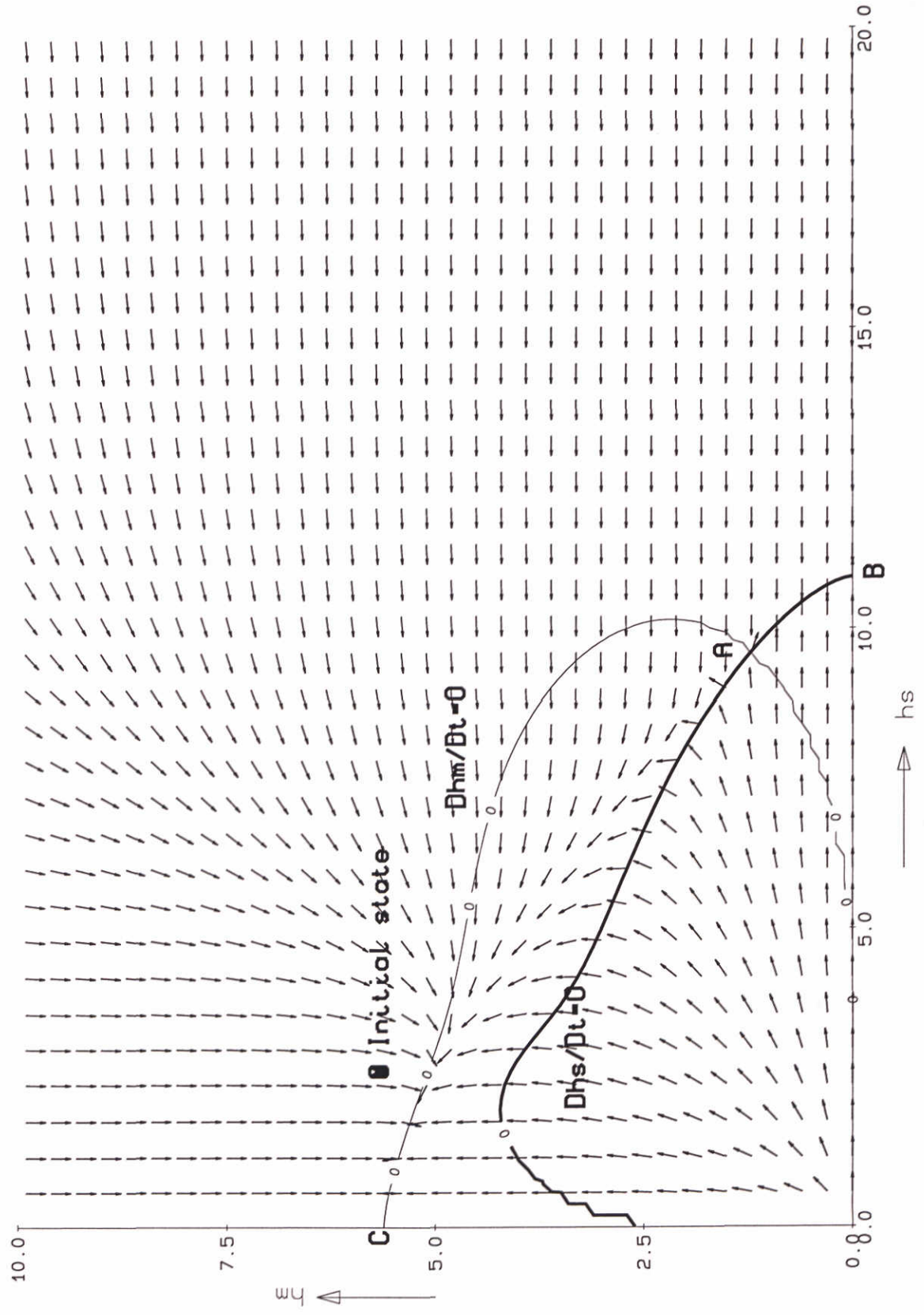

Equilibrium states and their stability
Width of the secondary channel doubled
k = 2.5

1994-11-01

DELFT HYDRAULICS

Fig.3.12

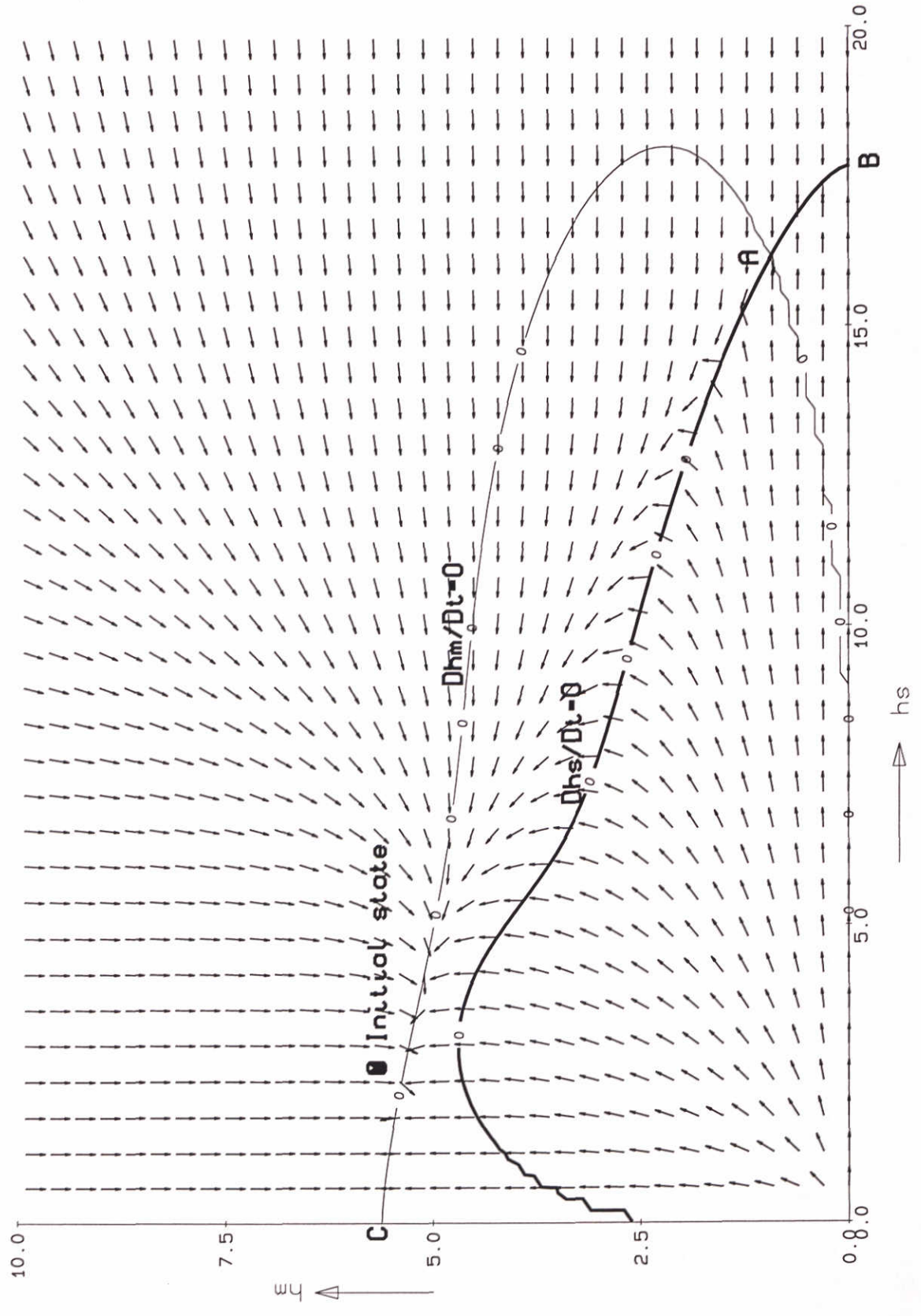

Equilibrium states and their stability
Decreased sediment transport
k = 2.5

1994-11-01

DELFT HYDRAULICS

Fig.3.13

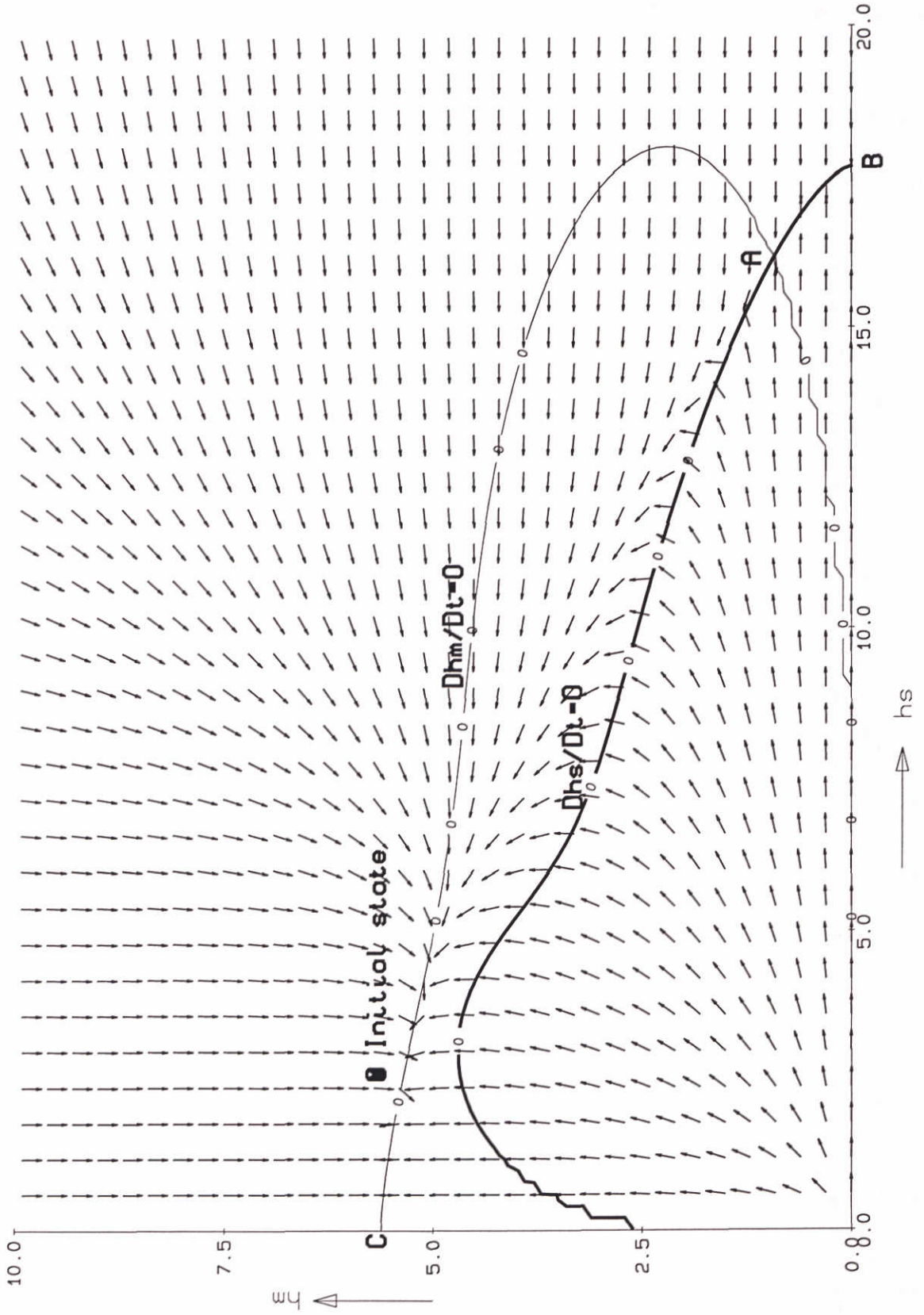

Equilibrium states and their stability
Increased sediment transport
k = 2.5

1994-11-01

DELFT HYDRAULICS

Fig.3.14

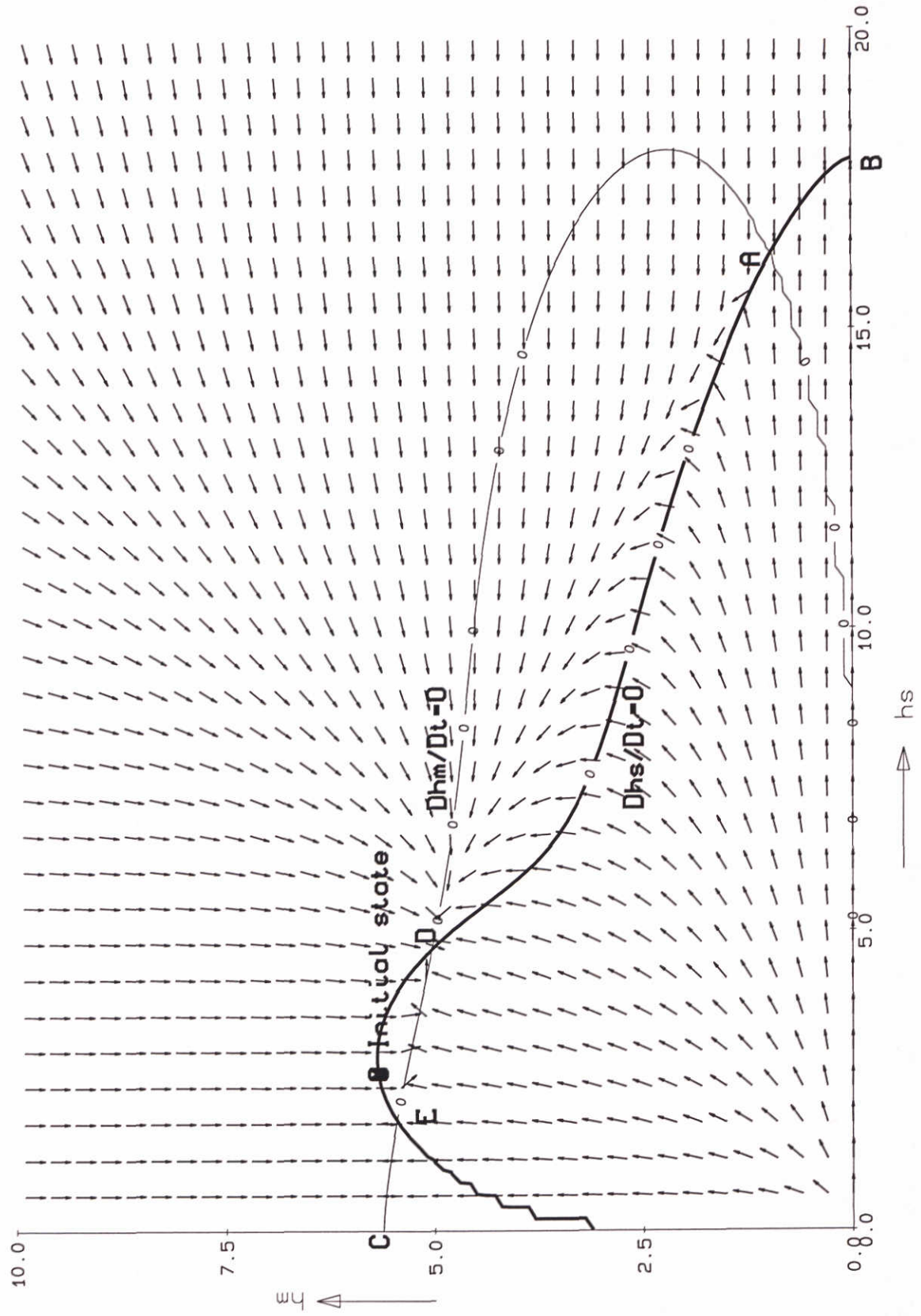

Equilibrium states and their stability
Grain size in the secdary channel halved
k = 2.5

1994-11-01

DELFT HYDRAULICS

Fig.3.15

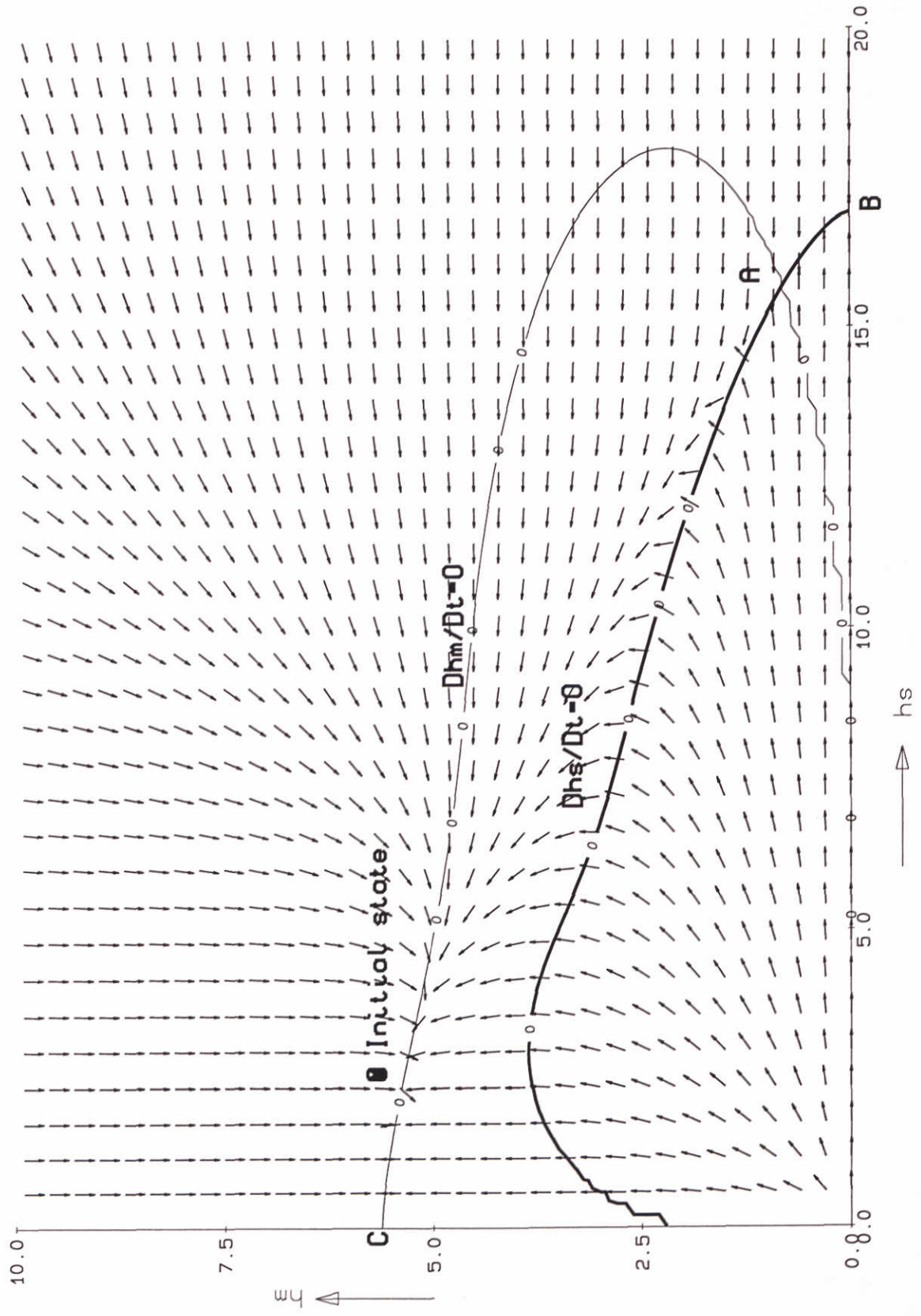

Equilibrium states and their stability
Grain size in the secdary channel doubled
k = 2.5

1994-11-01

DELFT HYDRAULICS

Fig.3.16

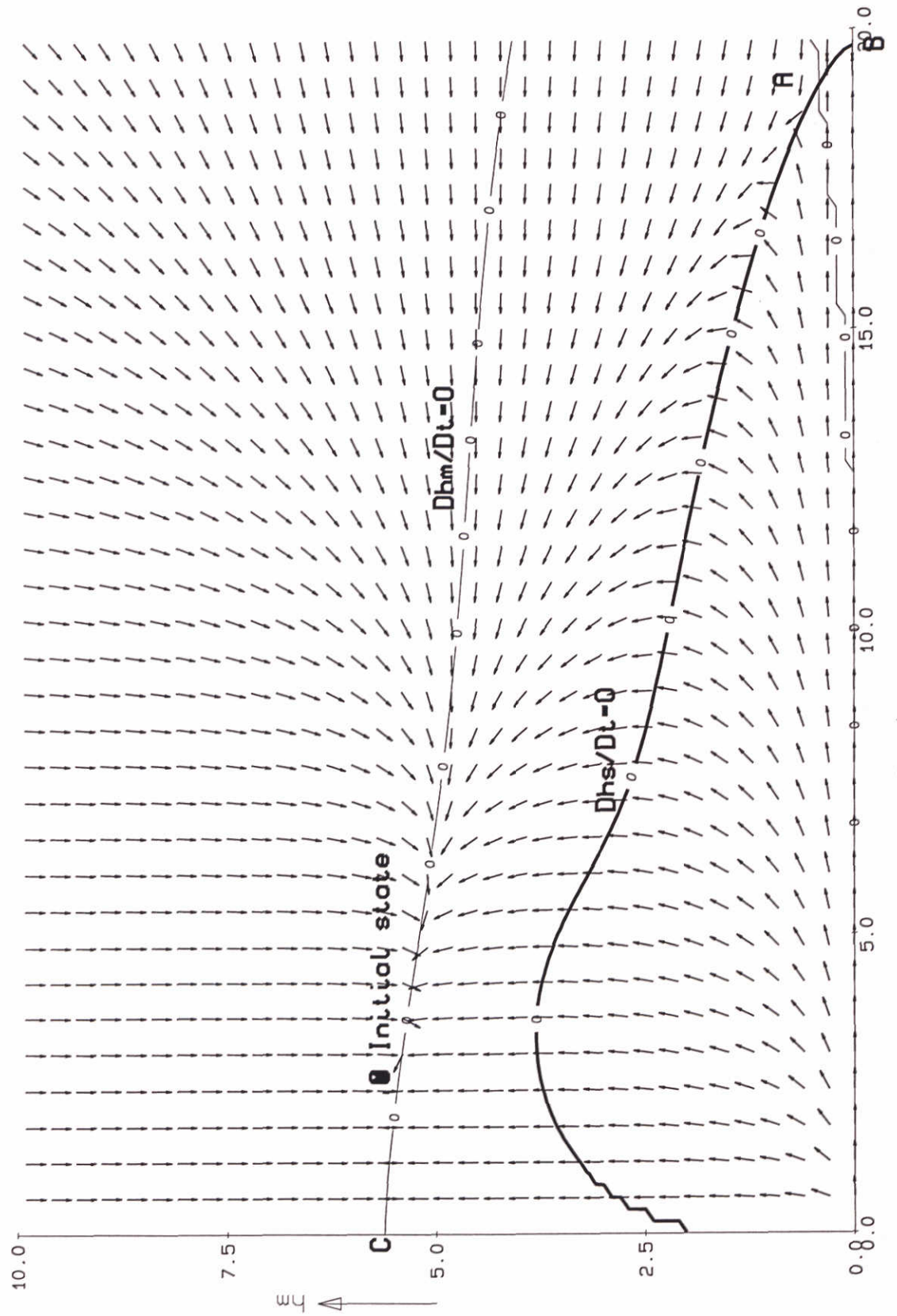

Equilibrium states and their stability
Smaller Chezy coefficient
k = 2.5

1994-11-01

DELFT HYDRAULICS

Fig.3.17

DELFT HYDRAULICS

Bed level differences reference case
Discharge 1600 m^3/s
Water depth approximately 5.61 m

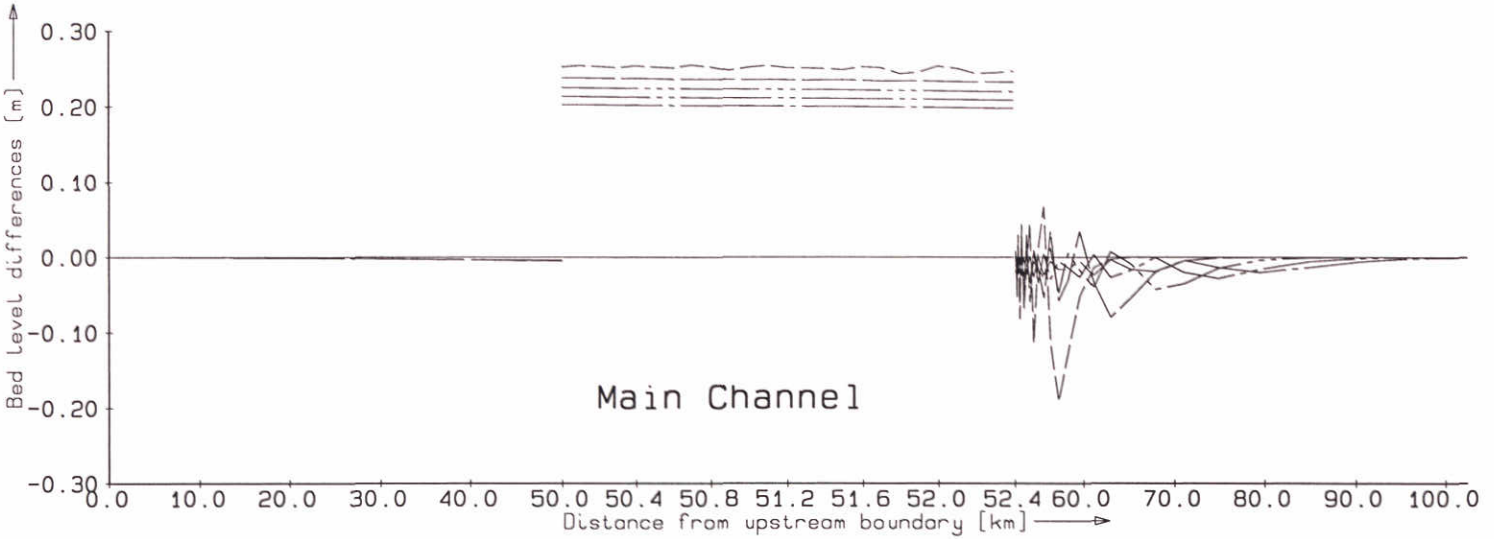

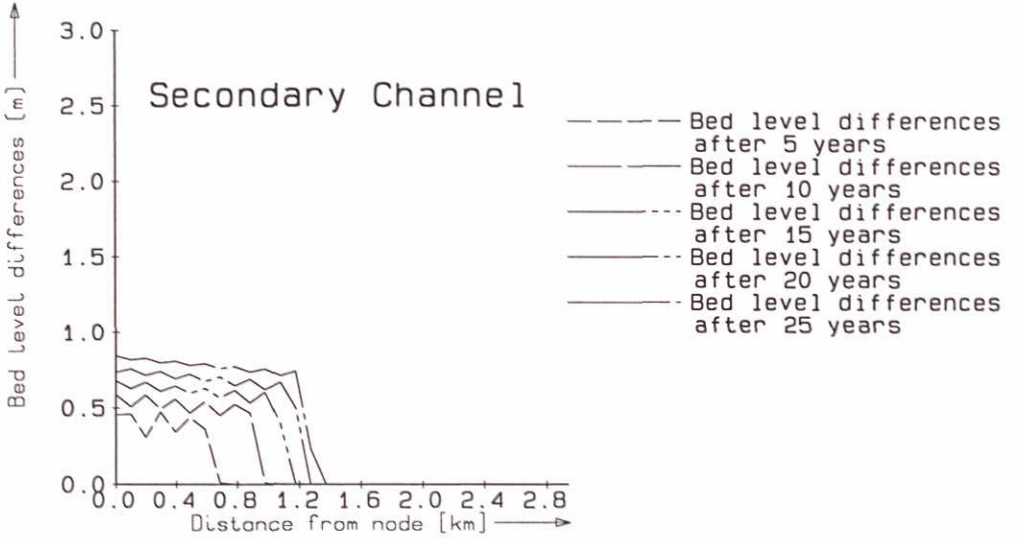

Q-1963

Fig. 4.1

Relative discharge through main channel

DELFT HYDRAULICS

Q-1963

Fig. 4.2

Bed level differences
Upstream node secondary channel

DELFT HYDRAULICS

Q-1963

Fig. 4.3

Bed level differences
Upstream node main channel

DELFT HYDRAULICS

Q-1963

Fig. 4.4

DELFT HYDRAULICS

Bed level differences case 001
Time varying boundary conditions

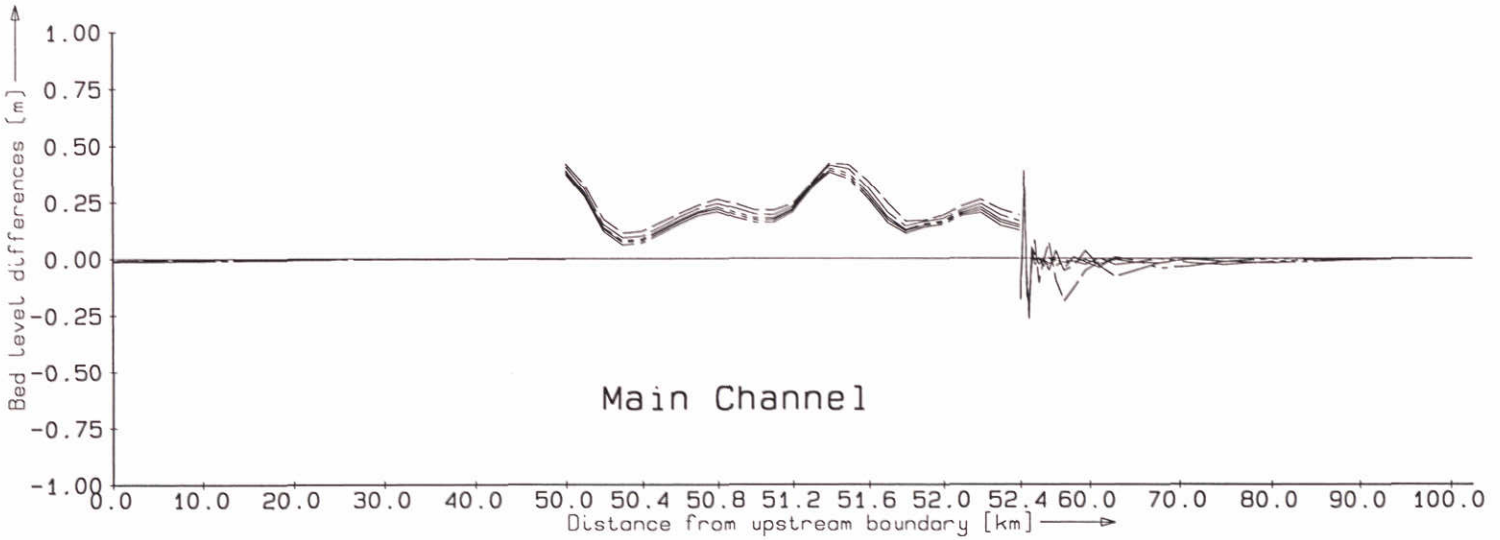

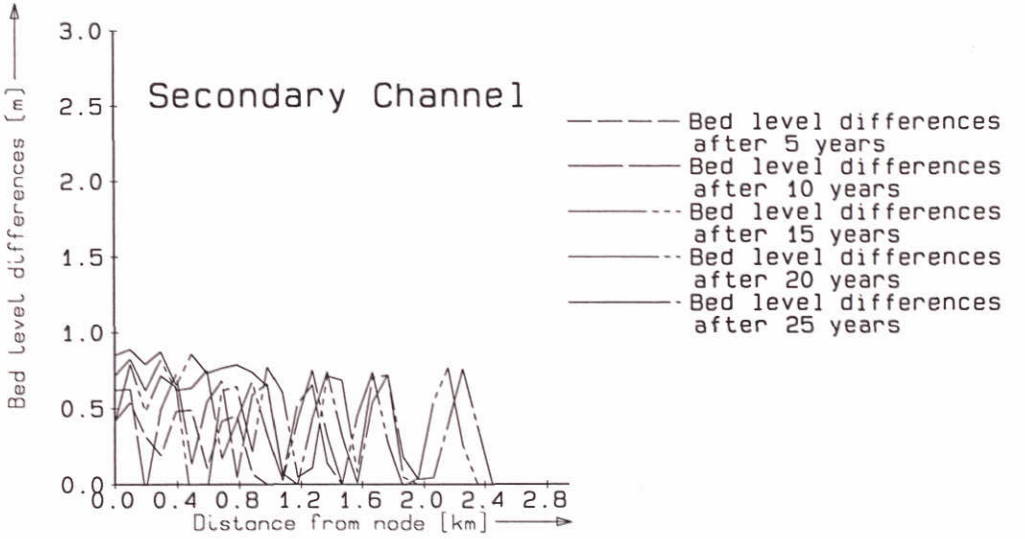

Q-1963

Fig. 4.5

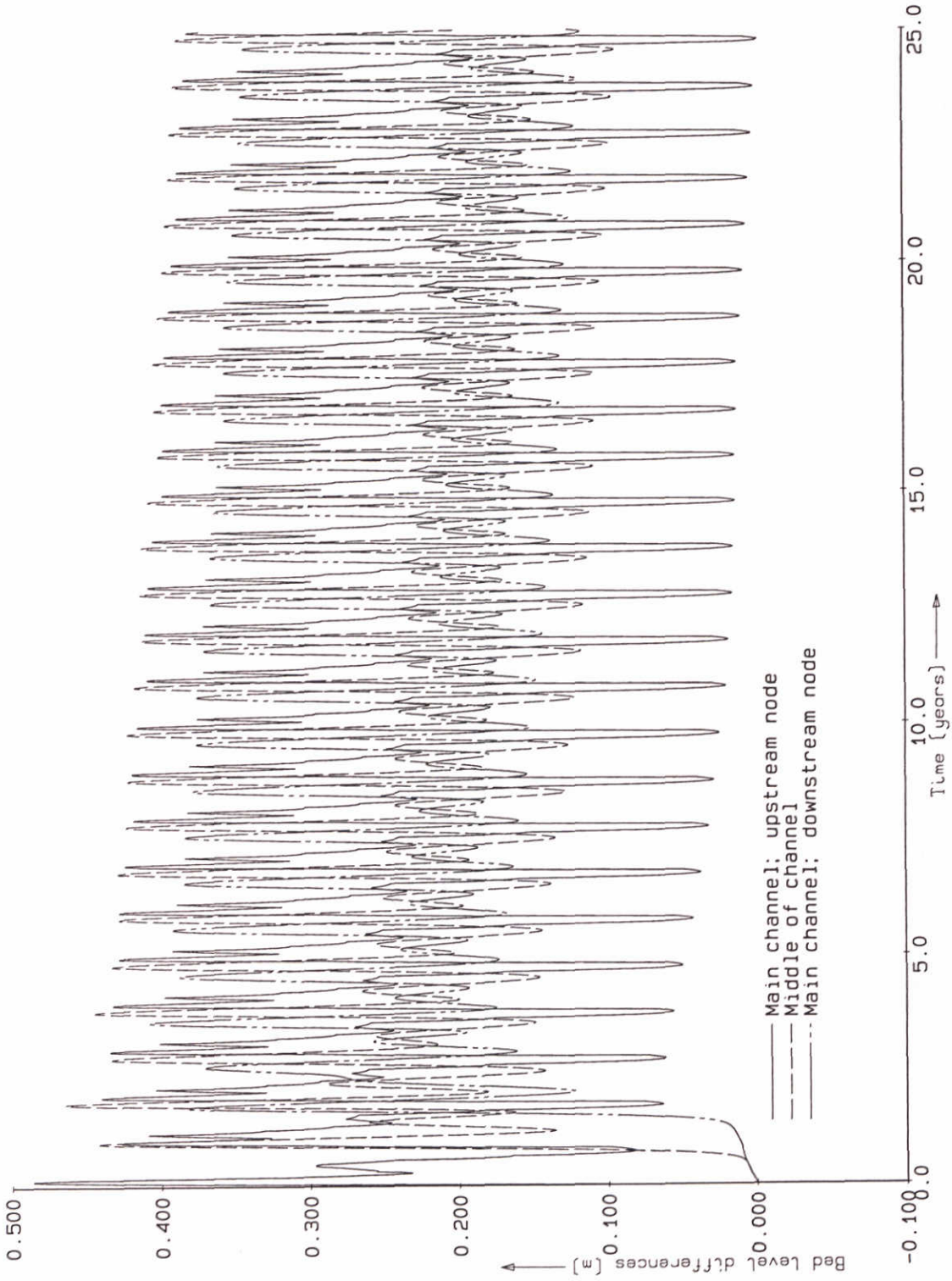

Bed level difference case 001
Time varying boundary conditions
Main channel

DELFT HYDRAULICS

Fig.4.6

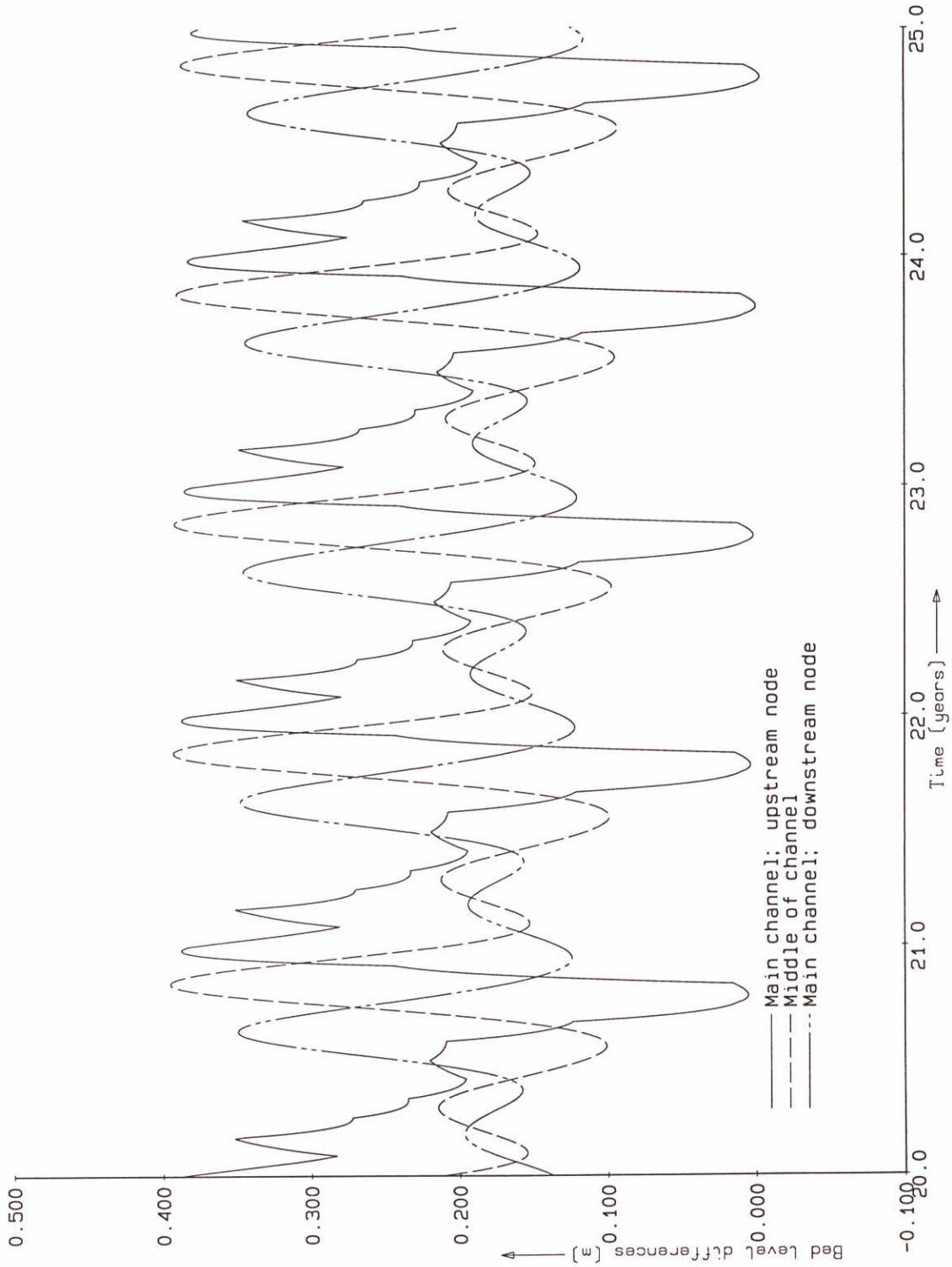

Bed level difference case 001
Time varying boundary conditions
Main channel

DELFT HYDRAULICS

Fig.4.7

DELFT HYDRAULICS

Bed level differences
Upstream node secondary channel

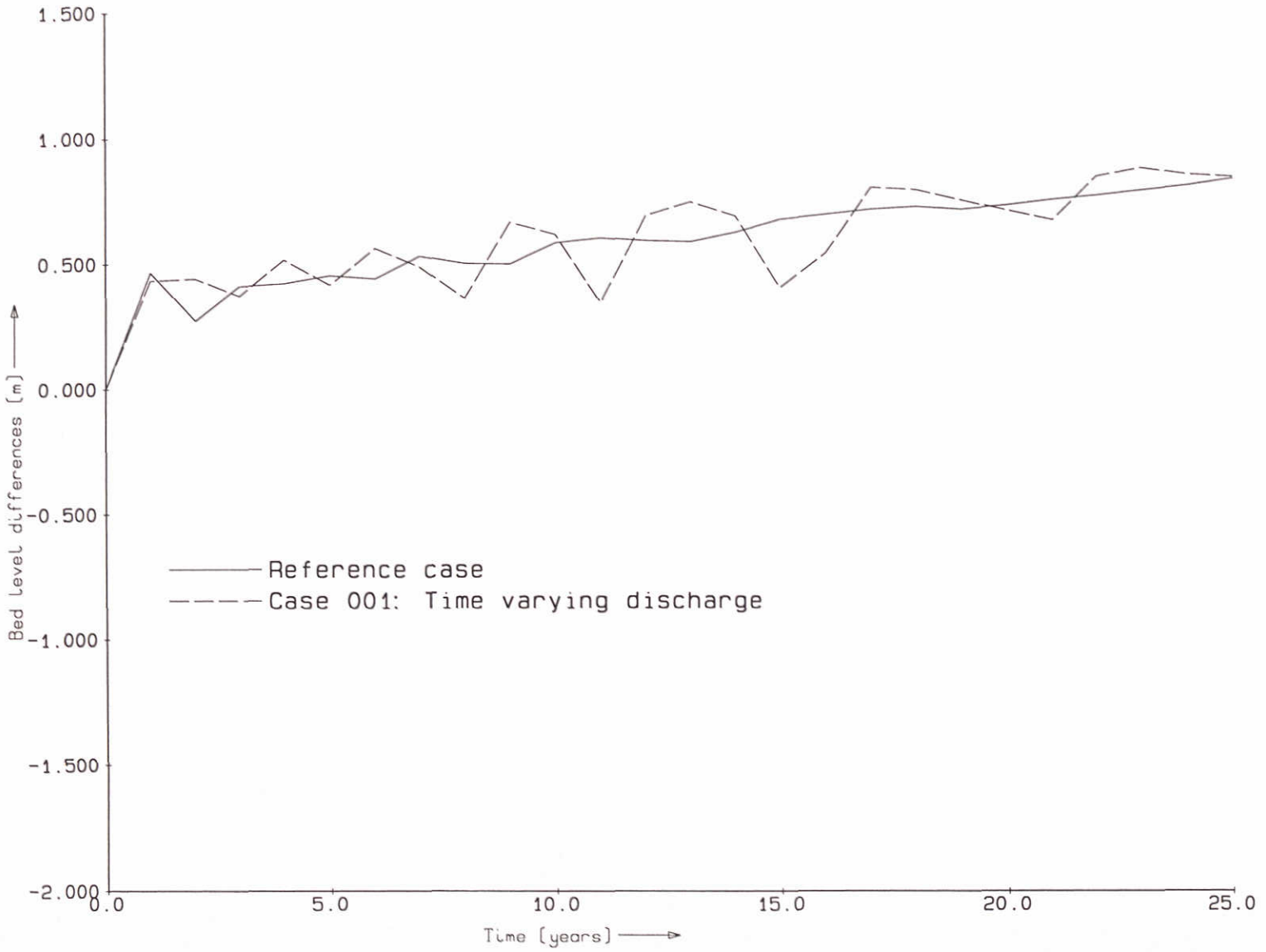

Q-1963

Fig. 4.8

DELFT HYDRAULICS

Bed level differences case 002
Power transport distribution equal to 5

Q-1963

Fig. 4.9

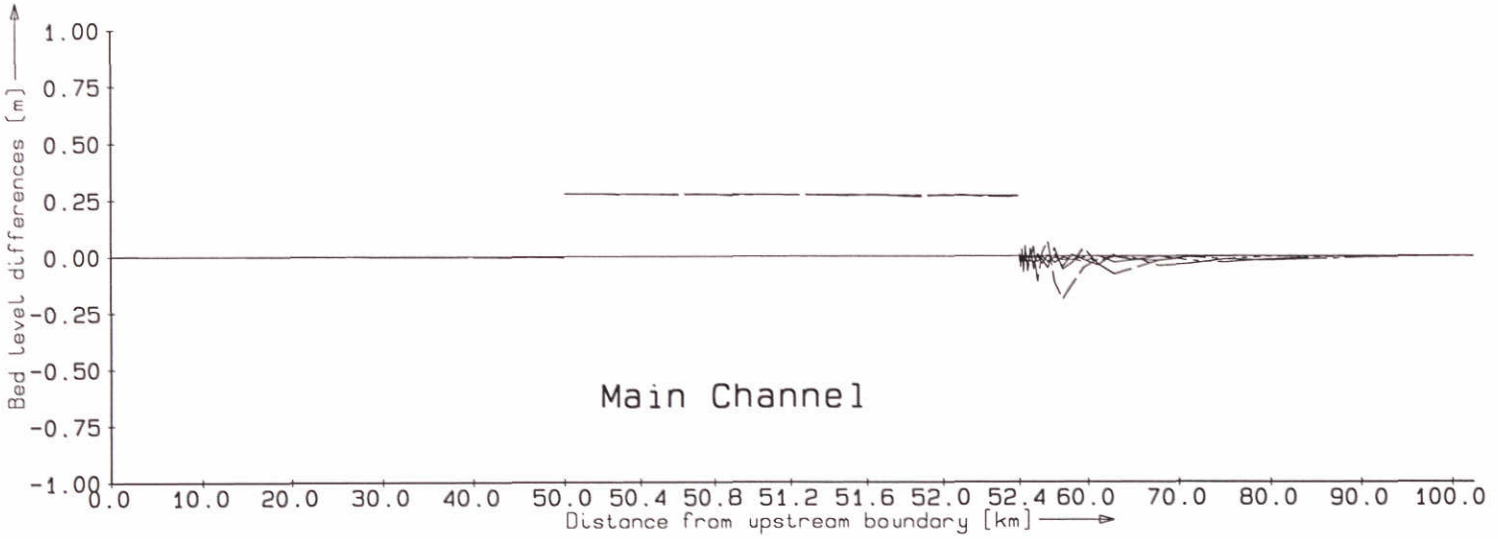

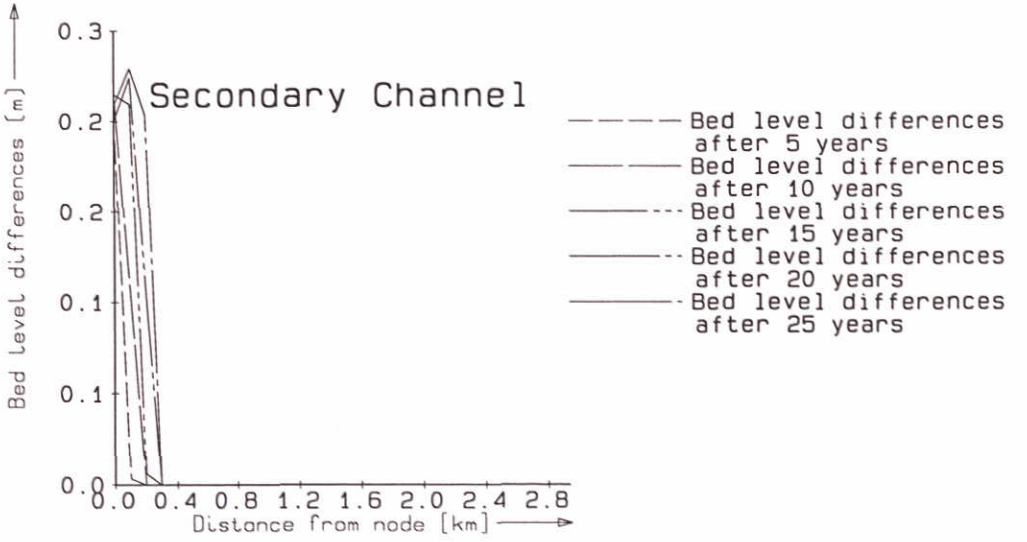

DELFT HYDRAULICS

Relative discharge through main channel

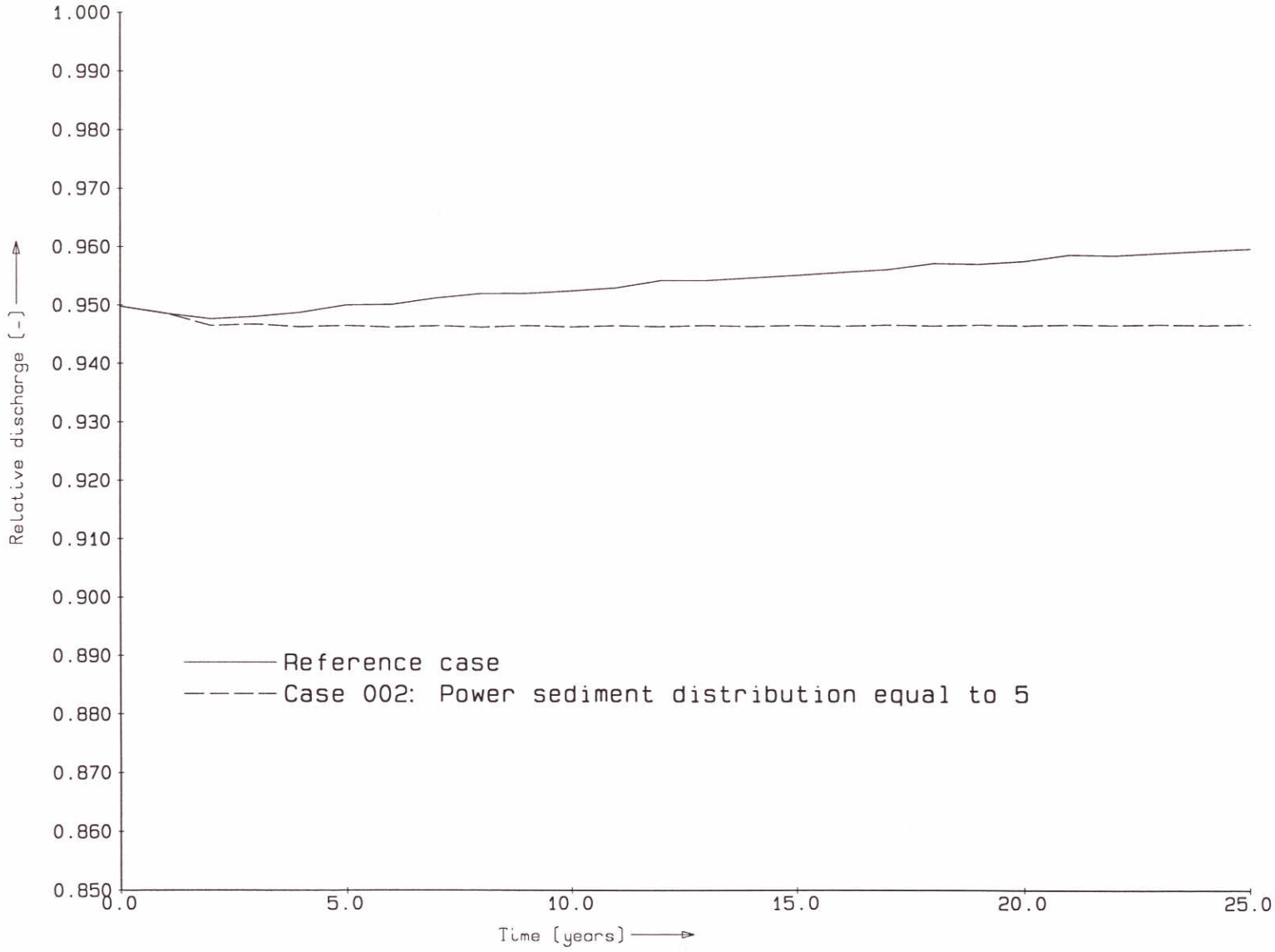

Q-1963

Fig. 4.10

DELFT HYDRAULICS

Bed level differences
Upstream node main channel

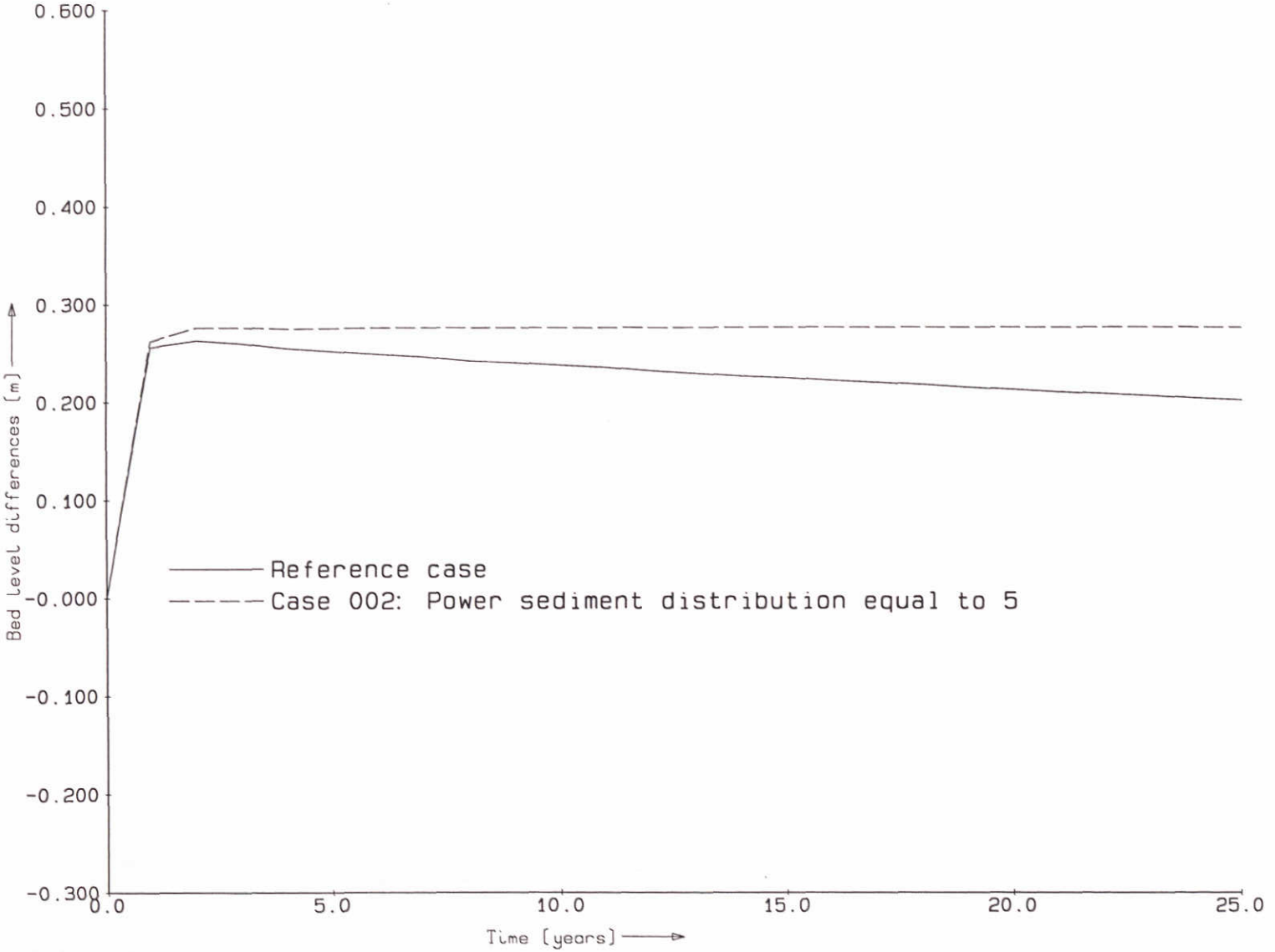

Q-1963

Fig. 4.11

DELFT HYDRAULICS

Bed level differences
Upstream node secondary channel

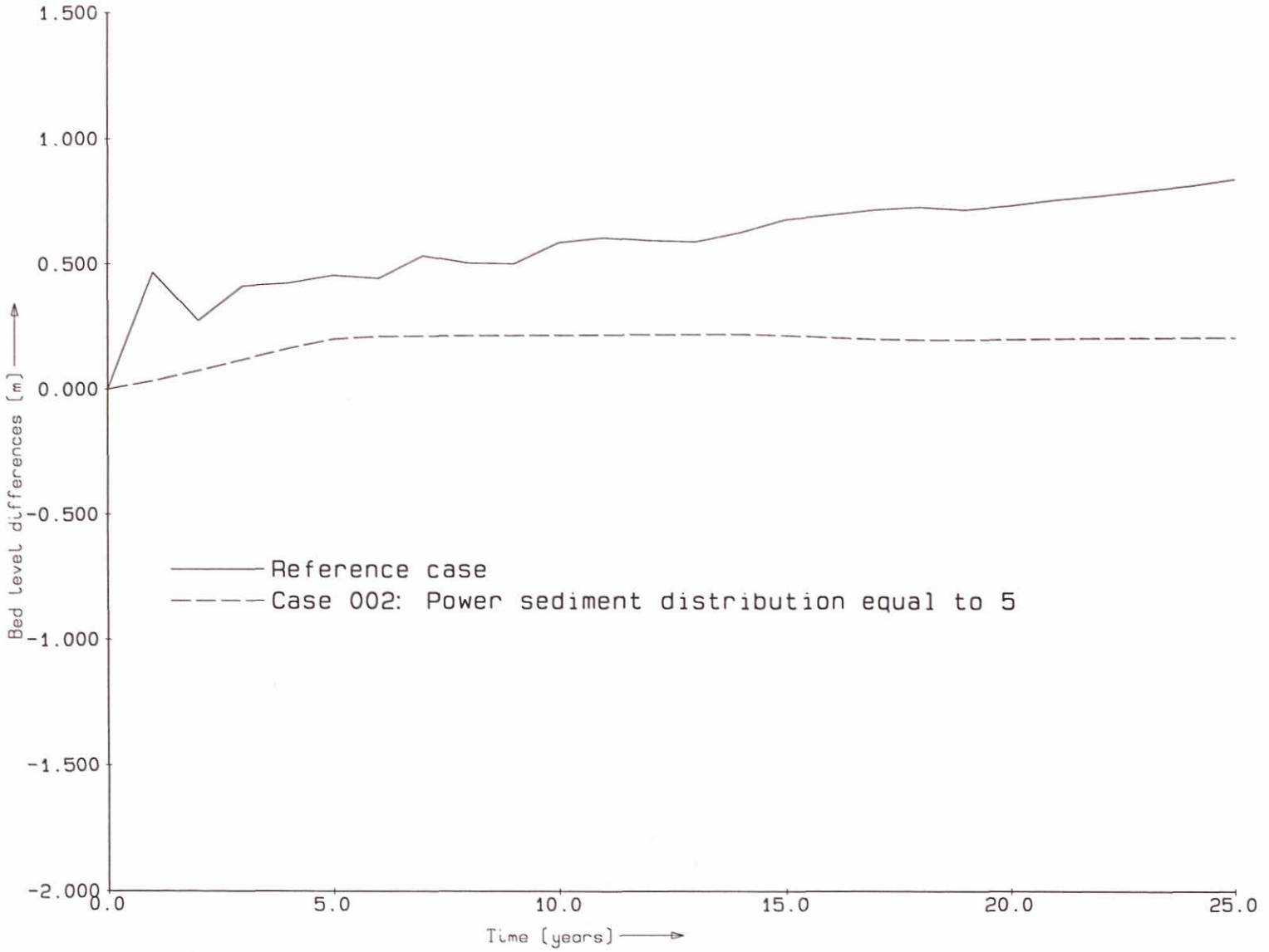

Q-1963

Fig. 4.12

DELFT HYDRAULICS

Bed level differences
Power transport distribution equal to 5
Depth secondary channel equals depth main channel

Q-1963

Fig. 4.13

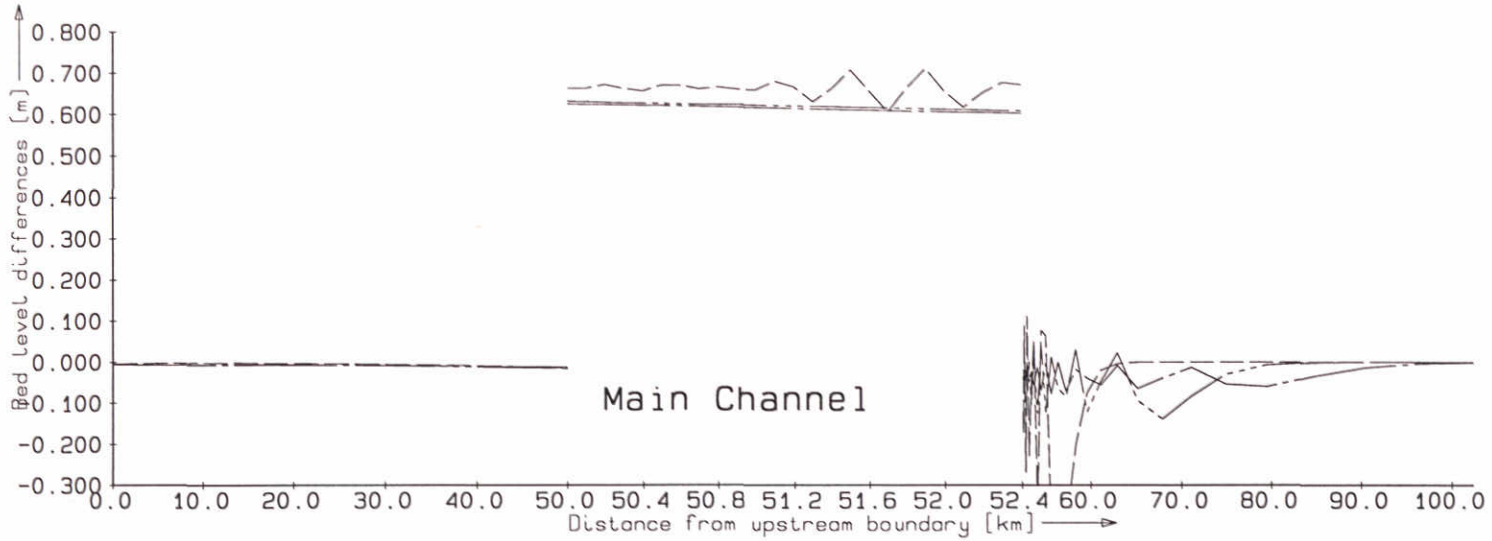

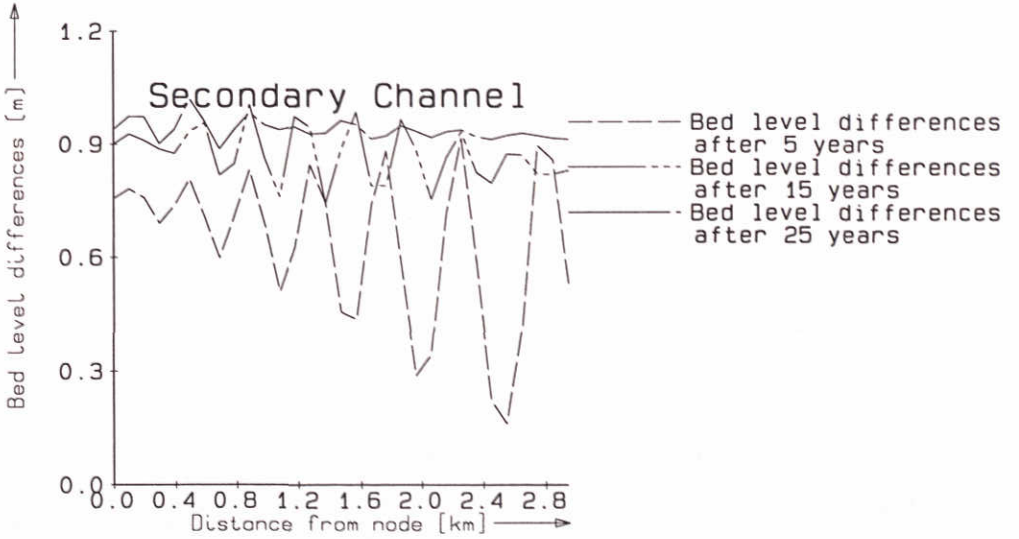

DELFT HYDRAULICS

Bed level differences
Power transport disribution equal to 10

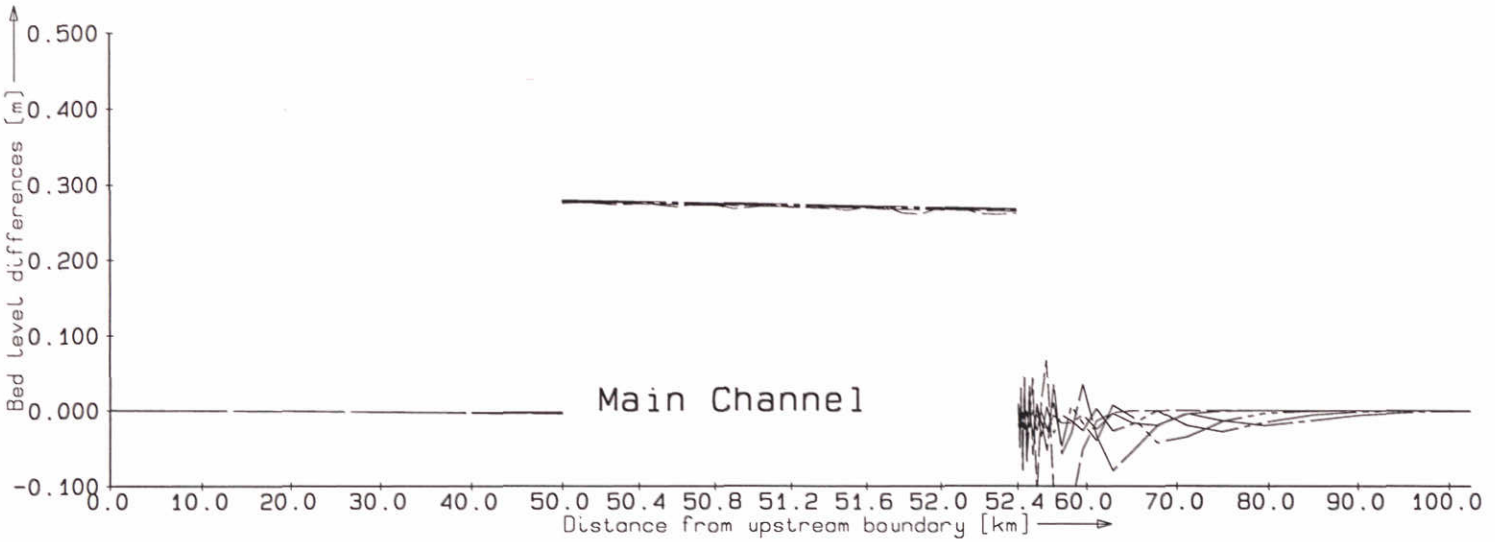

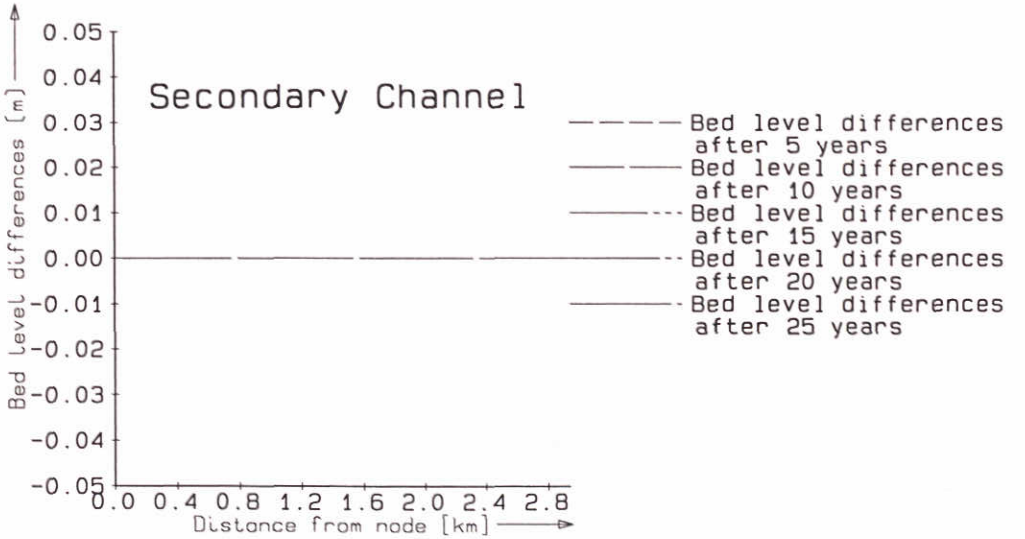

Q-1963

Fig. 4.14

DELFT HYDRAULICS

Bed level differences case 003
Enlarged width secondary channel

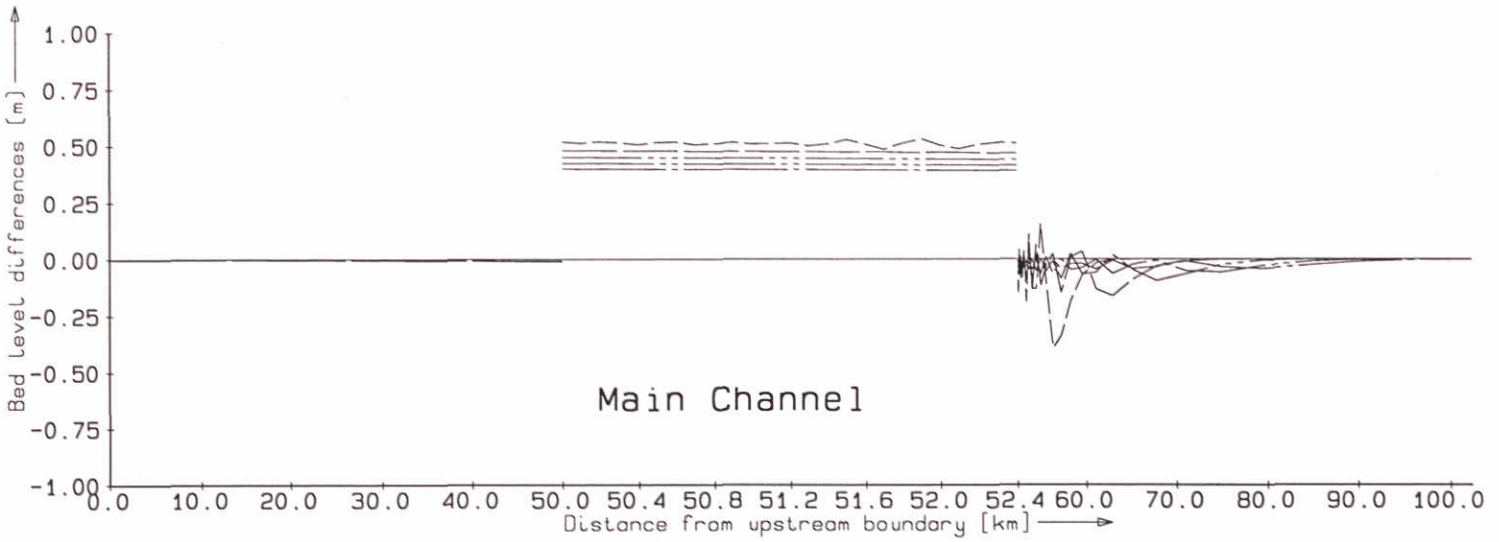

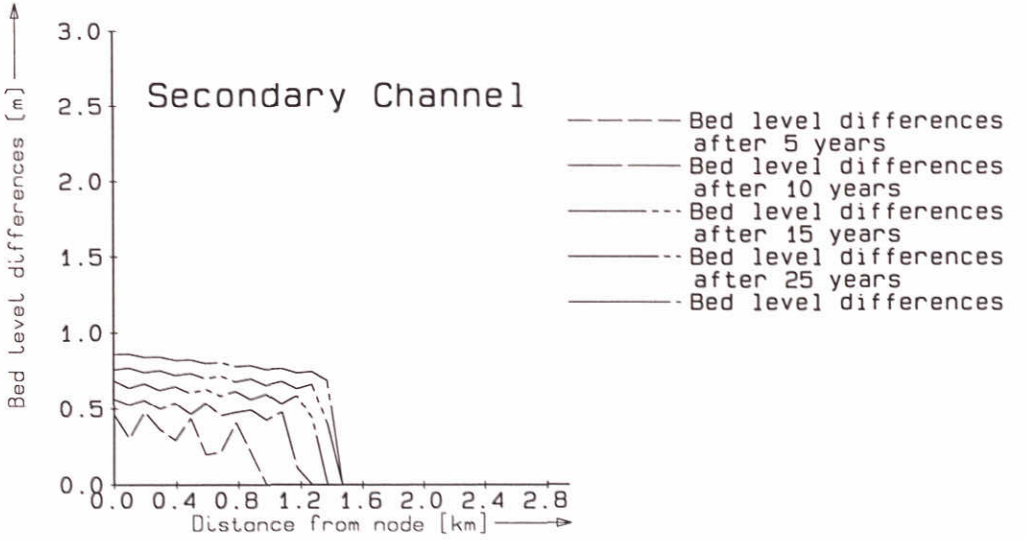

Q-1963

Fig. 4.15

Relative discharge through main channel

DELFT HYDRAULICS

Q-1963

Fig. 4.16

DELFT HYDRAULICS

Bed level differences
Upstream node main channel

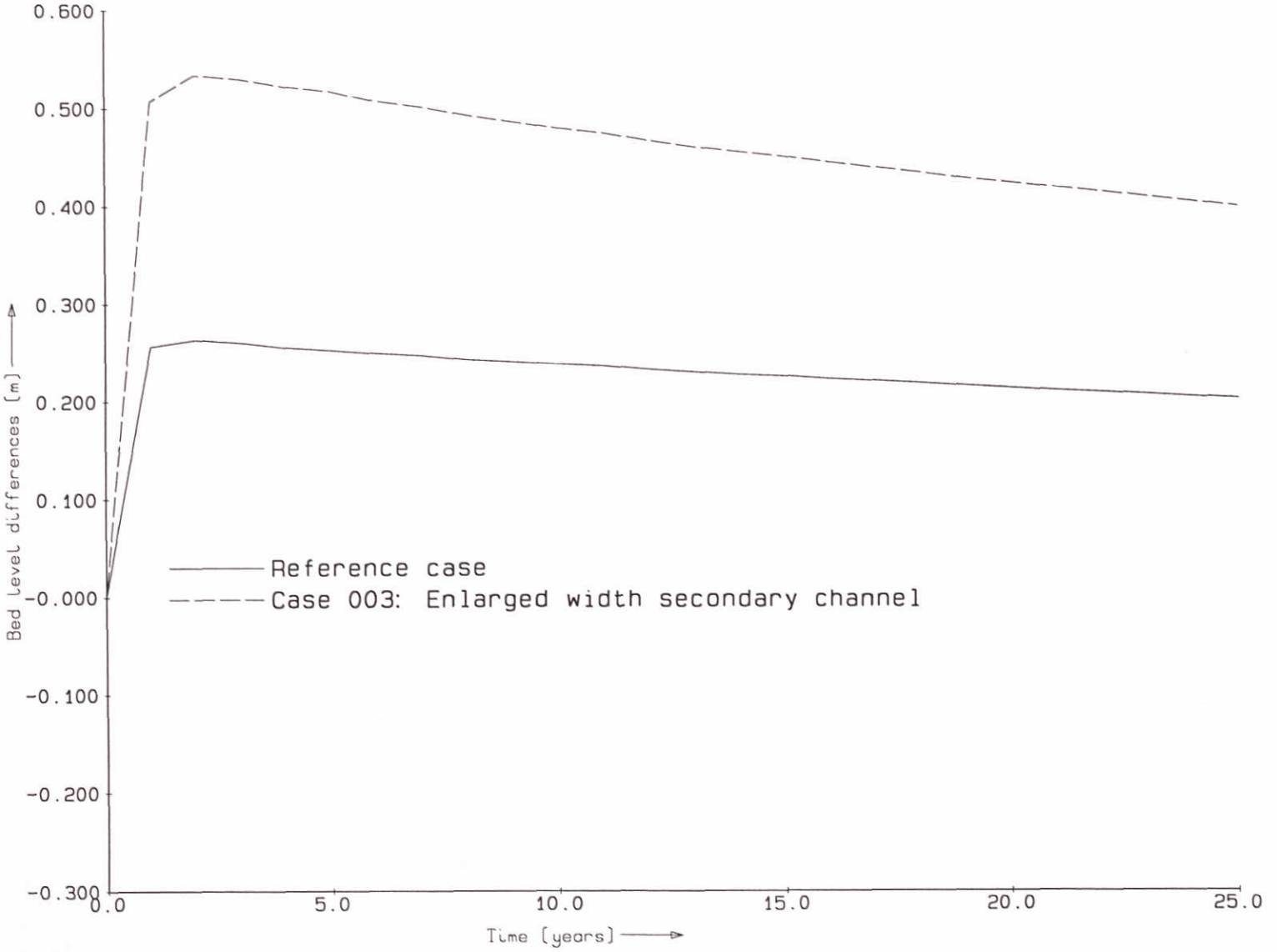

Q-1963

Fig. 4.17

DELFT HYDRAULICS

Bed level differences
Upstream node secondary channel

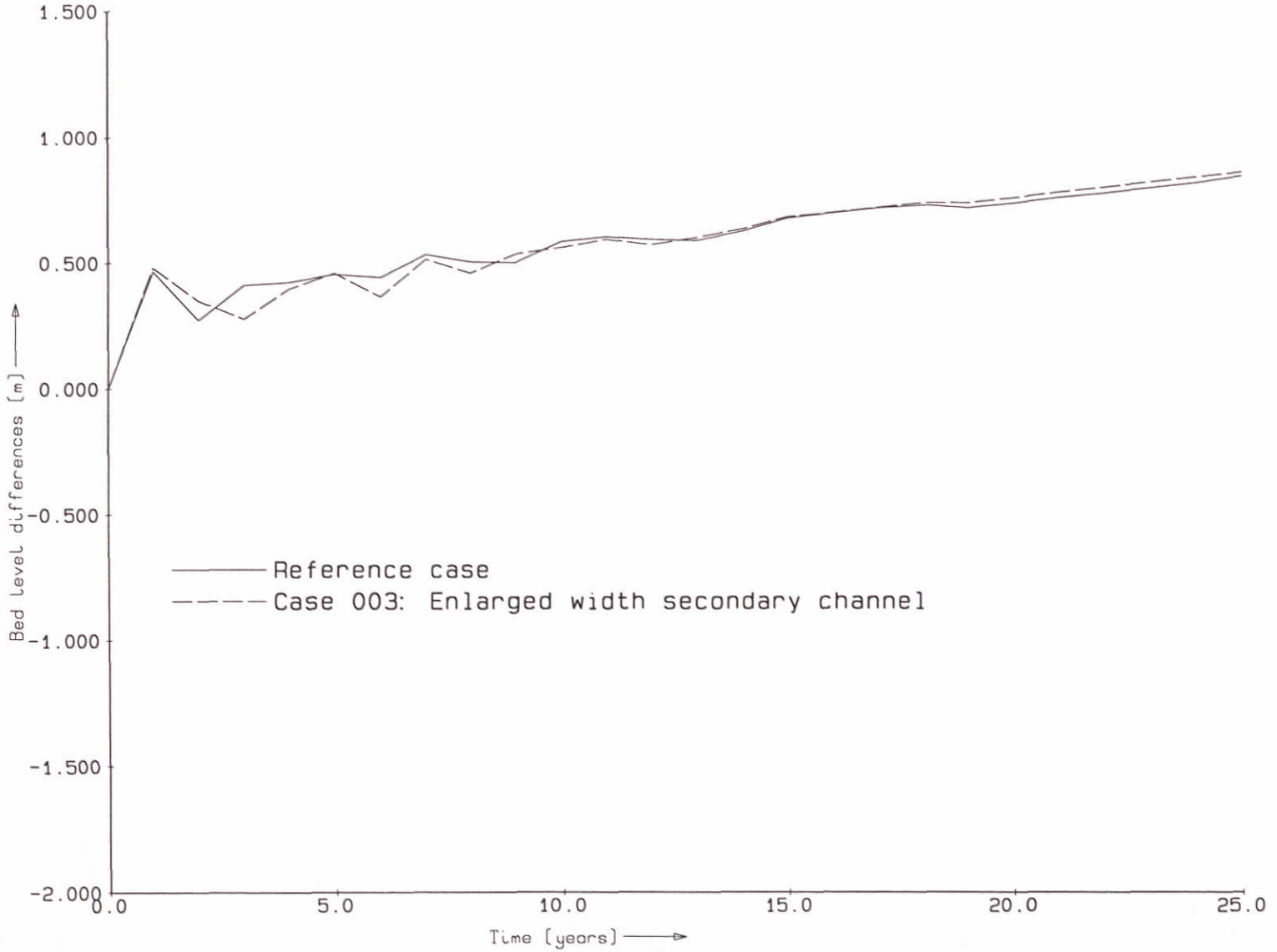

Q-1963

Fig. 4.18

DELFT HYDRAULICS

Bed level differences case 004
Decreased sediment transport

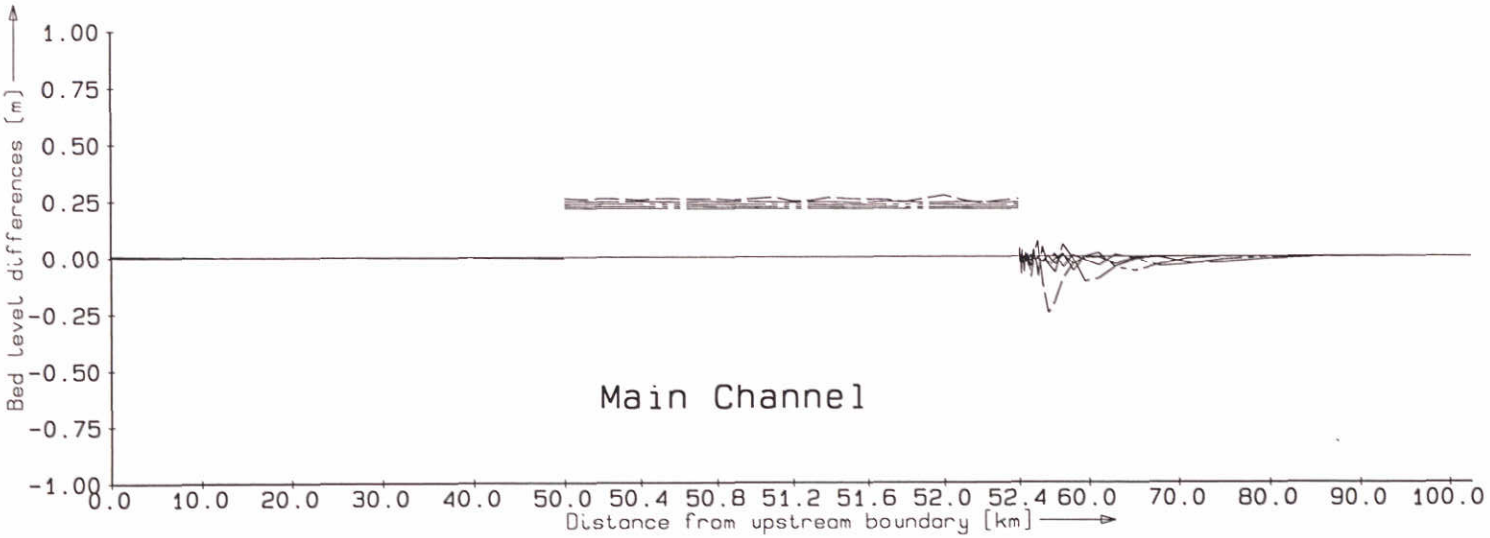

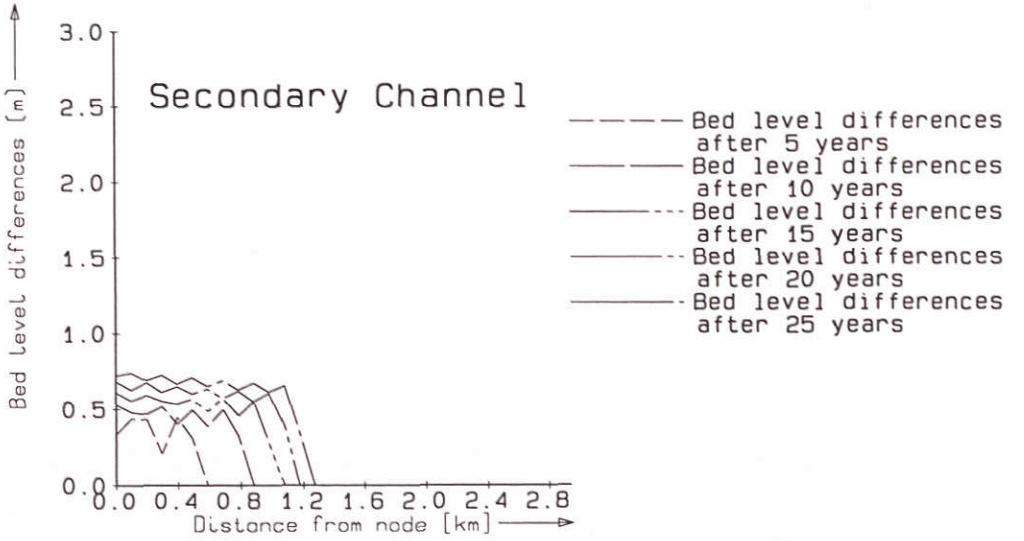

Q-1963

Fig. 4.19

DELFT HYDRAULICS

Relative discharge through main channel

Q-1963

Fig. 4.20

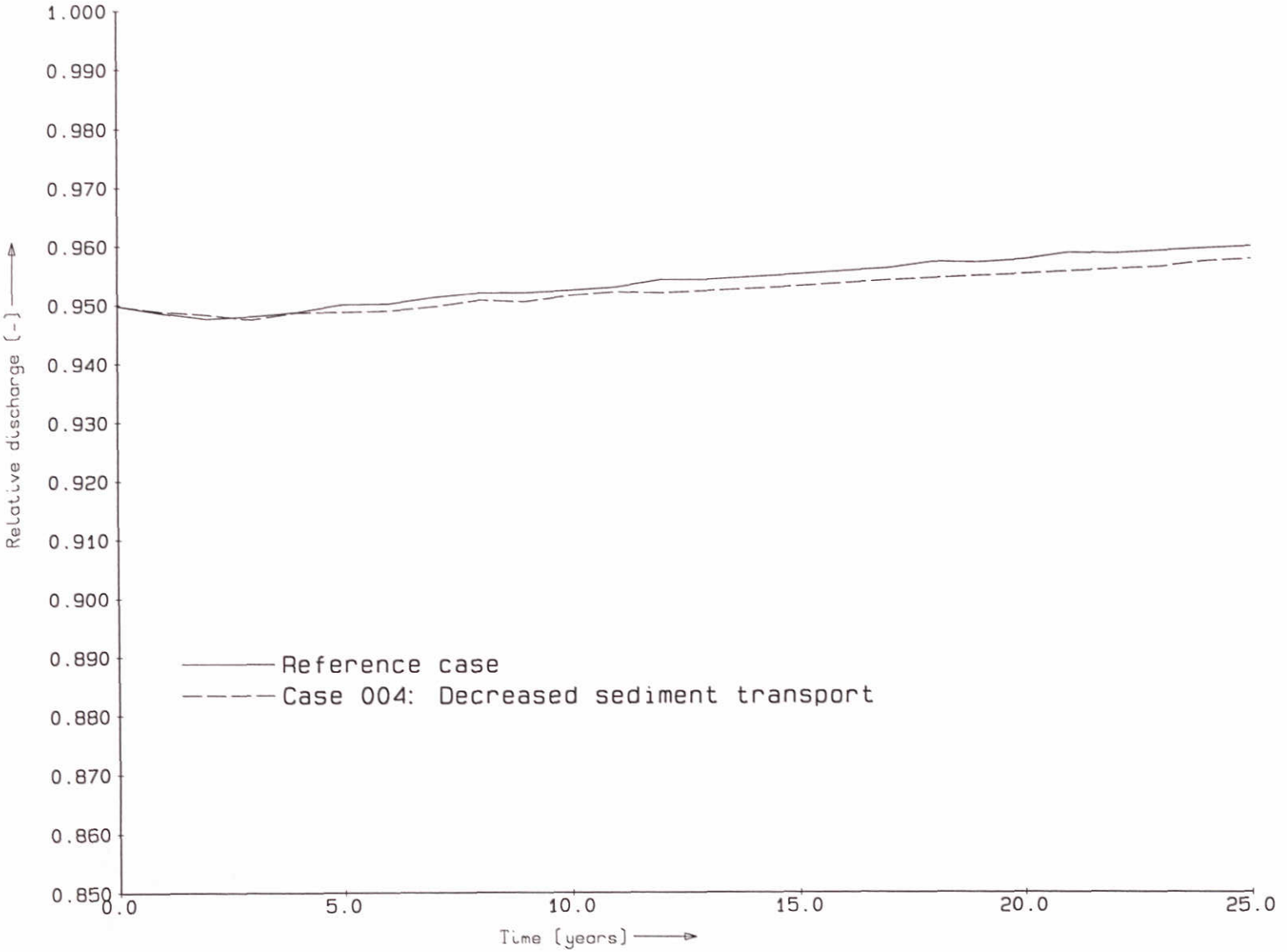

Bed level differences
Upstream node main channel

DELFT HYDRAULICS

Q-1963

Fig. 4.21

DELFT HYDRAULICS

Bed level differences
Upstream node secondary channel

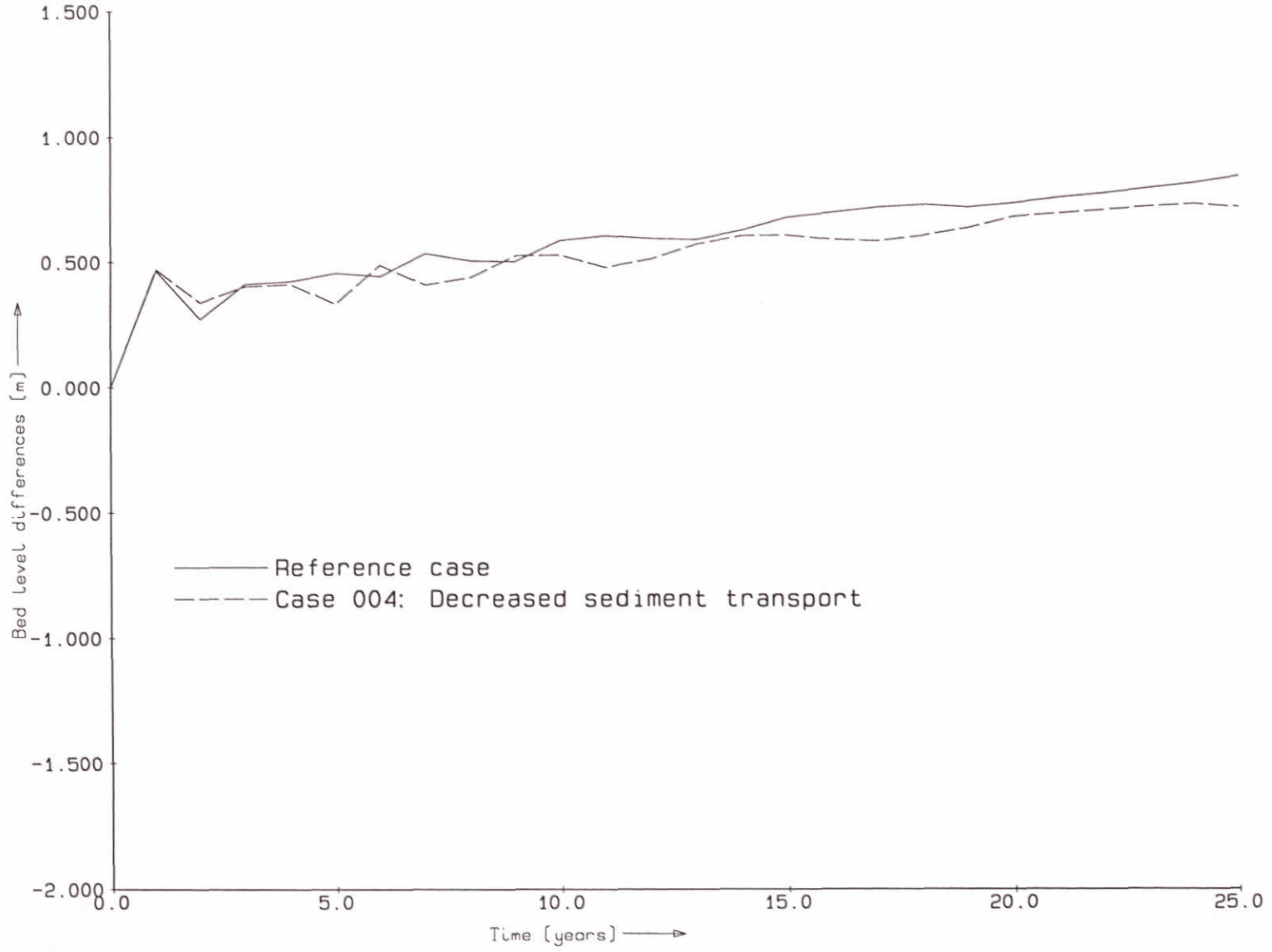

Q-1963

Fig. 4.22

DELFT HYDRAULICS

Bed level differences case 005
Increased sediment transport

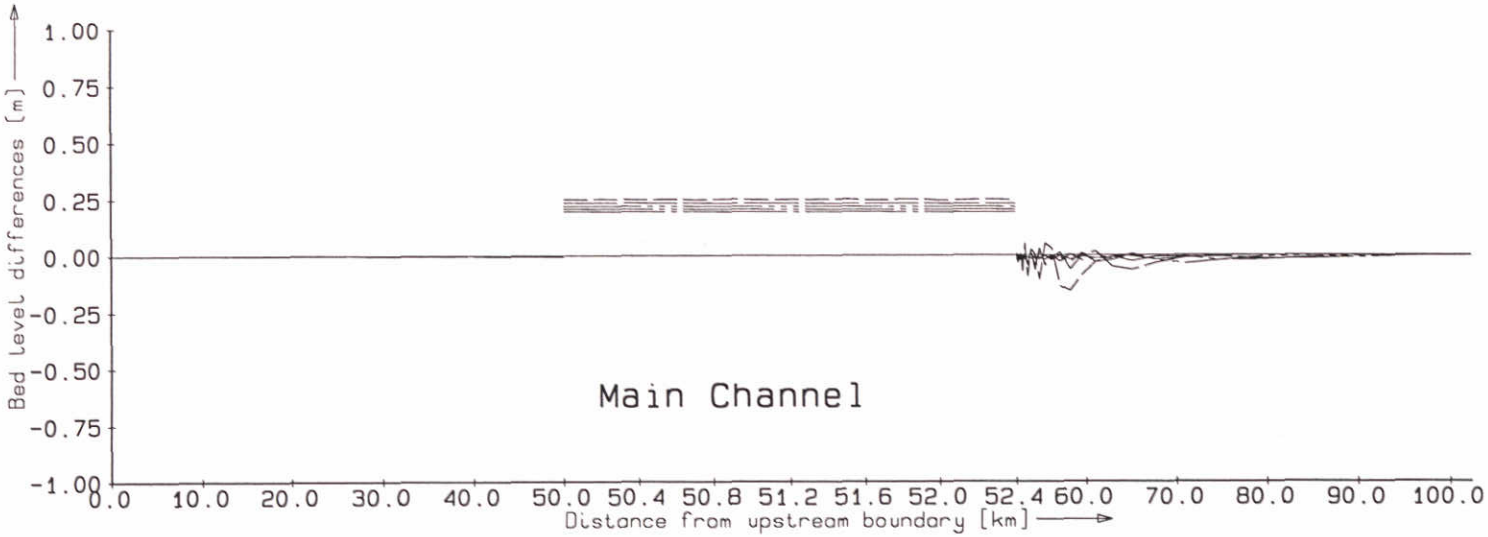

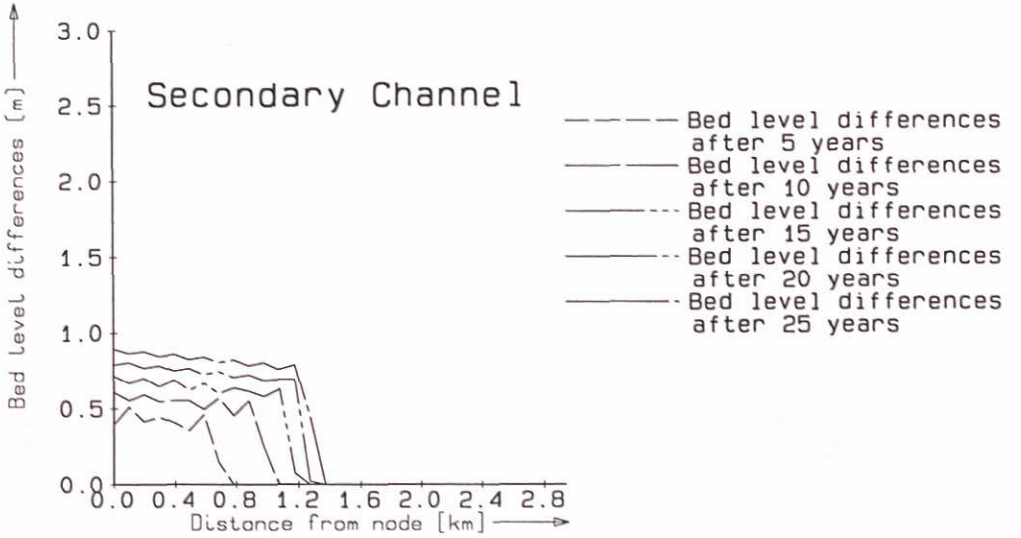

Q-1963

Fig. 4.23

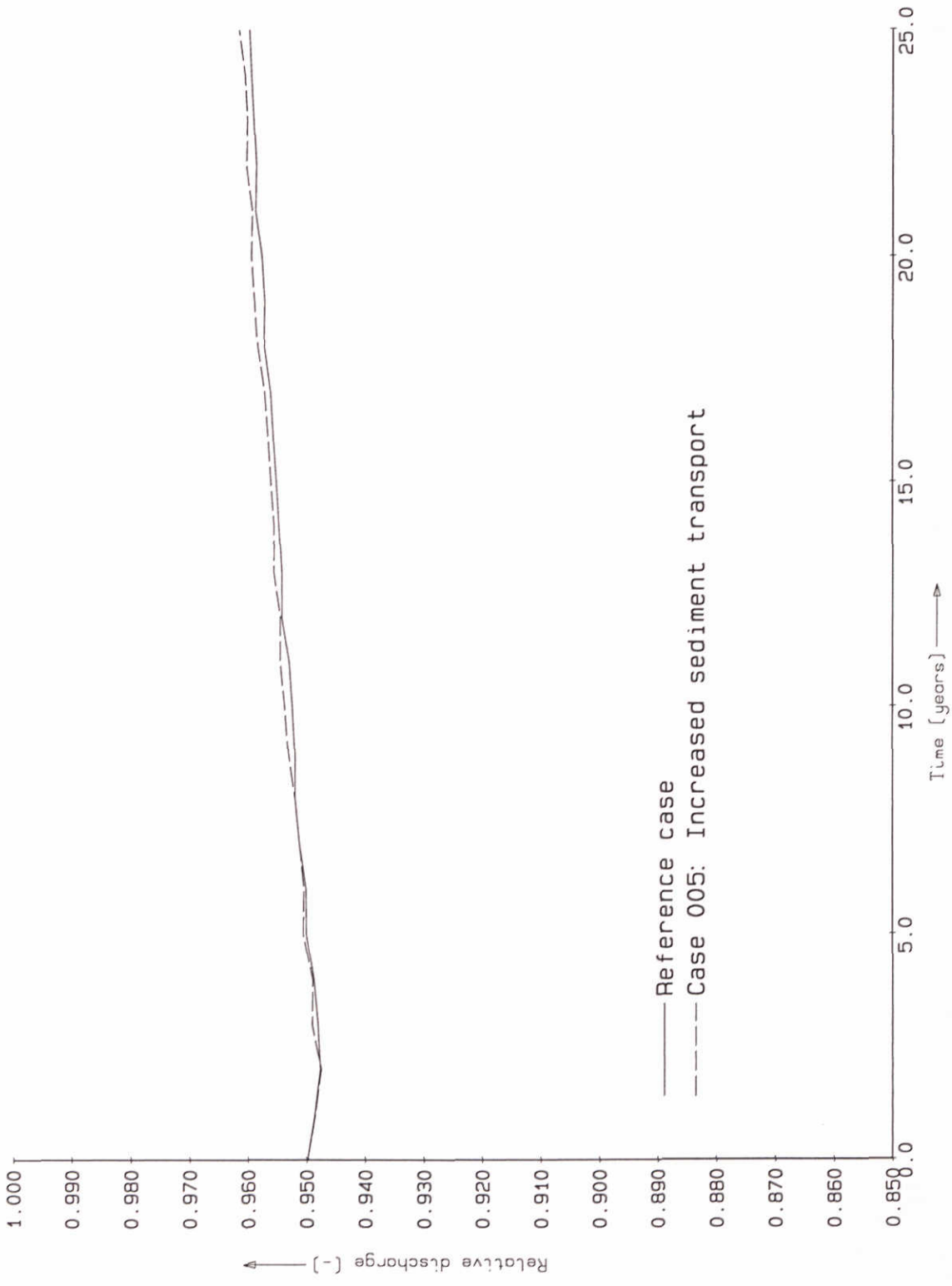

Relative discharge through main channel

DELFT HYDRAULICS

Q-1963

Fig. 4.24

DELFT HYDRAULICS

Bed level differences
Upstream node main channel

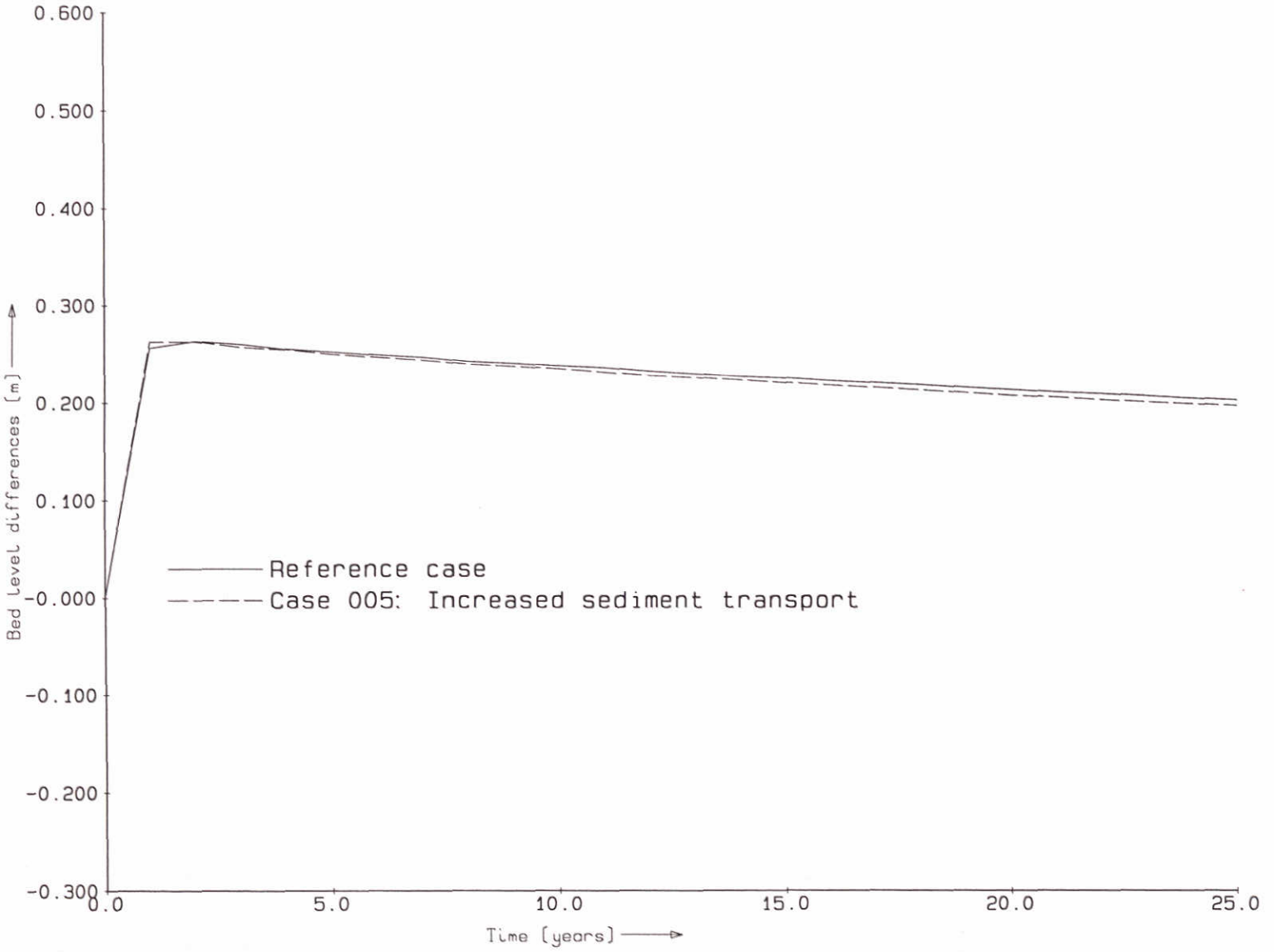

Q-1963

Fig. 4.25

DELFT HYDRAULICS

Bed level differences
Upstream node secondary channel

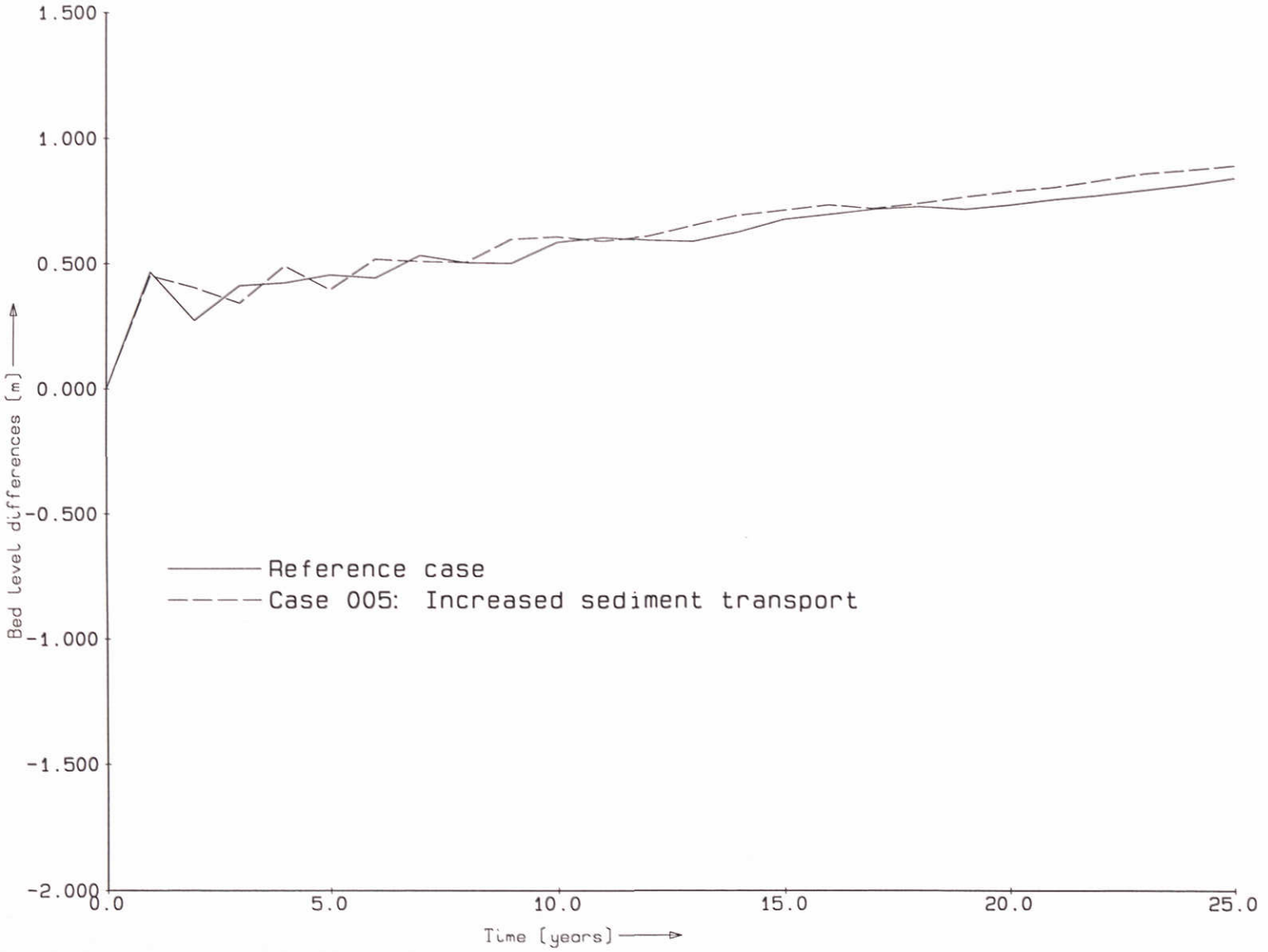

Q-1963

Fig. 4.26

DELFT HYDRAULICS

Bed level differences case 006
Grain size secondary channel halved

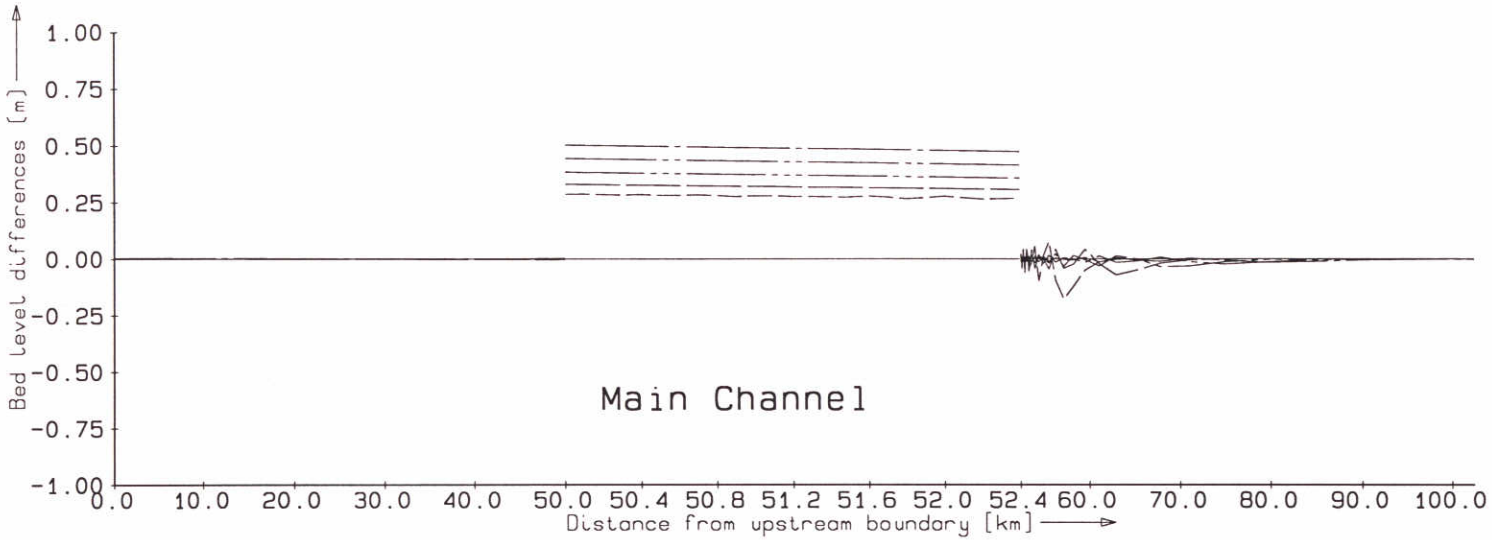

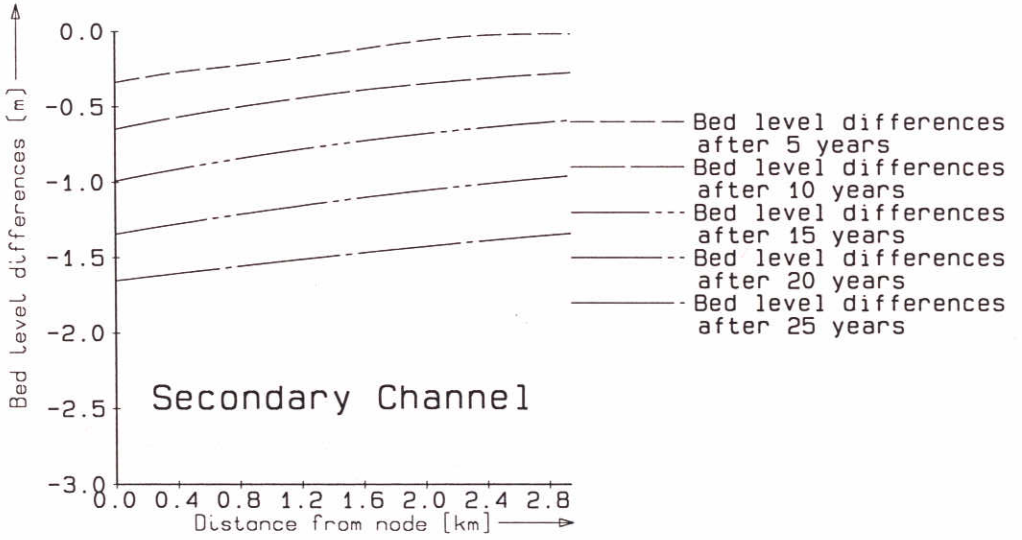

Q-1963

Fig. 4.27

Relative discharge through main channel

DELFT HYDRAULICS

Q-1963

Fig. 4.28

Bed level differences
Upstream node main channel

DELFT HYDRAULICS

Q-1963

Fig. 4.29

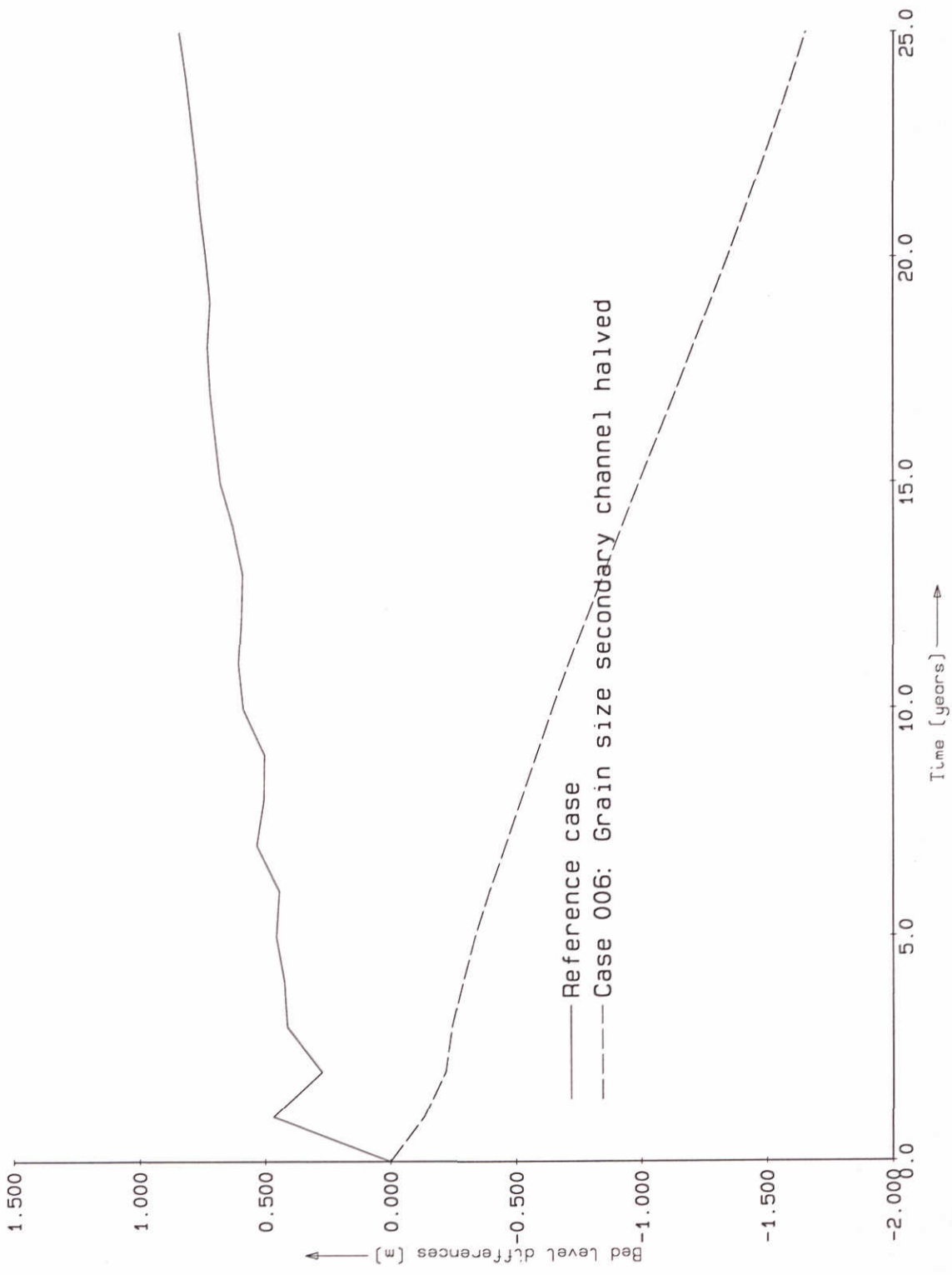

Bed level differences
Upstream node secondary channel

DELFT HYDRAULICS | Q-1963 | Fig. 4.30

DELFT HYDRAULICS

Bed level differences case 007
Grain size secondary channel doubled

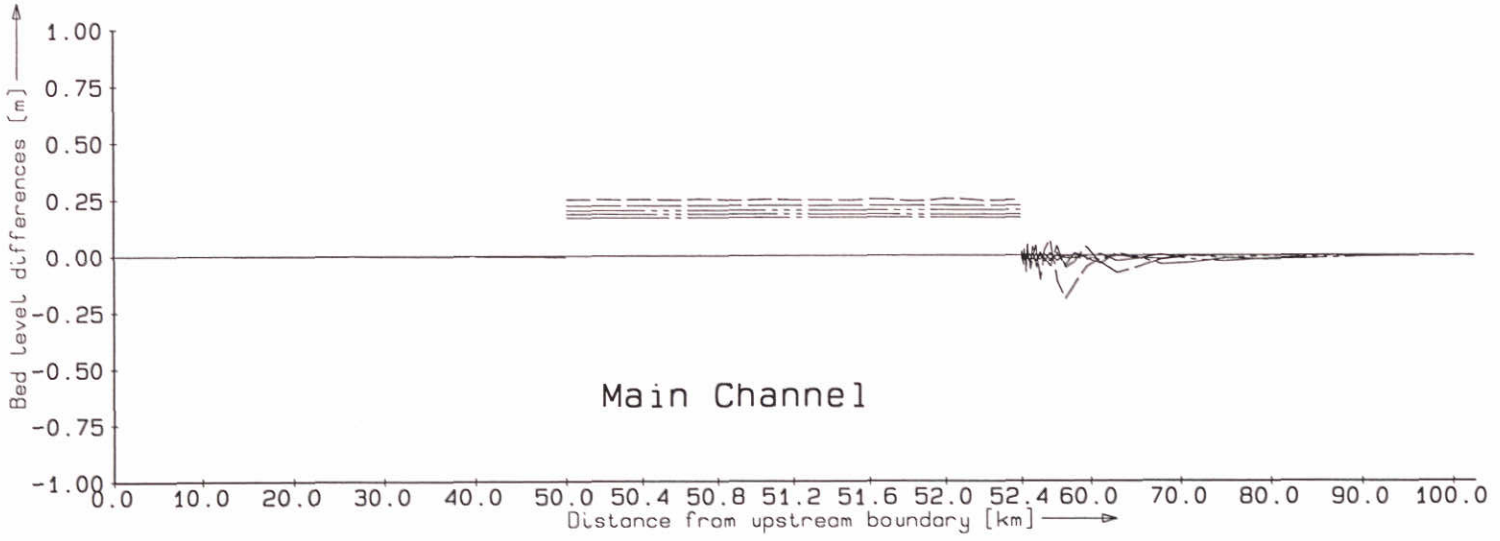

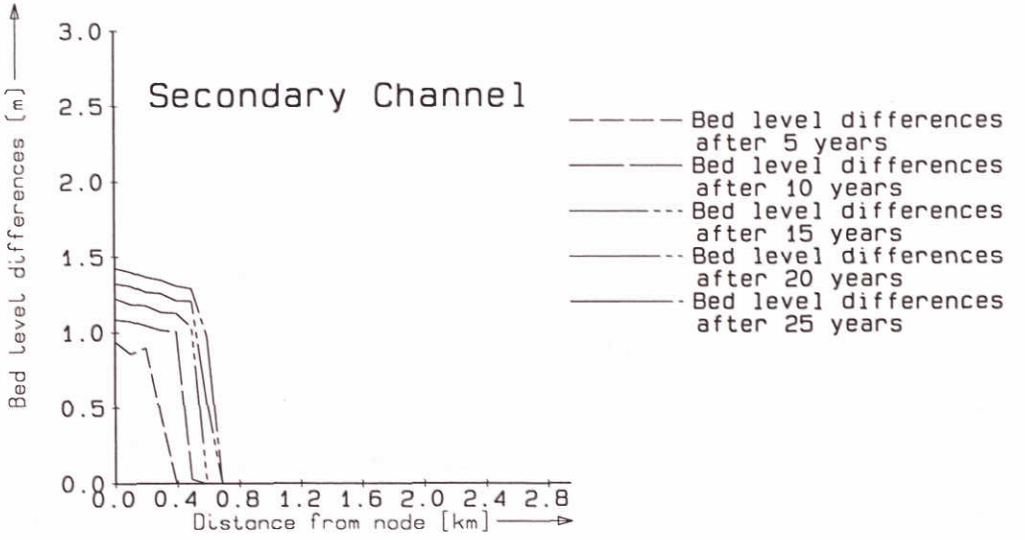

Q-1963

Fig. 4.31

DELFT HYDRAULICS

Relative discharge through main channel

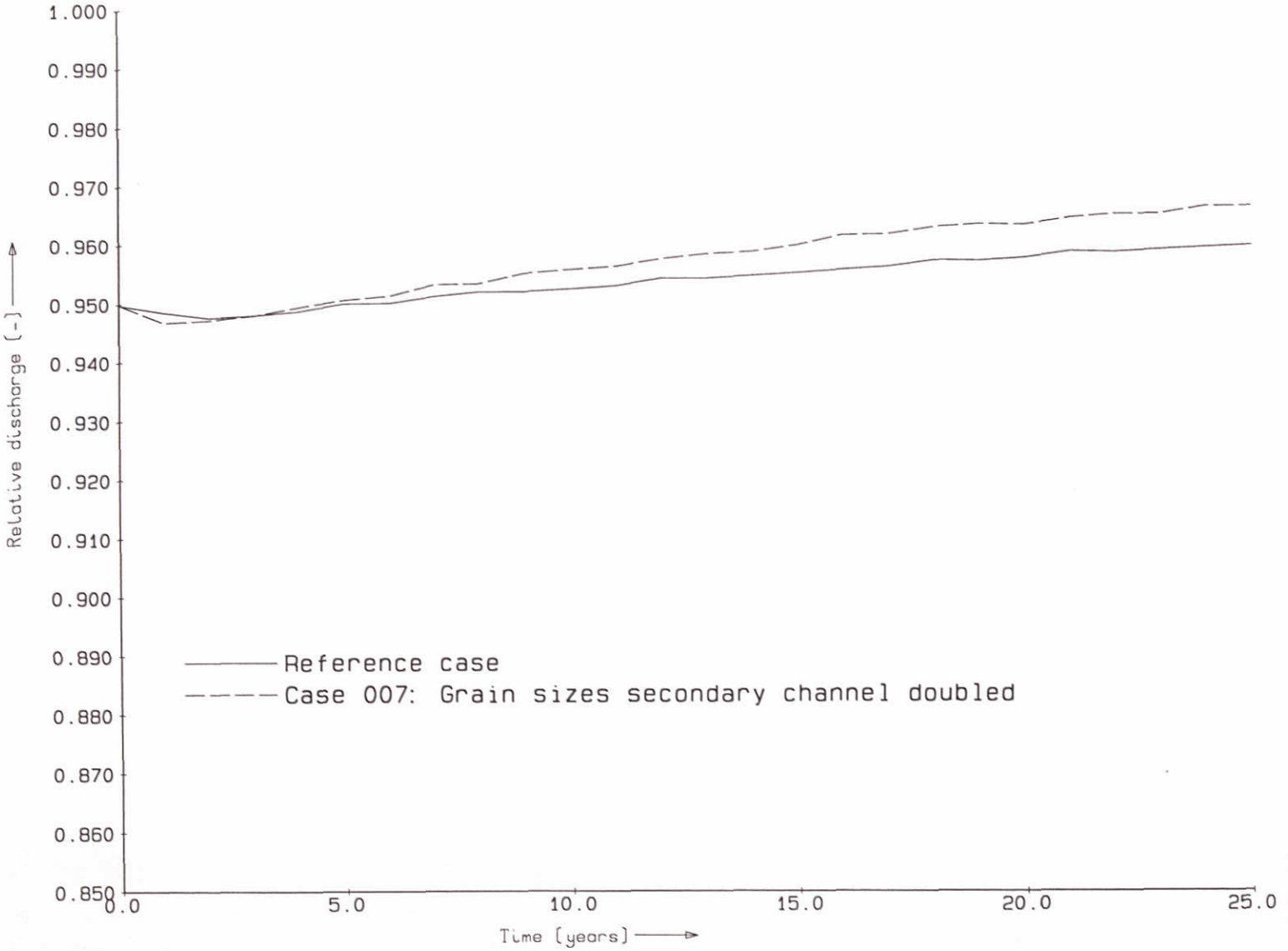

Q-1963

Fig. 4.32

DELFT HYDRAULICS

Bed level differences
Upstream node main channel

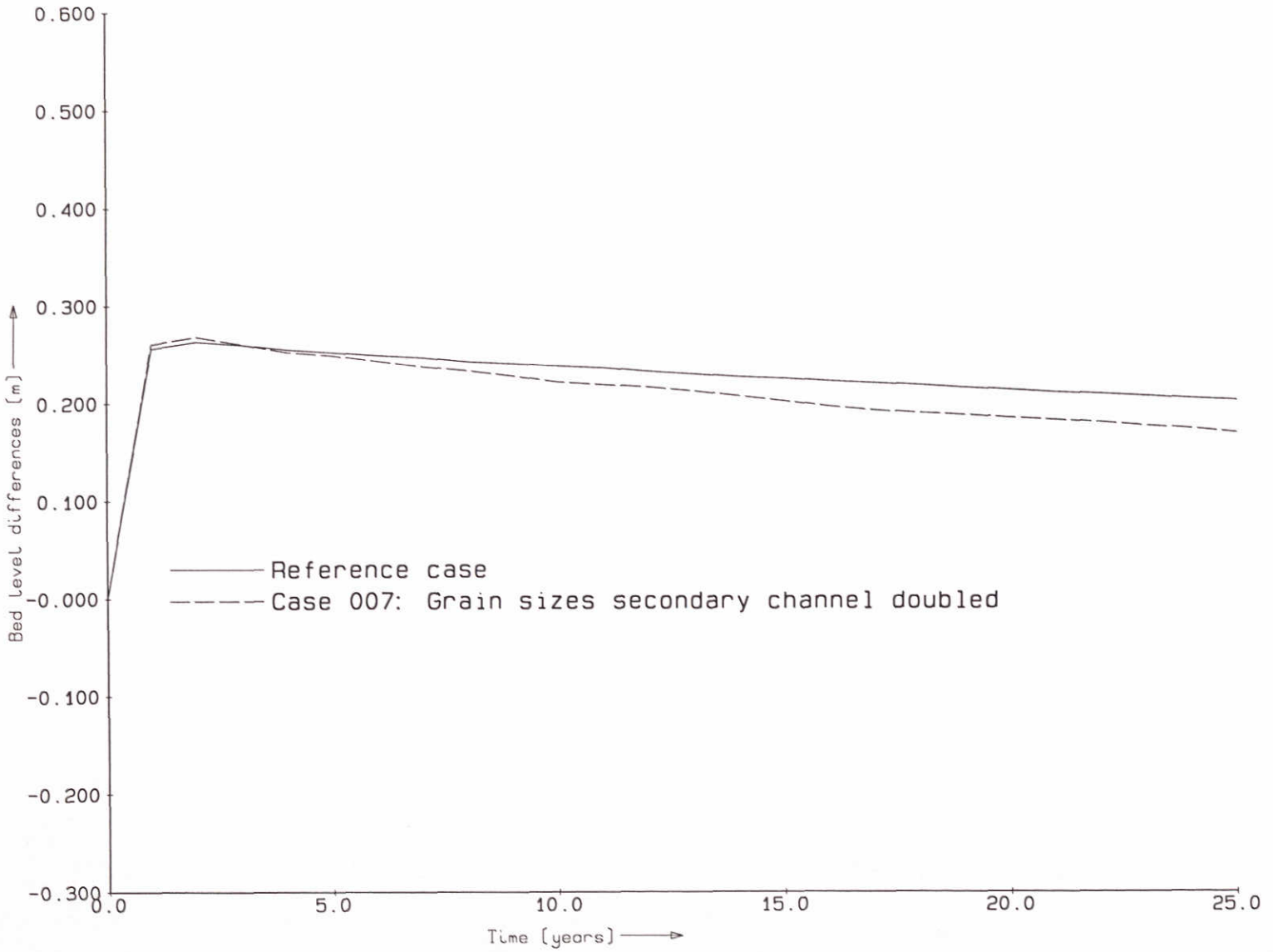

Q-1963

Fig. 4.33

DELFT HYDRAULICS

Bed level differences
Upstream node secondary channel

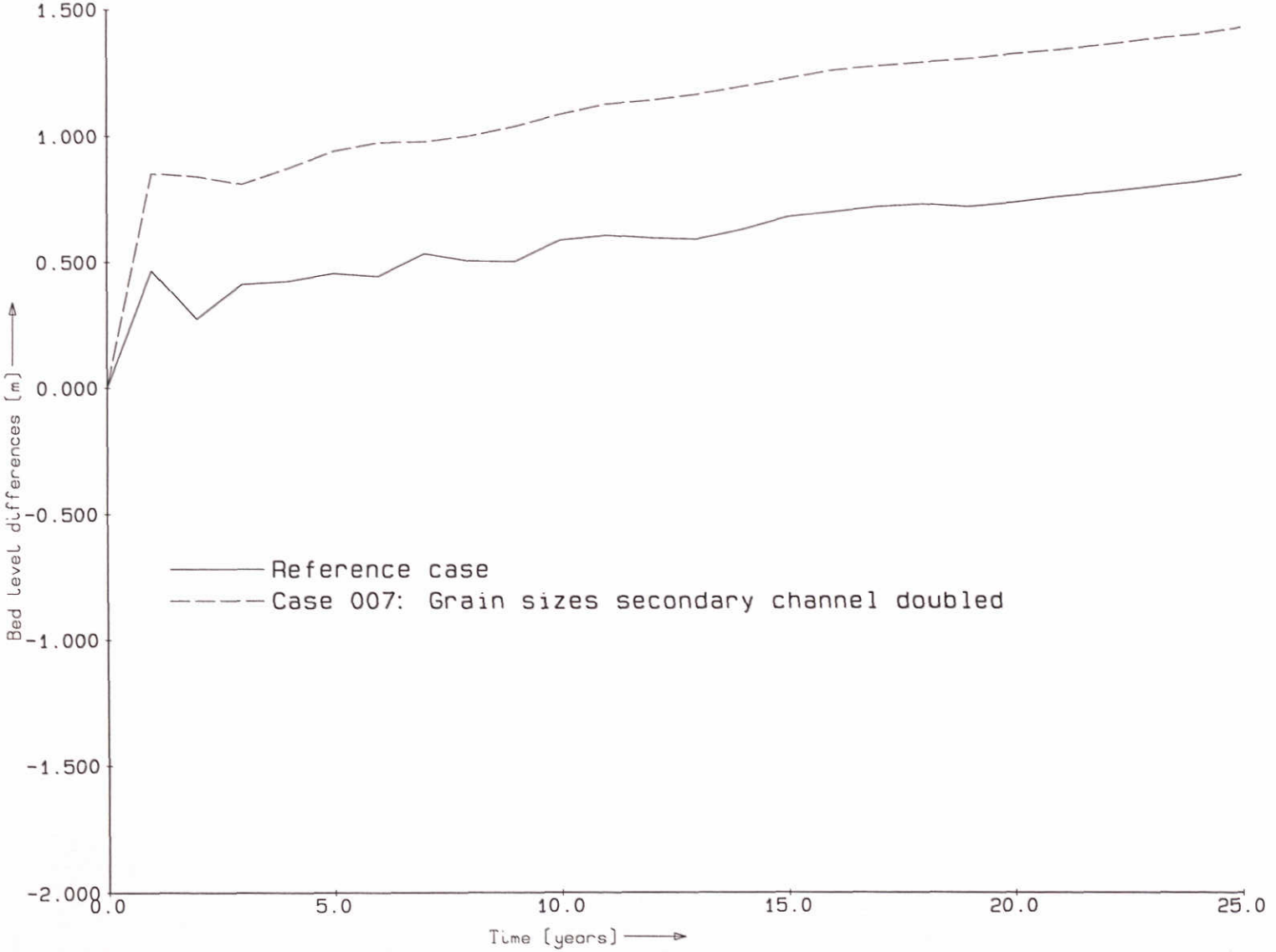

Q-1963

Fig. 4.34

DELFT HYDRAULICS

Bed level differences case 008
Enlarged friction secondary channel

Q-1963

Fig. 4.35

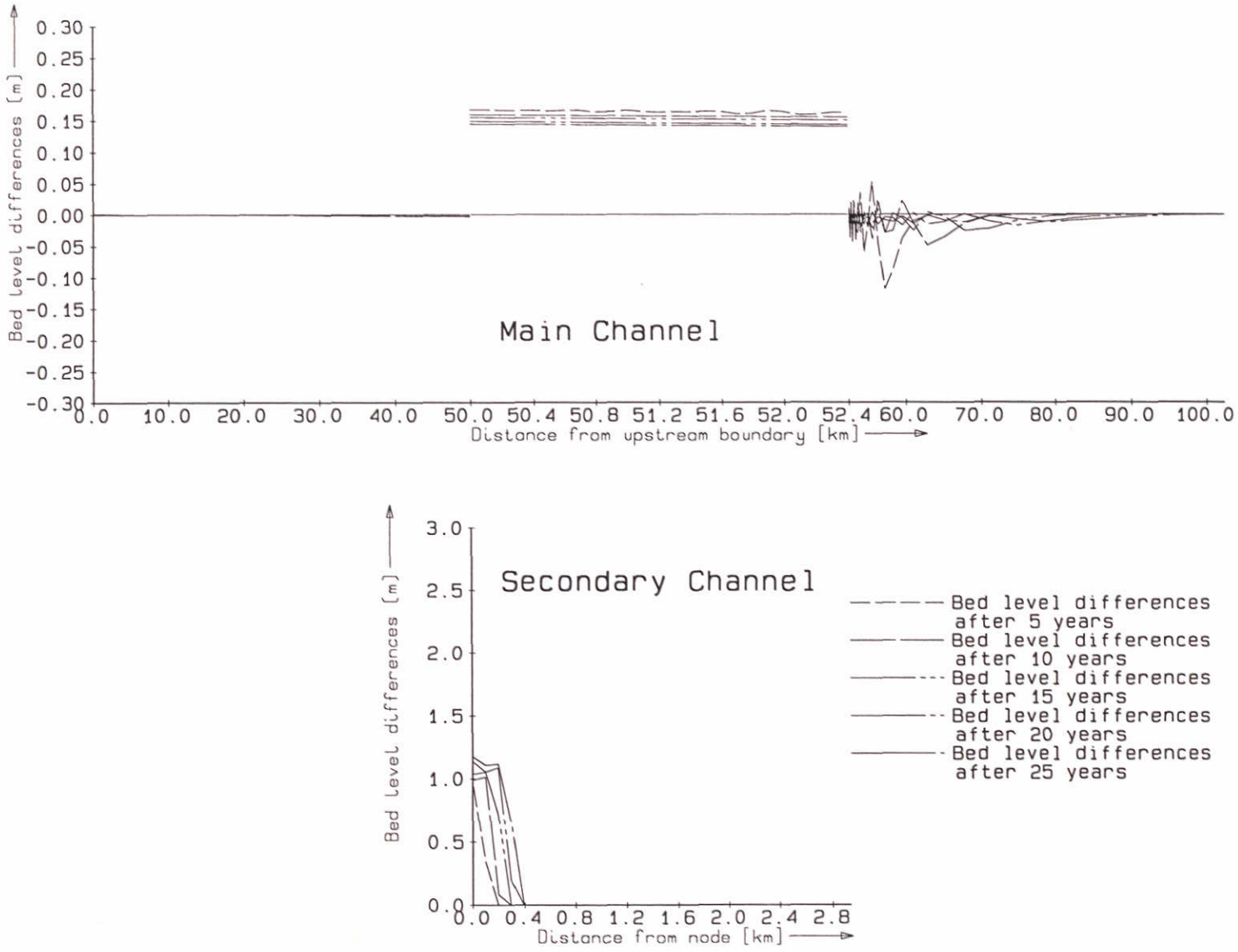

Relative discharge through main channel

DELFT HYDRAULICS

Q-1963

Fig. 4.36

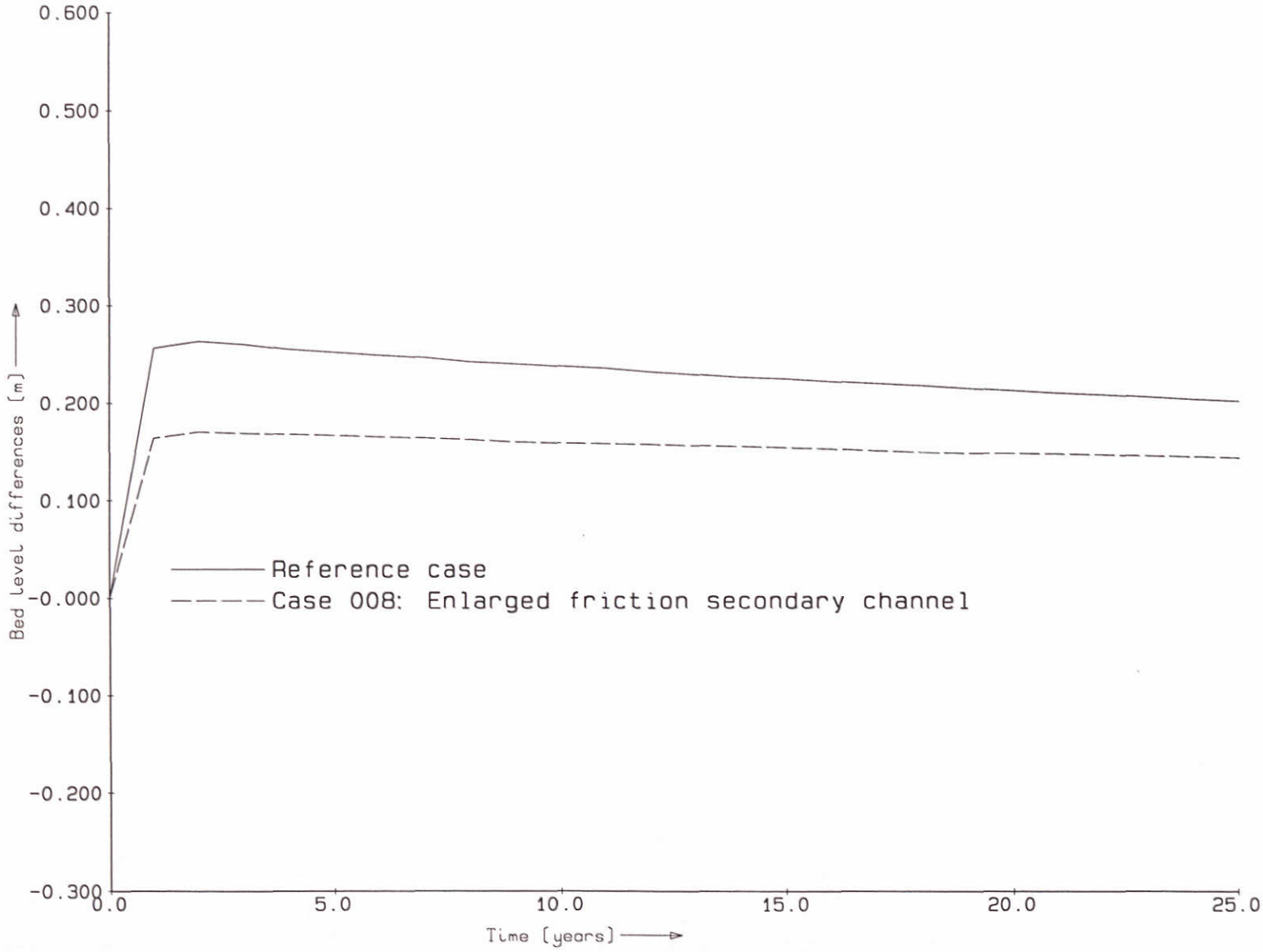

Bed level differences
Upstream node main channel

DELFT HYDRAULICS

Q-1963

Fig. 4.37

DELFT HYDRAULICS

Bed level differences
Upstream node secondary channel

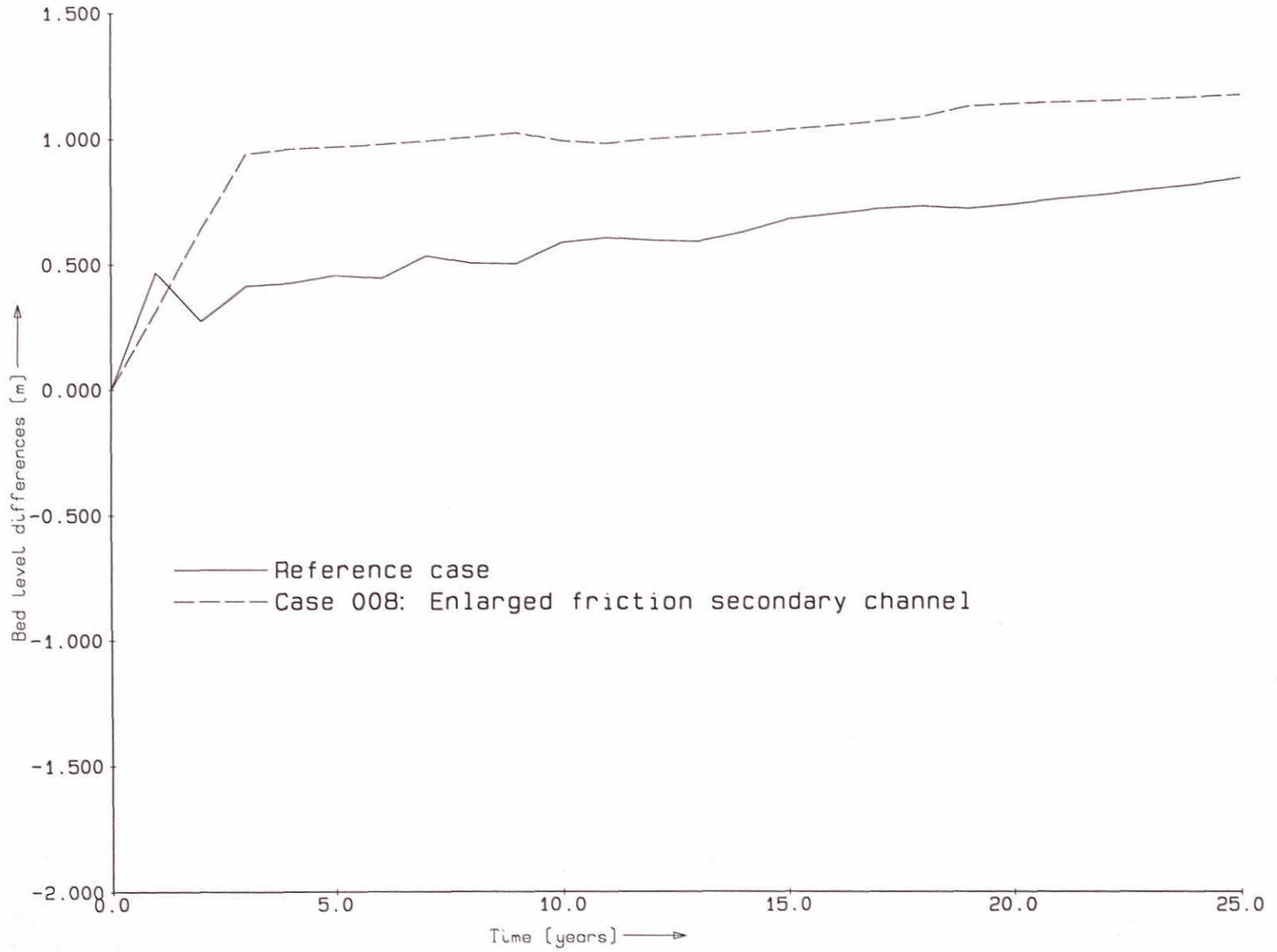

Q-1963

Fig. 4.38

main office
Rotterdamseweg 185
p.o. box 177
2600 MH Delft
The Netherlands
telephone (31) 15 - 56 93 53
telefax (31) 15 - 61 96 74
telex 38176 hydel-nl

location 'De Voorst'
Voorsterweg 28, Marknesse
p.o. box 152
8300 AD Emmeloord
The Netherlands
telephone (31) 5274 - 29 22
telefax (31) 5274 - 35 73
telex 42290 hylvo-nl